



저작자표시-비영리-변경금지 2.0 대한민국

이용자는 아래의 조건을 따르는 경우에 한하여 자유롭게

- 이 저작물을 복제, 배포, 전송, 전시, 공연 및 방송할 수 있습니다.

다음과 같은 조건을 따라야 합니다:



저작자표시. 귀하는 원저작자를 표시하여야 합니다.



비영리. 귀하는 이 저작물을 영리 목적으로 이용할 수 없습니다.



변경금지. 귀하는 이 저작물을 개작, 변형 또는 가공할 수 없습니다.

- 귀하는, 이 저작물의 재이용이나 배포의 경우, 이 저작물에 적용된 이용허락조건을 명확하게 나타내어야 합니다.
- 저작권자로부터 별도의 허가를 받으면 이러한 조건들은 적용되지 않습니다.

저작권법에 따른 이용자의 권리는 위의 내용에 의하여 영향을 받지 않습니다.

이것은 [이용허락규약\(Legal Code\)](#)을 이해하기 쉽게 요약한 것입니다.

[Disclaimer](#)

약학박사 학위논문

**Glutamyl-Prolyl tRNA Synthetase Controls
Collagen and Fibronectin Expression *via* STAT
Signaling in Pulmonary and Hepatic Fibrogenesis**

글루타밀-프롤릴 tRNA 합성효소의
폐 및 간 섬유화에서 STAT Signaling을 통한
Collagen과 Fibronectin의 발현 조절 연구

2019년 2월

서울대학교 대학원
약학대학 의약생명과학전공
송 대 근

**Glutamyl-Prolyl tRNA Synthetase Controls
Collagen and Fibronectin Expression *via* STAT Signaling
in Pulmonary and Hepatic Fibrogenesis**

**By
Dae-Geun Song**

**A thesis submitted in
partial fulfillment of the requirements
for the Degree of**

Doctor of Philosophy

(Pharmacy: Pharmaceutical Bioscience Major)

**Under the supervision of Professor Jung Weon Lee
at the College of Pharmacy**

Seoul National University

February, 2019

ABSTRACT

Background: Fibrosis is characterized by the increased accumulation of extracellular matrix (ECM), which drives abnormal cell proliferation and progressive organ dysfunction in many inflammatory and metabolic diseases. Studies have shown that halofuginone, a racemic halogenated derivative of febrifugine, purified from *Dichroa febrifuga*, inhibits glutamyl-prolyl-tRNA-synthetase (EPRS)-mediated fibrosis. However, the mechanism by which this occurs was only focused on the translational function of EPRS and *in vivo* efficacies were not studied. Thus, in order to develop efficacious drugs targeting EPRS, more studies are needed.

Methods: In this study, I explored the mechanistic aspects of how EPRS could develop hepatic and pulmonary fibrotic phenotypes in cells and animal models. CCl₄ administration, bile duct ligation operation, and bleomycin administration were used in order to induce fibrosis in wild type (*Eprs*^{+/+}) or *Eprs*^{-/+} C57B/L6 mice. **Results:** Treatment of transforming growth factor β 1 (TGF β 1) up-regulated extracellular matrix proteins, including fibronectin and collagen I, in LX2 hepatic stellate cells and A549 alveolar epithelial cells. This effect was inhibited in EPRS-suppressed cells and enhanced in PRS-overexpressed cells. Using the promoter luciferase assay, TGF β 1-mediated *COL1A1* (collagen I, α 1 chain) and *LAMC2* (laminin γ 2) transcription in LX2 and A549 cells were down-regulated by EPRS suppression, suggesting that EPRS may play roles in ECM production at transcriptional levels. Furthermore, signal transducer and activator of transcription (STAT) signaling activation was involved in the effects of TGF β 1 on ECM expression in an EPRS-dependent manner. This was mediated via a protein-protein complex formation consisting of TGF β 1 receptor, EPRS, Janus kinases, and STATs. Additionally, ECM expression in fibrotic livers and lungs were overlapped with EPRS expression along fibrotic septa regions and was positively correlated with STAT6 activation in fibrosis mouse models.

This was less obvious in livers and lungs of *Eprs*^{-/+} mice. **Conclusion:** These findings suggest that during fibrosis development, EPRS plays roles in non-translational processes of ECM expression via the TGFβ1/STAT signaling pathway. Therefore, EPRS can be used as a potential target to develop anti-fibrosis treatments.

Keywords: EPRS, fibrosis, STAT, TGFβ1, SMAD, CCl₄, bile duct ligation, bleomycin

Student Number: 2015-30498

TABLE OF CONTENTS

ABSTRACT.....	ii
TABLE OF CONTENTS.....	iv
LIST OF FIGURES	vii
LIST OF TABLES.....	xi
LIST OF ABBREVIATIONS	xii

BACKGROUND..... 1

i. Fibrosis.....	2
ii. Hepatic fibrosis	4
iii. Pulmonary fibrosis	8
iv. TGF β 1 Pathway	11
v. EPRS	13
vi. Halofuginone	22

CHAPTER 1. GLUTAMYL-PROLYL-TRNA SYNTHETASE INDUCES FIBROTIC EXTRACELLULAR MATRIX VIA BOTH TRANSCRIPTIONAL AND TRANSLATIONAL MECHANISMS 26

1.1. ABSTRACT.....	27
1.2. INTRODUCTION.....	28
1.3. MATERIALS AND METHODS.....	31
Reagents and plasmids.....	31
Cell culture.....	31

Western blot analysis	32
ECM deposition assay and collagen footprint assay.....	32
Quantitative reverse-transcription (qRT) PCR.....	33
Co-immunoprecipitation.....	33
Luciferase assay.....	34
Animal experiments.....	34
Liver organoid culture.....	35
Immunohistochemistry and staining.....	35
1.4. RESULTS.....	39
Inhibition or suppression of EPRS in LX2 HSCs decreased the production and deposition of ECMs under TGF β 1 signaling	39
EPRS-mediated transcriptional regulation of ECMs involved STAT6 activation.....	42
EPRS-mediated signaling occurred downstream of TGF β 1	44
<i>In vivo</i> liver tissues from fibrotic mice showed EPRS-dependent STAT6 phosphorylation and ECM production.....	45
Liver organoids in a three-dimensional (3D) Matrigel system revealed EPRS-dependent regulation of ECM induction.....	47
1.5. DISCUSSION	65

CHAPTER 2. GLUTAMYL-PROLYL-TRNA SYNTHETASE REGULATES EPITHELIAL EXPRESSION OF MESENCHYMAL MARKERS AND EXTRACELLULAR MATRIX PROTEINS: IMPLICATIONS FOR IDIOPATHIC PULMONARY FIBROSIS 69

2.1. ABSTRACT.....	70
2.2. INTRODUCTION.....	71
2.3. MATERIALS AND METHODS.....	73
Reagents and plasmids.....	73

Cell culture.....	73
Western blot analysis	74
qRT-PCR.....	74
Co-immunoprecipitation.....	74
Luciferase assay.....	75
Animal experiments.....	75
Immunohistochemistry and staining.....	76
Statistics	76
2.4. RESULTS.....	79
EPRS expression regulated ECM production in A549 alveolar type II cells upon TGFβ1 stimulation.....	79
Regulation of TGFβ1-induced ECM protein synthesis by EPRS occurred via STAT activation	80
TGFβ1-mediated SMAD3 phosphorylation upregulated phosphorylation of STAT6 depending on EPRS expression.	81
EPRS-mediated signaling in TGFβ1-treated cells involved the formation of a multi-protein complex consisting of STAT6 and TGFβ1R.....	81
Lung tissues from bleomycin-treated mice showed EPRS-dependent STAT6 phosphorylation and ECM protein production <i>in vivo</i>	82
2.5. DISCUSSION	93
 CONCLUSIONS & PERSPECTIVES.....	 97
 REFERENCES	 101
 ABSTRACT IN KOREAN.....	 112

LIST OF FIGURES

Figure 1.

Anatomy of liver; hepatic lobules.

Figure 2.

Sinusoidal events during fibrosing liver injury.

Figure 3.

Pathways of hepatic stellate cell activation.

Figure 4.

Pathobiologic features of idiopathic pulmonary fibrosis.

Figure 5.

Major components of the TGF β signaling pathway.

Figure 6.

General action mechanism of aminoacyl-tRNA synthetase.

Figure 7.

Structure of EPRS.

Figure 8.

Two-site phosphorylation of EPRS during release from MSC.

Figure 9.

Schematic representation of mTORC1–S6K1 activation of EPRS and its translocation to plasma membrane in adipocytes.

Figure 10.

Structures of Febrifugine and Halofuginone.

Figure 11.

Model of AAR Activation by inhibition of tRNA charging.

Figure 1. 1.

EPRS specific inhibitors can dose dependently down-regulate expression of fibronectin.

Figure 1. 2.

EPRS promotes expression of extracellular matrix (ECM) chains.

Figure 1. 3.

Suppression of different aminoacyl-tRNA synthetases (ARS) showed no significant changes in ECM chain mRNA levels.

Figure 1. 4.

ECM induction and deposition in human foreskin fibroblasts were dependent on EPRS expression.

Figure 1. 5.

STAT6 phosphorylation upon TGFβ1 treatment to LX2 cells was required for ECM production.

Figure 1. 6.

EPRS-dependent regulation of signaling downstream of TGFβ1.

Figure 1. 7.

CCl₄-treated mice showed EPRS-dependent ECM production.

Figure 1. 8.

Bile duct ligation in mice showed EPRS-dependent ECM production.

Figure 1. 9.

Liver organoid models prepared from WT or *Eprs*^{-/+} hetero-KO mice also showed EPRS-dependent fibronectin expression.

Figure 1. 10.

The working model for EPRS-dependent ECM expression on TGFβ1 treatment to LX2 cells.

Figure 2. 1.

EPRS expression regulates ECM protein production in A549 alveolar type II cells treated with TGFβ1.

Figure 2. 2.

Regulation of TGF β 1-induced ECM protein synthesis by EPRS occurs via STAT activation.

Figure 2. 3.

TGF β 1-mediated SMAD3 phosphorylation upregulates phosphorylation of STAT6 depending on EPRS expression.

Figure 2. 4.

EPRS-mediated signaling in TGF β 1-treated cells involves the formation of a multi-protein complex consisting of STAT6 and TGF β 1R.

Figure 2. 5.

Lung tissues from bleomycin-treated mice showed EPRS-dependent STAT6 phosphorylation and ECM protein production *in vivo*.

Figure 2. 6.

Working model for EPRS-dependent signaling during TGF β 1-mediated ECM expression of ECMs.

LIST OF TABLES

Table 1.

FDA approved drugs for IPF

Table 2.

Pharmacologic management of IPF.

Table 3.

Percentage of proline residue in ECM proteins.

Table 1. 1.

Antibodies and their dilution ratio used in Chapter 1.

Table 1. 2.

qRT-PCR primers used in Chapter 1.

Table 2. 1.

Antibodies and their dilution ratio used in Chapter 2.

Table 2. 2.

qRT-PCR primers used in Chapter 2.

LIST OF ABBREVIATIONS

3D	three dimension
α -SMA	α -smooth muscle actin
AAR	amino acid starvation response
COL1A1	Collagen I A1
ECM	extracellular matrix
EPRS	glutamyl-prolyl-tRNA-synthetase
ERS	glutamyl-tRNA-synthetase
FN	Fibronectin
HCC	hepatocellular carcinoma
HF	Halofuginone
HSCs	hepatic stellate cells
JAKs	Janus kinases
LAMC2	Laminin γ 2
PRS	prolyl-tRNA-synthetase
STAT	Signal transducer and activator of transcription
TGF β 1	Transforming growth factor beta 1

BACKGROUND

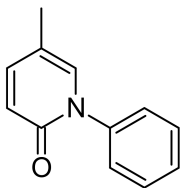
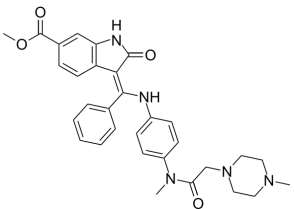
I. FIBROSIS

Fibrosis can be defined as the excessive production and deposition of extracellular matrix (ECM) outside of cells following chronic injury-mediated inflammation [1]. If not properly treated, fibrosis may progress into organ dysfunction. Fibrosis can develop in various organs in our body. Among the inflammatory and metabolic diseases are idiopathic pulmonary fibrosis (IPF), advanced liver disease, advanced kidney disease, cardiac fibrosis, and dermal fibrosis [2]. In spite of recent advances in our understanding of disease mechanisms, the disease conditions remain poorly treated [2].

Fibrosis is usually developed by following injury. Damaged tissues typically initiate a series of homeostatic reparative processes to restore organ integrity, structure and function. The time and the type of cause of injury may vary. The type may be exposure to toxic substances, infection or physical trauma. These insults may come through both acute and chronic processes. Such tissue injuries can trigger the development of fibrosis through the excessive production of ECM [2].

Until now, there are only two FDA drug for fibrosis treatment- pirfenidone and nintedanib. Pirfenidone (table i, compound 1) was recently approved as the first specific therapy for IPF [3]. Pirfenidone is known to target multiple molecules; TGF β [4, 5], TNF, IL-10 [6, 7], and p38 α [8]. However, the major target of pirfenidone remains unclear. Despite the unclear mechanism of action of pirfenidone, it serves as a gold standard in preclinical and clinical testing. Nintedanib (table i, compound 2) has also recently obtained approval as a therapy for IPF. The action mechanism of nintedanib is blocking pro-angiogenic receptor tyrosine kinases; i.e. nintedanib is a triple angiokine inhibitor [9].

Table 1. FDA approved drugs for IPF.

Compound	Molecular target(s); mechanism(s) and selected <i>in vitro</i> pharmacology	Evidence for anti-fibrotic activity and preclinical and/or clinical data (trial name)	Clinical trials; indication (status); identifier (trial name)
<p>1. Pirfenidone</p> 	<p>Multiple targets TGFβ [4, 5] TNF, IL-10 [6, 7] p38α (IC₅₀ 165 μM), and MRC5 (human lung fibroblast) cell inhibition (IC₅₀ 14 mM) [8]</p>	<p>Anti-fibrotic in animal models [10] Reduced deterioration in lung function in IPF (CAPACITY) [11] Reduced disease progression in IPF (ASCEND) [3]</p>	<p>IPF (marketed) IPF (Phase III, completed); NCT01366209 (ASCEND) SSc-ILD (Phase II); NCT01933334 (LOTUSS) Diabetic nephropathy (Phase II, completed); NCT00063583</p>
<p>2. Nintedanib</p> 	<p>Inhibits multiple tyrosine kinases [9] VEGFR1, VEGFR2 and VEGFR3 (IC₅₀ 13-34 nM) FGFR1 (IC₅₀ 69 nM) FGFR2 (IC₅₀ 37 nM) PDGFRα (IC₅₀ 59nM) FLT3 (IC₅₀ 26 nM) LCK (IC₅₀ 16 nM)</p>	<p>Anti-fibrotic and anti-inflammatory in experimental pulmonary fibrosis [12] Reduced FVC decline in two Phase III IPF trials (INPULSIS-1 and INPULSIS-2) [13]</p>	<p>IPF (marketed) IPF (Phase III); NCT01619085 and NCT01979952</p>

Reprinted by permission from Springer Nature: *Nature Reviews Drug Discovery*, Dissecting fibrosis: therapeutic insights from the small-molecule toolbox, Nanthakumar, C. B. *et al.*, copyright 2015.

II. HEPATIC FIBROSIS

Chronic liver disease can progress to advanced fibrosis and cirrhosis, can accompany abnormal liver vascular architecture and functional failure, and can eventually lead to hepatocellular carcinoma (HCC) [14]. Significant advances in different cell and organism models have revealed molecular mechanisms that underlie the progression of liver fibrosis [15]. Liver fibrosis involves a several-fold increase in the ECM [1]. Liver ECM is produced mostly by hepatic stellate cells (HSCs) [16], and collagen I is the main component of the fibrous septa related to activated HSCs [17]. Many previous studies have shown that hepatocytes produce ECM *in vitro*. Furthermore, numerous other ECM molecules can be either indicators or therapeutic targets for manipulating fibrosis [18], and the mammalian ECM consists of approximately 300 proteins [19]. Because previous studies have mostly focused on the role of collagen I in liver malignancy, it is important to study the roles of other ECM molecules in liver fibrosis.

Pharmaceutical agents can be designed to prevent the progression of fibrosis and reverse steatohepatitis [20]. Excessive ECM production by activated HSCs, portal myofibroblasts (MF), and activated sinusoidal endothelial cells can be targeted in the development of anti-fibrotic agents [14]. Moreover, ductular reactions or epithelial-mesenchymal transition-like changes can stimulate cholangiocytes, which then activate MF and result in the progression of cirrhosis and the development of HCC [21]. Many different molecules are involved in signaling pathways for ECM production and deposition in these processes leading to liver fibrosis. In particular, prolyl-tRNA synthetase (PRS) has been targeted to block fibrotic collagen production [22].

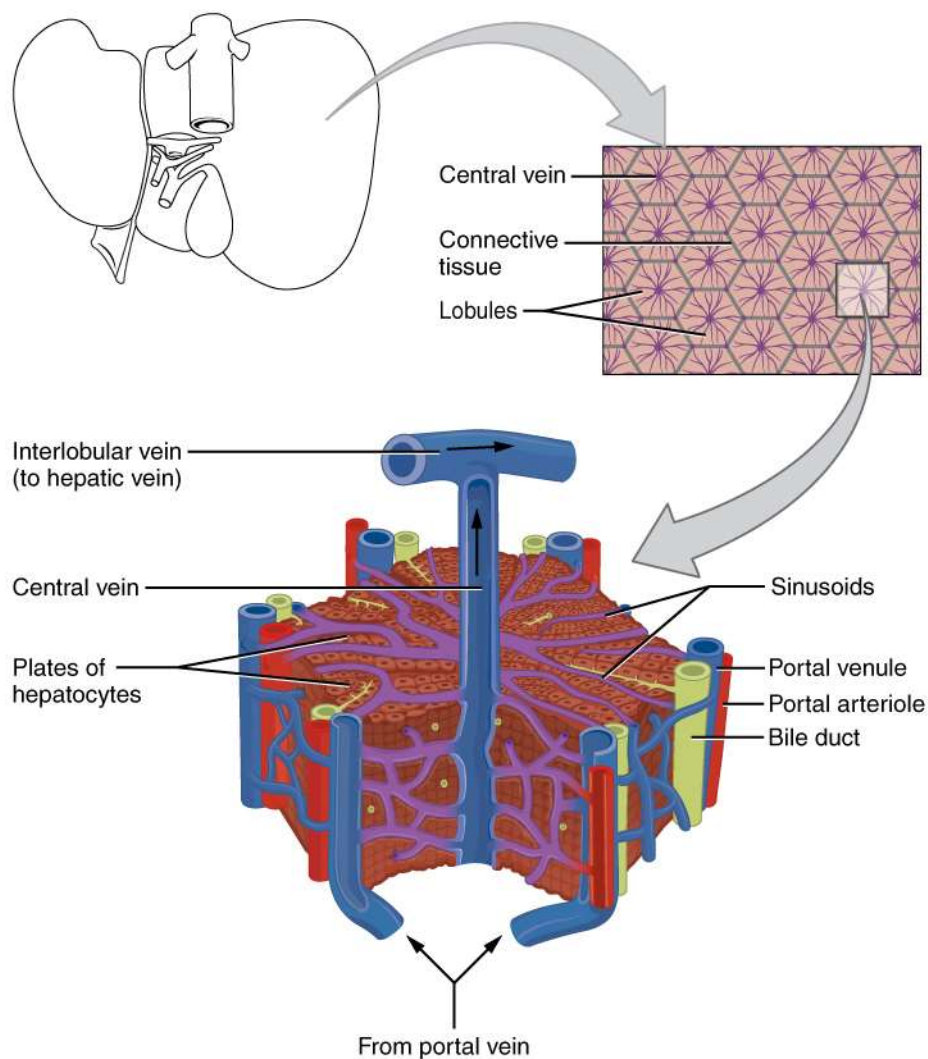


Figure 1. Anatomy of liver; hepatic lobules. Adopted from Anatomy & Physiology by Rice University available at <https://cnx.org/contents/FPtK1zmh@6.27:esgfrPlv@3/Accessory-Organ-in-Digestion-The-Liver-Pancreas-and-Gallbladder> under Creative Commons Attribution 4.0 License. Copyright 1999-2018.

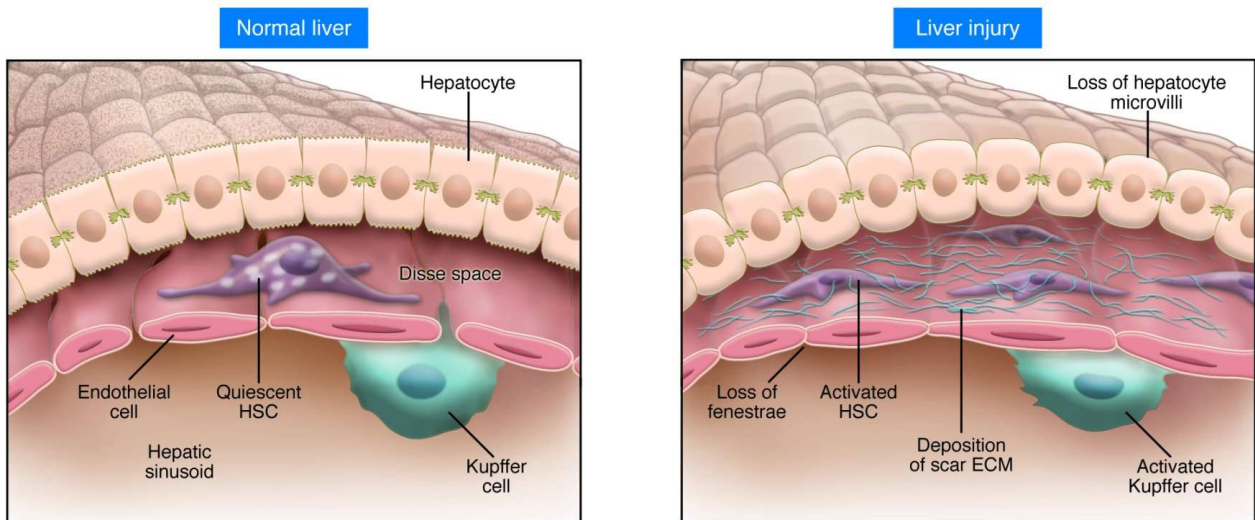


Figure 2. Sinusoidal events during fibrosing liver injury. Republished with permission of American Society for Clinical Investigation, *Journal of Clinical Investigation*, John P. Iredale, Vol 117(3), pp. 539-48, 2007; permission conveyed through Copyright Clearance Center, Inc. [23, 24].

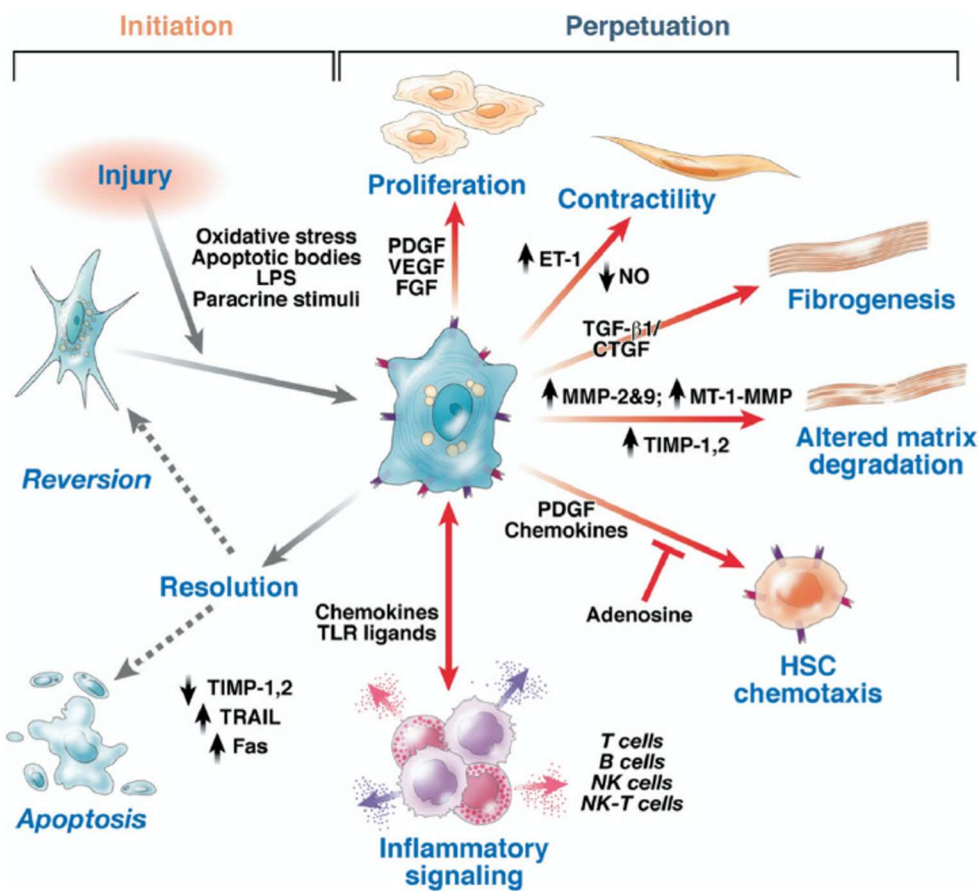


Figure 3. Pathways of hepatic stellate cell activation. Reprinted from *Gastroenterology*, Vol 134(6), Scott L. Friedman, Mechanisms of Hepatic Fibrogenesis, pp 1655–1669, copyright 2008, with permission from Elsevier. [23, 25, 26].

III. PULMONARY FIBROSIS

Idiopathic pulmonary fibrosis (IPF) is a critical type of pulmonary fibrosis which can be defined as chronic, progressive, fatal, fibrotic interstitial lung disease of unknown cause [27-30]. Typical clinical symptoms include dyspnoea, decreased exercise capacity, and dry cough; most patients survive for 2.5-5 years after diagnosis [31]. Like most other fibrotic symptoms, IPF is characterized by the excessive accumulation of extracellular matrix (ECM) components, which correlates with the proliferation and activation of fibroblasts, myofibroblasts, and abnormal lung epithelial cells [32]. Although the origins and activation of invasive lung myofibroblasts remain unclear, some potential causes include activation of lung resident fibroblasts, recruitment of circulating fibrocytes and blood mesenchymal precursors, and mesenchymal transformation of alveolar type II epithelial cells, endothelial cells, pericytes, and/or mesothelial cells [33].

Current pharmacologic treatments for IPF include two U.S. Food & Drug Administration-approved drugs (nintedanib and pirfenidone) that improve symptoms but do not cure the disease [27]. Given the limited treatment options, it is urgent to investigate the mechanisms of IPF pathogenesis [30].

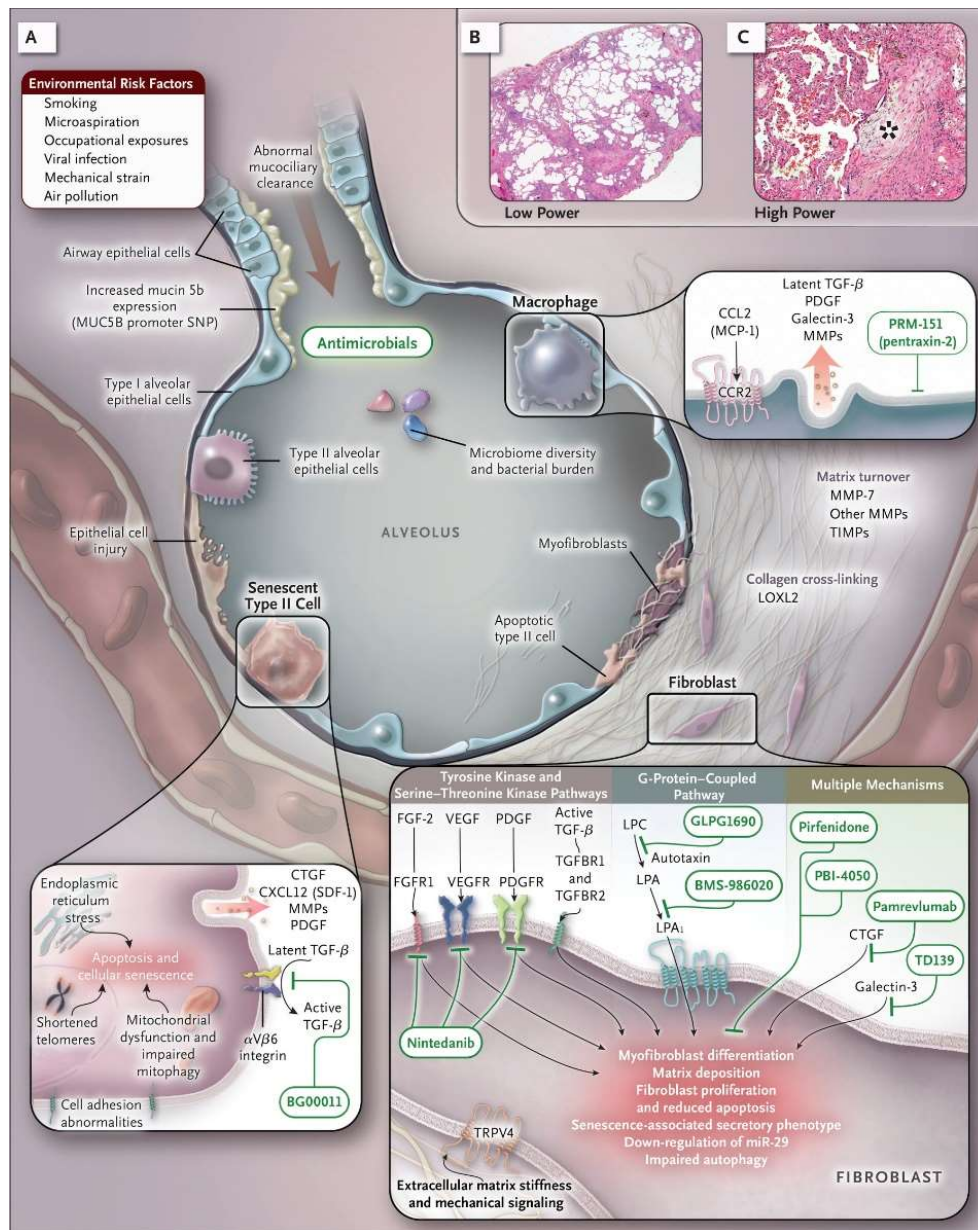


Figure 4. Pathobiologic features of idiopathic pulmonary fibrosis. Reproduced with permission from *New England Journal of Medicine*. Lederer *et al.*, Idiopathic Pulmonary Fibrosis, 2018, Vol 378(19), pp 1811-23, Copyright Massachusetts Medical Society [27].

Table 2. Pharmacologic management of IPF.

Variable	Nintedanib	Pirfenidone
Mechanism of action	Tyrosine kinase inhibition	Inhibition of TGF- β production and downstream signaling, collagen synthesis, and fibroblast proliferation (selected list)
Efficacy	Slows FVC decline by 50%	Slows FVC decline by 50%
FDA-approved dose	150 mg by mouth twice daily	801 mg by mouth thrice daily
Common side effects	Diarrhea	Anorexia, nausea, photosensitivity
Enzyme metabolism	Ester cleavage (major), CYP 3A4 (minor)	CYP 1A2 (major), other CYP enzymes (minor)
Cautions	Risks of both bleeding and arterial thrombosis; risk of gastrointestinal perforation (rare); anticoagulant and prothrombotic drugs should be avoided	CYP 1A2 inhibitors (e.g., fluvoxamine and ciprofloxacin) can raise pirfenidone levels; CYP 1A2 inducers (e.g., omeprazole and smoking) can lower pirfenidone levels
Need for liver-function monitoring	Yes†	Yes‡
Clinical strategies to minimize side effects	Use of antidiarrheal agents, temporary dose reduction to 100 mg twice daily	Slow dose increase over 14-day period, medication to be taken with food, use of antacids, use of antiemetic agents, sun avoidance

Reproduced with permission from *New England Journal of Medicine*. Lederer *et al.*, Idiopathic Pulmonary Fibrosis, 2018, Vol 378(19), pp 1811-23, Copyright Massachusetts Medical Society [27].

IV. TGF β 1 PATHWAY

Transforming growth factor β 1 (TGF β 1) is a multifunctional cytokine that regulates immune responses during homeostasis and inflammation [34, 35]. The role of TGF β 1 in human health is well summarized in the following literature.

“TGF- β has important homeostatic roles in the control of wound healing and tissue repair, epithelial integrity, and innate and adaptive immune responses [35, 36]. Aberrant TGF- β regulation is associated with inherited conditions, such as hereditary hemorrhagic telangiectasia, Loeys–Dietz syndrome, familial pulmonary hypertension, Camurati–Engelmann disease, Marfan syndrome and fibrodysplasia ossificans progressiva, cancers, both hereditary (e.g. juvenile polyposis and Cowden syndrome) and sporadic (breast, colon, lung and pancreas), and fibrosing disorders such as post-angioplasty restenosis, pulmonary fibrosis, glomerulosclerosis and SSc [35, 37]. Reduced TGF- β signaling resulting from decreased expression of the type I TGF- β receptor confers a substantially increased risk of colorectal cancer, first in mice and then in humans [35, 38, 39]. The functional duality of TGF- β was illustrated in a mouse model of autoimmunity, where it was shown to be necessary for maintaining immune tolerance while promoting tissue fibrosis [35, 40]. These conditions demonstrate that either insufficient or excessive TGF- β activity is harmful; therefore, therapeutic targeting of TGF- β must consider the impact of TGF- β blockade on physiological as well as pathological processes [35].”¹

¹ Text excerpted by permission from Springer Nature: *Nature Reviews Rheumatology*, Transforming growth factor β as a therapeutic target in systemic sclerosis, John Varga and Boris Pasche, copyright 2009.

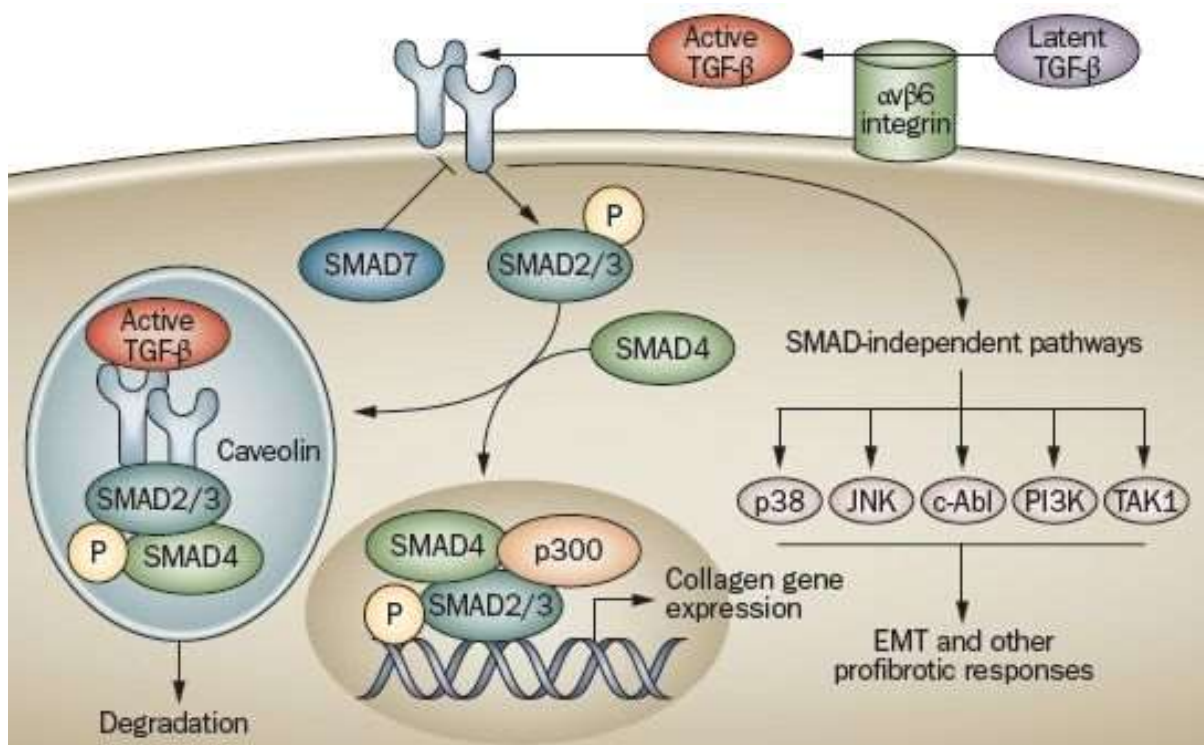


Figure 5. Major components of the TGFβ signaling pathway. Reprinted by permission from Springer Nature: *Nature Reviews Rheumatology*, Transforming growth factor β as a therapeutic target in systemic sclerosis, John Varga and Boris Pasche, copyright 2009 [35].

V. EPRS

Glutamyl-prolyl-tRNA synthetase (EPRS) catalyzes the attachment of glutamate or proline to transfer RNA (tRNA) during translation [41, 42]. The canonical and non-canonical function of EPRS has been summarized in the following literature.

“EPRS is a member of aminoacyl-tRNA synthetases (AARS) whose canonical function is to decipher the genetic code by accurate ligation of amino acids to their cognate tRNAs [42-44]. The AARS are ancient and ubiquitous enzymes with catalytic cores conserved in bacteria, archaea, and eukarya. The 20 AARS are divided into 2 classes of 10 enzymes each, distinguished by structures and signature sequences in their catalytic domains. During evolution, certain AARS acquired structural characteristics and functions beyond those required for protein synthesis. For example, many chordate AARS are distinguished from their bacterial counterparts by a greater degree of complexity exemplified by noncanonical functions unrelated to aminoacylation, by intracellular organization into large complexes, and by noncatalytic appended domains [45, 46]. These features of chordate AARS appear to be interrelated, e.g., the appendages facilitate interactions between AARS and other proteins (or inter-AARS interactions), and they may contribute to AARS noncanonical activities [47].

Via their noncanonical activities, several AARS may be important regulators of diverse cellular processes, including several related to inflammation. For example, mast cell LysRS exerts transcriptional control via its catalytic product Ap4A [48] and, upon secretion, triggers a proinflammatory response [49]. GlnRS prevents apoptosis by inhibiting the kinase activity of apoptosis signal-regulated kinase 1 [50]. Proteolytic fragments of TyrRS and TrpRS exhibit opposing, cytokine-like activities that regulate

angiogenesis [51]. In humans and other chordates, GluRS (or ERS) and ProRS (or PRS) are linked to form a single bifunctional protein, glytamyl-prolyl tRNA synthetase (GluProRS or EPRS) [52]. Human EPRS exhibits a noncanonical function as a posttranscriptional regulator of inflammatory gene expression [53]. In some cases, domains that are neither a part of the enzymatic core nor present in bacterial homologs contribute to noncanonical functions [46, 54]. These domains are usually appended to the N or C terminus and include EF1Bg- like domains, an endothelial monocyte-activating polypeptide II-like domain, and a helix-turn-helix domain termed the WHEP- TRS (after three AARS containing them, i.e., Trp(W)RS, His(H)RS, and GluPro(EP)RS); GlyRS and MetRS also contain appended WHEP domains. Interestingly, no other proteins contain this domain, and all five WHEP domain-bearing proteins express noncanonical functions [46, 53, 55]. In mammalian cells, 9 of the 20 AARS activities are organized in a cytosolic, 1.5 mDa tRNA multisynthetase complex (MSC) [45, 48]. The complex also contains three AARS-interacting multifunctional proteins (AIMP) that lack synthetase activity, AIMP1/p43, AIMP2/p38, and AIMP3/p18, which may serve as a scaffold for the complex but also express additional cellular functions [45, 55]. The function of the MSC remains unclear, but it may facilitate channeling of amino-acylated tRNAs to the ribosome during protein biosynthesis [56]. In addition, the complex can serve as a depot for AARS and non-AARS proteins released to perform noncanonical activities in a stimulus- or context-dependent manner [57].”²

² Text excerpted from *Molecular Cell*, Vol 35(2), Arif, A. *et al.*, Two-Site Phosphorylation of EPRS Coordinates Multimodal Regulation of Noncanonical Translational Control Activity, pp 164–80, copyright 2009, with permission from Elsevier.

The example of translation-inhibiting-noncanonical activity of EPRS induced by the interferon- γ is described in the following paragraph. It also describes the mechanism of the dissociation of EPRS from MSC.

“Human EPRS is a 172 kDa monomeric protein that displays all of the characteristics that differentiate eukaryotic AARS from their bacterial counterparts. The protein contains two distinct appended domains, namely an N-terminal EF1Bg-like domain and a linker domain containing three tandem WHEP repeats that connects the catalytic domains. EPRS resides exclusively in the MSC, but in monocytic cells, it is released upon interferon (IFN)- γ activation to join three other proteins to form the cytosolic IFN- γ -activated inhibitor of translation (GAIT) complex [53]. The GAIT complex binds a defined RNA element (GAIT element) consisting of a stem loop with an internal bulge in the 3' untranslated region (UTR) of target transcripts—e.g., vascular endothelial growth factor (VEGF)-A, ceruloplasmin (Cp), death-associated protein kinase, zipper-interacting protein kinase, several chemokines, and their receptors—and silences their translation [57-61]. The GAIT complex forms in two stages. After about 2 hr of IFN- γ stimulation, EPRS is phosphorylated and released from its MSC residence to interact with NS1-associated protein (NSAP1) and form the inactive pre-GAIT complex. About 14–16 hr later, ribosomal protein L13a and glyceraldehyde 3-phosphate dehydrogenase (GAPDH) join the pre-GAIT complex to form the active four-protein complex that binds GAIT element-bearing mRNAs and suppresses their translation by intercepting the 43S ribosomal subunit-binding site on eukaryotic initiation factor 4G (eIF4G) [60, 62]. As the sole target mRNA-binding protein, EPRS has a central role in GAIT system function [53]. The two upstream WHEP repeats are essential and sufficient for high-affinity binding to the GAIT

element [54]. RNA- binding activity of EPRS is both negatively and positively regulated. Coincident with its release from the MSC, NSAP1 binds EPRS in a domain partially overlapping the RNA-binding domain and efficiently inhibits binding to target transcripts. Upon subsequent joining of L13a and GAPDH to the pre-GAIT complex, RNA binding and translational silencing is restored.

Phosphorylation is a near-universal regulatory mechanism applied to both global and transcript-selective translational control [63-65]. Two key GAIT complex constituents, EPRS and L13a, are phosphorylated in response to IFN- γ [53, 58, 66]. EPRS phosphorylation is required for its release from the MSC and for formation of the functional GAIT complex [53, 54]. IFN- γ -inducible, two-site phosphorylation of EPRS at Ser886 and Ser999 in the linker domain choreographs the specific events required for noncanonical EPRS activity. These phosphorylation events are essential for induced release of EPRS from the MSC, for negative and positive regulation of EPRS binding to target mRNAs, for phospho-L13a binding to eIF4G, and, ultimately, for translational silencing of inflammatory gene expression [42].”³

The additional mechanism which can dissociate EPRS from MSC has been explained in other literature.

“In adipocytes, insulin stimulated S6K1-dependent EPRS phosphorylation and release from the multisynthetase complex. Interaction screening revealed that phospho-EPRS binds SLC27A1 (that is, fatty acid transport protein 1, FATP1) [67],

³ Text excerpted from *Molecular Cell*, Vol 35(2), Arif, A. *et al.*, Two-Site Phosphorylation of EPRS Coordinates Multimodal Regulation of Noncanonical Translational Control Activity, pp 164–80, copyright 2009, with permission from Elsevier.

inducing its translocation to the plasma membrane and long-chain fatty acid uptake. Thus, EPRS and FATP1 are terminal mTORC1–S6K1 axis effectors that are critical for metabolic phenotypes [67].”⁴

⁴ Text extracted by permission from Springer Nature: *Nature*, EPRS is a critical mTORC1–S6K1 effector that influences adiposity in mice, Arif, A., *et al.*, copyright 2017

Aminoacyl-tRNA Synthetase (ARS)

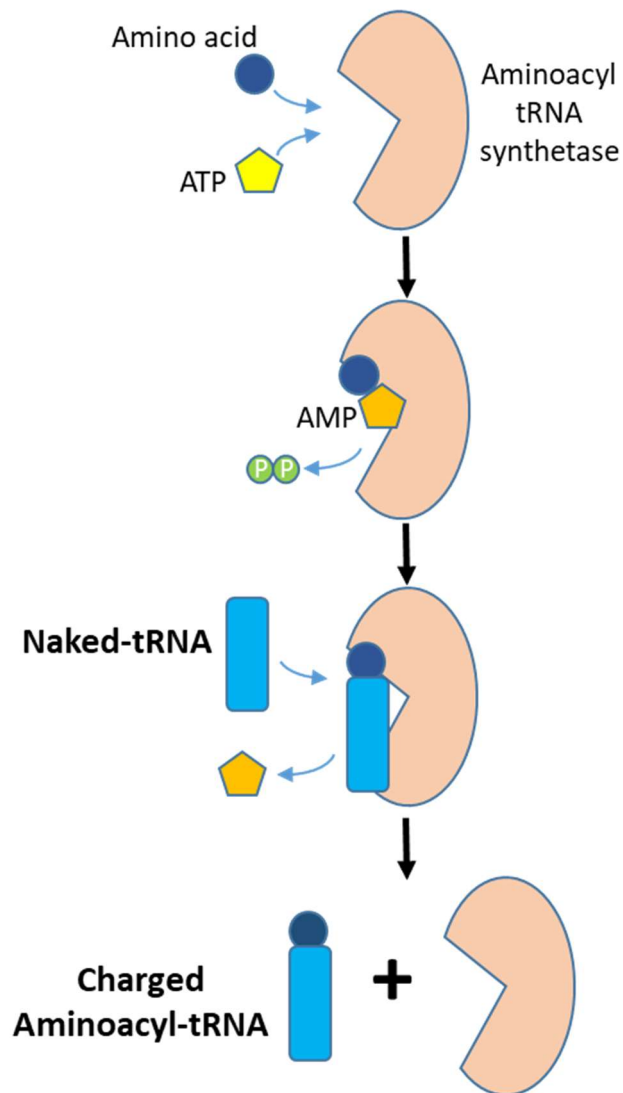


Figure 6. General action mechanism of aminoacyl-tRNA synthetase. Adapted from [68].

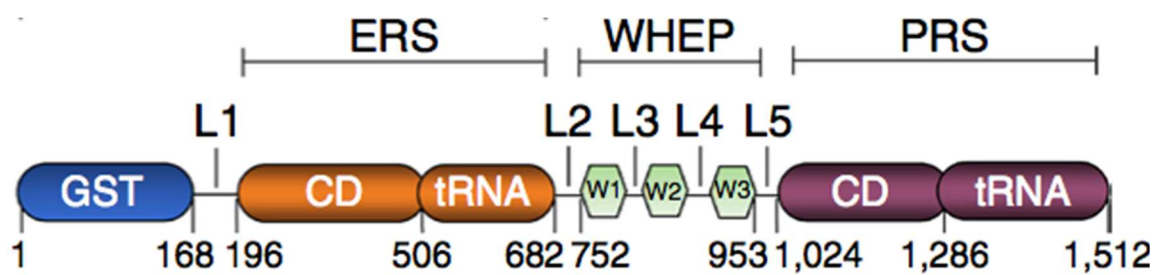


Figure 7. Structure of EPRS. Reprinted by permission from Springer Nature: *Nature Immunology*, Infection-specific phosphorylation of glutamyl-prolyl tRNA synthetase induces antiviral immunity, Lee, E.-Y., *et al.*, copyright 2016 [69]

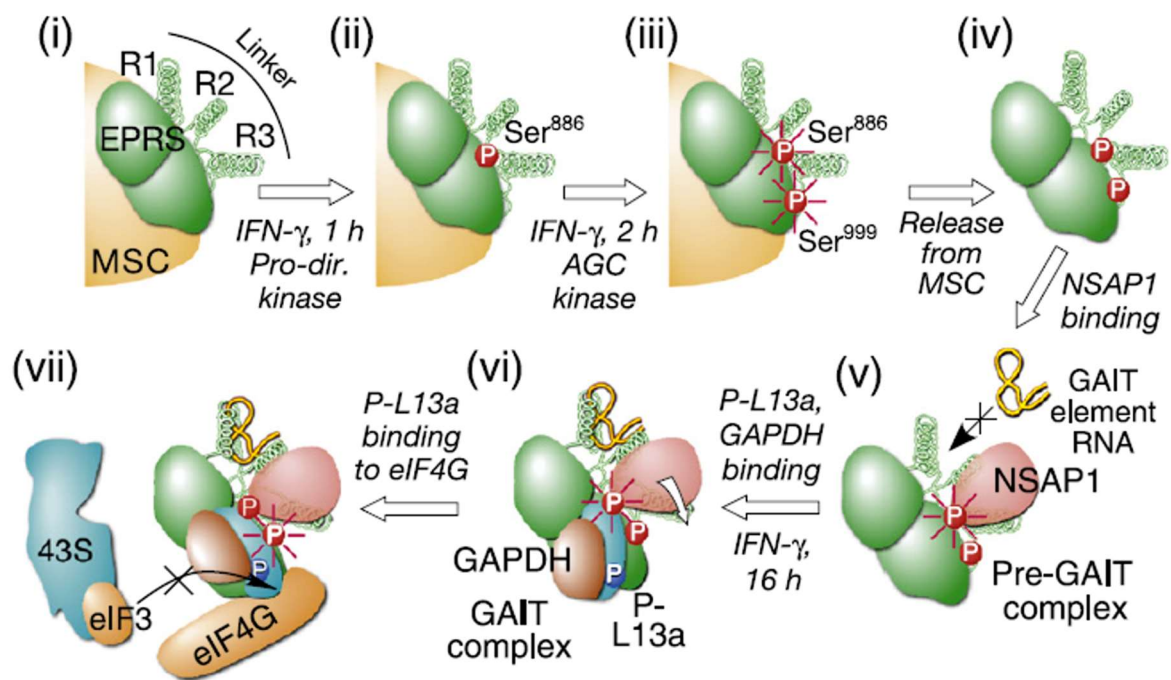


Figure 8. Two-site phosphorylation of EPRS during release from MSC. Reprinted from *Molecular Cell*, Vol 35(2), Arif, A. *et al.*, Two-Site Phosphorylation of EPRS Coordinates Multimodal Regulation of Noncanonical Translational Control Activity, pp 164–80, copyright 2009, with permission from Elsevier. [42].

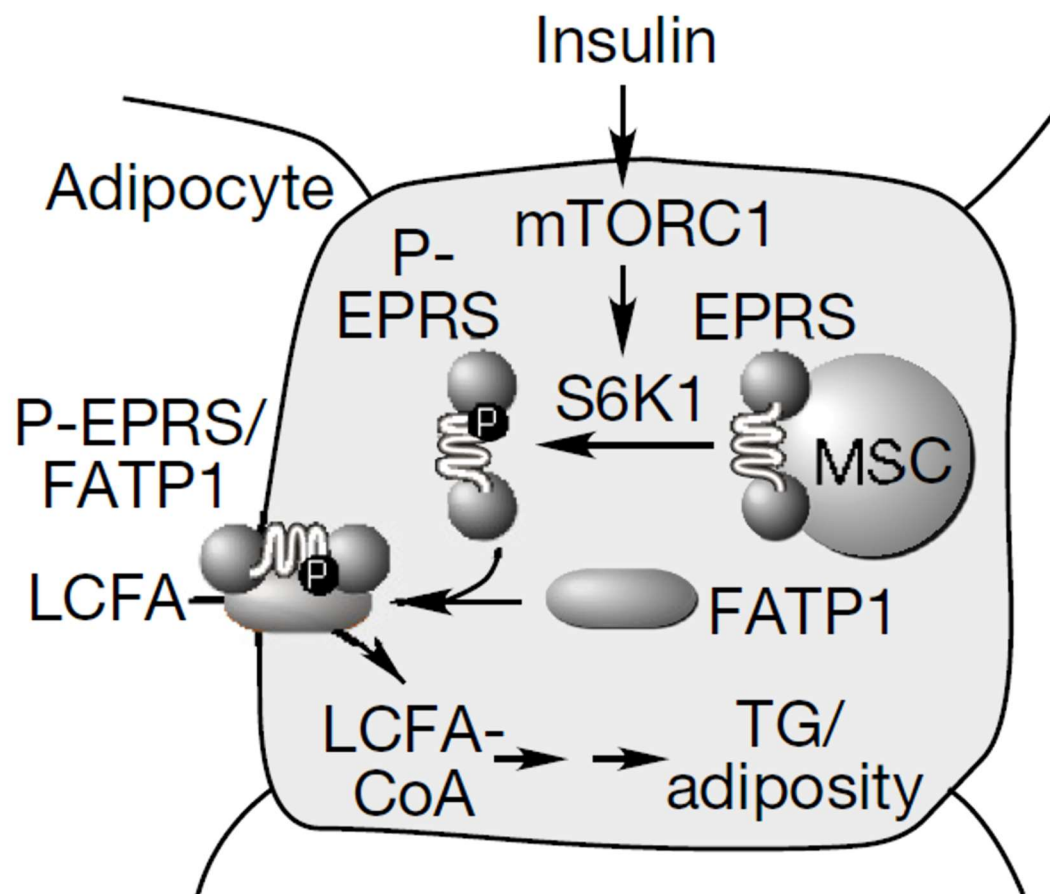


Figure 9. Schematic representation of mTORC1–S6K1 activation of EPRS and its translocation to plasma membrane in adipocytes. Reprinted by permission from Springer Nature: *Nature*, EPRS is a critical mTORC1–S6K1 effector that influences adiposity in mice, Arif, A., *et al.*, copyright 2017 [67].

VI. HALOFUGINONE

Halofuginone (HF) is an analog of the alkaloid febrifugine, which was originally isolated from the plant *Dichroa febrifuga*. HF is an excellent example of a bioactive agent that inhibits mRNA levels of collagen (*COL1A1* and *COL1A2*). Interestingly, these levels are restored by proline supplementation [22], indicating that HF can block the catalytic activity of PRS, which involves the loading of proline to transfer RNA (tRNA) during the translational process of proline-rich collagen. The observation that both COL1A1 (with 19% proline/total residues) and FN1 (fibronectin; with 7.9% proline/total residues) can be blocked by HF treatment [22] suggests that glutamyl-prolyl-tRNA synthetase (EPRS) may have roles beyond its translational tRNA charging activity. Limiting amino acids or inhibition of any of the aminoacyl-tRNA synthetases in animals activates the amino acid response (AAR) pathway after the accumulation of uncharged tRNAs is sensed and eukaryotic translation initiation factor 2 α (eIF2 α) is phosphorylated by GSN2 kinase [70]. These processes lead to decreased global protein synthesis [71] and induction of selected genes including activating transcription factor 4 (ATF4). ATF4 can then activate downstream genes to mediate the adaptation of cells to a stress environment, including C/EBP-homologous protein (CHOP, also known as DDIT3) [72]. Thus, ATF4 protein expression consequently activates multiple stress-induced genes, including AAR elements [73].

Because of its poor oral bioavailability, gastrointestinal (GI) toxicity, and limited patent life, the development of HF as an anti-fibrotic drug has been hindered [74]. Many of its side effects may be due to its inhibition of TGF β /SMAD3 signaling, which is important for homeostatic immune and inflammatory functions [34, 75]. Thus, the role of EPRS in the development of fibrosis, especially with regard to HF, requires further exploration.

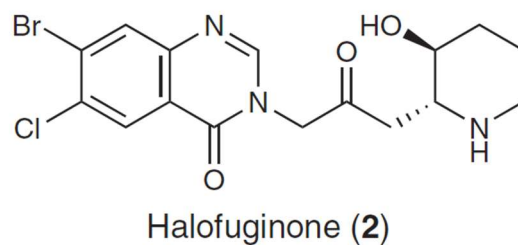
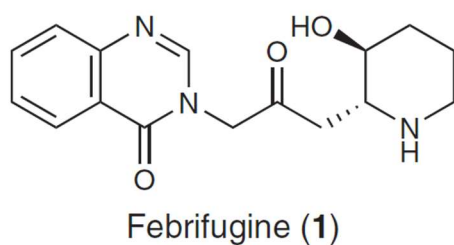


Figure 10. Structures of Febrifugine and Halofuginone. Reprinted by permission from Springer Nature: *Nature Chemical Biology*, Halofuginone and other febrifugine derivatives inhibit prolyl-tRNA synthetase, Keller, T. L., *et al.*, copyright 2012 [22].

Table 3. Percentage of proline residue in ECM proteins.

Protein	# Proline	Total residue	Proline/Total residue (%)	Entry #
HSA	24	609	3.9	P02768
BSA	28	607	4.6	P02769
FN1	189	2386	7.9	P02751
Col1A1	278	1464	19.0	P02452
Col4A1	324	1669	19.4	P02462
LAMC2 (laminin gamma 2)	55	1193	4.6	Q13753
PRB1	147	392	37.5	P04280

Total number of residues were obtained from UniProt Database (<https://www.uniprot.org/>).

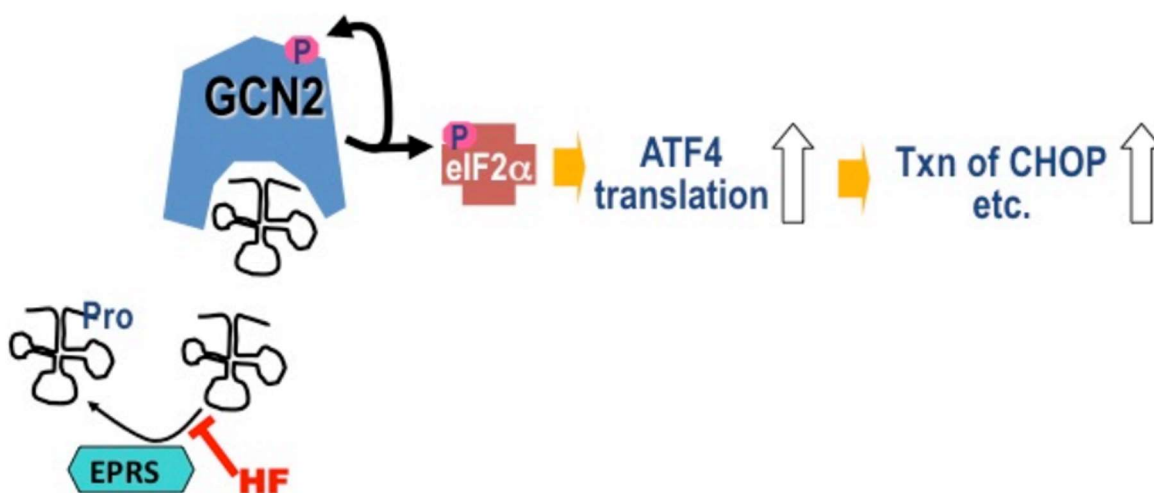


Figure 11. Model of AAR Activation by inhibition of tRNA charging. Reprinted by permission from Springer Nature: *Nature Chemical Biology*, Halofuginone and other febrifugine derivatives inhibit prolyl-tRNA synthetase, Keller, T. L., *et al.*, copyright 2012 [22].

CHAPTER 1.

Glutamyl-Prolyl-tRNA Synthetase Induces Fibrotic Extracellular Matrix via both Transcriptional and Translational Mechanisms

ABSTRACT

Background: Fibrosis is characterized by the increased accumulation of extracellular matrix (ECM), which drives abnormal cell proliferation and progressive organ dysfunction in many inflammatory and metabolic diseases. Studies have shown that halofuginone, a racemic halogenated derivative, inhibits glutamyl-prolyl-tRNA-synthetase (EPRS)-mediated fibrosis. However, the mechanism by which this occurs is unclear. **Methods:** In this study, I explored the mechanistic aspects of how EPRS could develop liver fibrotic phenotypes in cells and animal models. **Results:** Treatment of transforming growth factor $\beta 1$ (TGF $\beta 1$) up-regulated fibronectin and collagen I levels in LX2 hepatic stellate cells. This effect was inhibited in PRS-suppressed LX2 cells. Using the promoter luciferase assay, TGF $\beta 1$ -mediated *COL1A1* (collagen I, $\alpha 1$ chain) transcription and basal *LAMC2* (laminin $\gamma 2$) transcription in LX2 cells were down-regulated by EPRS suppression, suggesting that EPRS may play roles in ECM production at transcriptional levels. Furthermore, signal transducer and activator of transcription (STAT) signaling activation was involved in the effects of TGF $\beta 1$ on ECM expression in a PRS-dependent manner. This was mediated via a protein-protein complex formation consisting of TGF $\beta 1$ receptor, EPRS, Janus kinases, and STAT6. Additionally, ECM expression in fibrotic livers were overlapped with EPRS expression along fibrotic septa regions and was positively correlated with STAT6 activation in CCl₄-treated mice. This was less obvious in livers of *Eprs*^{-/+} mice. **Conclusion:** These findings suggest that during fibrosis development, EPRS plays roles in non-translational processes of ECM expression via intracellular signaling regulation upon TGF $\beta 1$ stimulation.

1.1. INTRODUCTION

Liver fibrosis involves the excessive production and deposition of extracellular matrix (ECM) outside of cells following chronic injury-mediated inflammation [1]. Chronic liver disease can progress to advanced fibrosis and cirrhosis, can accompany abnormal liver vascular architecture and functional failure, and can eventually lead to hepatocellular carcinoma (HCC) [14]. Significant advances in different cell and organism models have revealed molecular mechanisms that underlie the progression of liver fibrosis [15]. Liver fibrosis involves a several-fold increase in the ECM [1]. Liver ECM is produced mostly by hepatic stellate cells (HSCs) [16], and collagen I is the main component of the fibrous septa related to activated HSCs [17]. Many previous studies have shown that hepatocytes produce ECM *in vitro*. Furthermore, numerous other ECM molecules can be either indicators or therapeutic targets for manipulating fibrosis [18], and the mammalian ECM consists of approximately 300 proteins [19]. Because previous studies have mostly focused on the role of collagen I in liver malignancy, it is important to study the roles of other ECM molecules in liver fibrosis.

Pharmaceutical agents can be designed to prevent the progression of fibrosis and reverse steatohepatitis [20]. Excessive ECM production by activated HSCs, portal myofibroblasts (MF), and activated sinusoidal endothelial cells can be targeted in the development of anti-fibrotic agents [14]. Moreover, ductular reactions or epithelial-mesenchymal transition-like changes can stimulate cholangiocytes, which then activate MF and result in the progression of cirrhosis and the development of HCC [21]. Many different molecules are involved in signaling pathways for ECM production and deposition in these processes leading to liver fibrosis. In particular, prolyl-tRNA synthetase (PRS) has been targeted to block fibrotic collagen production [22]. Halofuginone (HF) is an analog of the alkaloid febrifugine, which was originally isolated from the plant *Dichroa febrifuga*. HF is an excellent example of a bioactive

agent that inhibits mRNA levels of collagen (*COL1A1* and *COL1A2*). Interestingly, these levels are restored by proline supplementation [22], indicating that HF can block the catalytic activity of PRS, which involves the loading of proline to transfer RNA (tRNA) during the translational process of proline-rich collagen. The observation that both *COL1A1* (with 19% proline/total residues) and FN1 (fibronectin; with 7.9% proline/total residues) can be blocked by HF treatment [22] suggests that glutamyl-prolyl-tRNA synthetase (EPRS) may have roles beyond its translational tRNA charging activity. Limiting amino acids or inhibition of any of the aminoacyl-tRNA synthetases in animals activates the amino acid response (AAR) pathway after the accumulation of uncharged tRNAs is sensed and eukaryotic translation initiation factor 2 α (eIF2 α) is phosphorylated by GSN2 kinase [70]. These processes lead to decreased global protein synthesis [71] and induction of selected genes including activating transcription factor 4 (ATF4). ATF4 can then activate downstream genes to mediate the adaptation of cells to a stress environment, including C/EBP-homologous protein (CHOP, also known as DDIT3) [72]. Thus, ATF4 protein expression consequently activates multiple stress-induced genes, including AAR elements [73].

TGF β 1 is a multifunctional cytokine that plays major roles in the initiation and progression of fibrogenesis and is the molecular basis of organ fibrosis [76]. In fibroblasts from human patients, treatment with HF reduces TGF β 1-mediated collagen synthesis [77] without altering TGF β receptor gene expression or TGF β levels [78], indicating that HF targets downstream of TGF β receptor 1 (TGF β R1). HF can also target the signaling activity of SMAD3 and other molecules in different cell types [75]. Furthermore, HF prevents the differentiation of Th17 cells, which are a subset of CD4⁺ T cells that express interleukin (IL)-17. This occurs when HF binds to EPRS and induces the accumulation of uncharged tRNA and the activation of the AAR pathway, and leads to the inhibition of autoimmune inflammation [79]. Human glutamyl-tRNA synthetase (ERS) and prolyl-tRNA synthetase (PRS) activities are contained within a single

polypeptide chain [80]. Because of its poor oral bioavailability, gastrointestinal (GI) toxicity, and limited patent life, the development of HF as an anti-fibrotic drug has been hindered [74]. Many of its side effects may be due to its inhibition of TGF β /SMAD3 signaling, which is important for homeostatic immune and inflammatory functions [34, 75]. Thus, the role of EPRS in the development of fibrosis, especially with regard to HF, requires further exploration.

In this study, I have focused on the mechanistic roles of EPRS in TGF β 1-mediated fibrosis. My findings revealed relationships between EPRS and STAT6 during TGF β 1-mediated ECM production in LX2 HSCs and CCl₄-mediated liver fibrosis.

1.2. MATERIALS AND METHODS

Reagents and plasmids

All cytokines and growth factors, including TGF β 1, were purchased from Peprotech (Rocky Hill, NJ, USA). Halofuginone, CCl₄, ascorbic acid, PSS [Poly(sodium 4-styrenesulfonate) solution, 200 kDa, 30 wt. % in H₂O], and the hydroxyproline assay kit were purchased from Sigma-Aldrich (St. Louis, MO, USA). EPRS specific inhibitors, DWN 10290, DWN 10620, DWN 10624, DWN 10993, DWN 11157, and DWN 11158, were gifts from Daewoong Pharm. CO., Ltd. (Seoul, Korea). Target-specific pooled siRNAs (siSTAT3 and siSTAT6) were purchased from Santa Cruz Biotechnology (Dallas, TX, USA). EPRS and its S999A mutant in pEXPR-103-Strep vector (IBA Lifesciences, Goettingen, Germany) were gifts from Dr. Myung Hee Kim at the Korea Research Institute of Bioscience and Biotechnology (KRIBB). The PRS domain of EPRS was cloned into the pEXPR-103-Strep vector (IBA Lifesciences, Goettingen, Germany). The generation of pRc/CMV-WT STAT3 was previously reported [81], and pCMV-STAT6-IRES-Neo was a gift from Axel Nohturfft (Addgene plasmid # 35482). Adenoviruses expressing SMAD2 or SMAD3 were explained in a previous study [82].

Cell culture

LX2 HSCs were a kind gift from Dr. Scott Friedman (Mount Sinai School of Medicine, NY, USA), and HFF cells were a kind gift from Dr. Jin Ho Chung (Seoul National University, Seoul, Korea). Cells were cultured in Dulbecco's Modified Eagle Medium (SH30243.01, Hyclone, South Logan, UT, USA). All media were supplemented with 10% fetal bovine serum (GenDEPOT, Barker, TX, USA) and 1% penicillin/streptomycin (GenDEPOT) and all cells were grown at 37°C in 5% CO₂. The SMARTvector shEPRS doxycycline-inducible knock-down cell line was established by treating lentiviral particles (EPRS mCMV-turboGFP

V2IHSMCG_687815, 687823, Dharmacon, Lafayette, CO, USA). Positive clones were enriched by treatment with 2 µg/ml puromycin (GenDEPOT) and maintained in complete media supplemented with 1 µg/ml puromycin. The siRNAs or cDNA plasmids were transiently transfected using Lipofectamine RNAiMAX or Lipofectamine 3000, respectively, following the manufacturer's instructions (Thermo Fisher Scientific, Waltham, MA, USA).

Western blot analysis

Subconfluent cells or animal tissues were harvested for whole-cell or tissue extracts using radioimmunoprecipitation assay buffer. Lysates were separated in Tris-Glycine sodium dodecyl sulfate (SDS)-polyacrylamide gel at concentrations ranging from 8 to 12%, after which they were transferred to nitrocellulose membranes (Thermo Fisher Scientific). Target-specific antibodies used in this study are summarized in table 1. The resulting western blot images were quantified using ImageJ software (version 1.50b, NIH, USA). Quantitated values were normalized using either loading control or their total forms. The values were displayed under the images.

ECM deposition assay and collagen footprint assay

Control or shEPRS cells were grown on glass coverslips and treated with TGFβ1 or vehicle. Following treatment, cells were washed in cold PBS, fixed in 4% formaldehyde in PBS, washed in PBS, and blocked in 5% bovine serum albumin (BSA) in PBS. Without permeabilization, cells were incubated with collagen I or fibronectin antibody (supplementary table S1) overnight at 4°C, followed by an Alexa Fluor 488-conjugated secondary anti-rabbit IgG antibody (Thermo Fisher Scientific). Antibodies were diluted in 5% BSA. DAPI (4',6-Diamidino-2-Phenylindole) was used to stain nuclei. Immunofluorescent images were acquired on a fluorescence microscope (BX51TR, Olympus, Tokyo, Japan) or a confocal laser scanning

microscope (Nikon C2, Nikon, Tokyo, Japan), as previously described [83]. The fluorescence intensity was measured using ImageJ software (version 1.50b, NIH, USA). The collagen footprint assay was conducted as previously described [84]. Briefly, collagen deposition was first facilitated by treating cultured cells with ascorbic acid and PSS with or without TGF β 1. On the next day, the cells were washed with ice-cold PBS and lysed with 0.5% deoxycholate in PBS at 4°C with gentle agitation. The remaining collagen debris (footprint) was either immunostained for visualization or collected with 2 \times SDS-PAGE sample buffer and heated at 95°C for 5 min. The collagen footprint was analyzed according to the conventional western blotting method.

Quantitative reverse-transcription (qRT) PCR

Cells were infected or transfected to suppress the indicated genes for 24 h or 48 h. Total RNA from animal tissues, cells, or 3D organoids were isolated using Qiazol Reagent (Qiagen, Hilden, Germany), and their cDNAs were synthesized using amfiRivert Platinum cDNA synthesis master mix (GenDEPOT) according to the manufacturer's instructions. Quantitative qRT-PCR was performed with LaboPass™ EvaGreen Q Master (Cosmo Genetech, Seoul, Korea) and with the CFX Connect™ Real-Time PCR (Bio-Rad, Hercules, CA, USA). The mRNA levels were normalized against glyceraldehyde 3-phosphate dehydrogenase (GAPDH) and the CFX Maestro™ software (Sunnyvale, CA, USA) was used to analyze the data. Primers were purchased from Cosmo Genetech (Seoul, Korea). The primer sequences are shown in table 1. 2.

Co-immunoprecipitation

Whole-cell lysates were prepared using IP lysis buffer (40 mM HEPES pH7.4, 150 mM NaCl, 1 mM EDTA, 0.5% Triton X-100) and precipitated with Pierce High-Capacity Streptavidin

Agarose (Thermo Fisher Scientific) overnight at 4°C. Precipitates were washed three times with ice-cold lysis buffer and three times with IP wash buffer (40 mM HEPES pH 7.4, 500 mM NaCl, 1 mM EDTA, 0.5% Triton X-100), after which they were boiled in 2× SDS-PAGE sample buffer before immunoblotting.

Luciferase assay

To analyze the promoter activity, *LAMC2* (laminin $\gamma 2$) promoters (encoding regions of -1871 to +388) and *COL1A1* (collagen I $\alpha 1$) promoters (encoding regions of -2865 to +89) were amplified by PCR and cloned into the pGL3-basic vector. LX2 cells were seeded in 48 well plates and then transfected with plasmids using the Lipofectamine 3000 transfection reagent (Thermo Fisher Scientific) on the next day. β -Gal was co-transfected for normalization. One day after transfection, 2 ng/ml TGF β 1 was added to the culture media. After 24 h, luciferase activity was measured using the luciferase reporter assay kit (Promega, Madison, WI, USA) with a luminometer (DE/Centro LB960, Berthold Technologies, Oak Ridge, TN, USA), according to the manufacturer's instructions.

Animal experiments

WT *Eprs*^{+/+} and *Eprs*^{-/+} hetero-KO C57BL/6 mice were housed in a specific pathogen-free room with controlled temperature and humidity. Mouse protocols and animal experiments were approved by the Institutional Animal Care and Use Committee (IACUC) of Seoul National University (SNU-161201-1-3). To induce hepatic fibrosis in mice, CCl₄ treatment and bile duct ligation (BDL) methods were used. For the CCl₄-mediated liver fibrosis model, WT and *Eprs*^{-/+} mice aged 7 weeks ($n \geq 5$) were injected intraperitoneally with or without CCl₄ (Sigma-Aldrich, 1 mg/kg) in 40% olive oil once a week for 5 weeks. For BDL method, WT and *Eprs*^{-/+} mice aged 10 weeks ($n = 4$) were anesthetized with isoflurane and through a midline incision,

bile duct was isolated and doubly ligated according to the previous report [85]. Control animals were sham operated. After 5 weeks, mice were sacrificed and serum and tissue samples were collected for further analysis. Liver samples from both CCl₄-treated and BDL mice were either snap frozen in liquid nitrogen for western blot, qRT-PCR, and hydroxyproline analyses, or fixed in 4% formaldehyde in PBS for histological analyses. Serum ALT, AST and ALP levels were measured with their respective detection slides using DRI-Chem 3500i blood analyzer (FUJIFILM, Tokyo, Japan).

Liver organoid culture

Mouse liver organoids were prepared from WT or *Eprs*^{-/+} mice. Mouse livers were chopped and lysed in digestion solution containing collagenase and dispase II and isolated ducts were collected by hand under a microscope, as described previously [86]. Collected ducts were seeded onto 3D Matrigel (Corning, NY, USA, 10 µg/ml). Cells were supplemented with culture media containing specific growth factors, as described previously [86]. After 2-3 passages, organoids were differentiated. Differentiated or non-differentiated organoids were treated with 2 ng/ml TGFβ1 for 1 day and harvested for qRT-PCR analysis.

Immunohistochemistry and staining

Paraffin blocks and liver tissue sections were prepared by Abion Inc. (Seoul, Korea). The sections were subjected to immunohistochemistry analysis. Primary antibodies and their dilution ratios are listed in supplementary table S1. The vectastain ABC-HRP kit (Vector Laboratories, CA, USA) was used to visualize the stained samples. Mayer's hematoxylin (Sigma-Aldrich) was used for counter-staining the nuclei. Masson's trichrome staining was performed by Abion Inc. (Seoul, Korea). Fibrosis stage was determined according to METAVIR classification separately by two independent scientists.

Statistics: Statistical analyses were performed using the Prism software (version 7.0, GraphPad, La Jolla, CA). Two-way ANOVA in group analyses or Student's *t*-tests were performed to determine statistical significance. $P < 0.05$ was considered statistically significant.

Table 1. 1. Antibodies and their dilution ratio used in Chapter 1.

Name	Company	Catalog	WB dil.	IHC dil.
EPRS	Neomics	NMS-01-0004	1:5000	1:200
Fibronectin	DAKO	A0245	1:5000	1:200
Collagen I	Acris	R1038X	1:1000	1:200
β -actin	Abcam	AB133626	1:1000	
pY641-STAT6	Abcam	AB28829	1:1000	1:100
Total-STAT6	Cell Signaling Technology	#9362	1:1000	
pY705-STAT3	Abcam	AB76315	1:1000	
pY705-STAT3	Cell Signaling Technology	#9145		1:200
Total-STAT3	Santa Cruz Biotechnology	SC-482	1:1000	
pS465/467-SMAD2	Cell Signaling Technology	#3108	1:1000	1:100
Total-SMAD2	Cell Signaling Technology	#5339	1:1000	
pS423/425-SMAD3	Cell Signaling Technology	#9520	1:1000	
Total-SMAD3	Cell Signaling Technology	#9523	1:1000	
TGF β -receptor1	Santa Cruz Biotechnology	SC-399	1:500	
JAK1	Cell Signaling Technology	#3344	1:1000	
JAK2	Millipore	04-001	1:1000	
Total-STAT1	Santa Cruz Biotechnology	SC-346	1:1000	
Total-STAT5	Santa Cruz Biotechnology	SC-835	1:1000	
KRS	Neomics	NMS-01-0005	1:2000	
pT202/Y204-Erk	Cell Signaling Technology	#9101	1:1000	
Erk	Cell Signaling Technology	#9102	1:1000	
Anti-Strep	IBA life Sciences	2-1509-001	1:2500	
Alpha-SMA	Sigma	A2547	1:1000	1:200
Snail	Cell Signaling Technology	#3895	1:1000	
Laminin gamma2	Santa Cruz Biotechnology	SC-28330		1:200
Laminin	Abcam	AB11575	1:1000	
Ki67	Abcam	AB15580		1:200

Table 1. 2. qRT-PCR primers used in Chapter 1.

Gene name	Forward	Reverse	Size (bp)
Human <i>EPRS</i>	AGGAAAGACCAACACC TTCTC	CTCCTTGAACAGCCACTC TATT	87
Human <i>KRS</i>	GAGAAGGAGGCCAAAC AGAA	CTCAGGACCCACACCATT ATC	99
Human <i>GRS</i>	ATCTACCTCTACCTCAC GAAGG	CCCAACAGTCACAGGCAT AA	100
Human <i>LRS</i>	TGCCAGCTAAAGGGAA GAAG	GTAGAACAGACAGGGTGG TATG	114
Human <i>Collagen1A1</i> (<i>COL1A1</i>)	CAGACTGGCAACCTCA AGAA	CAGTGACGCTGTAGGTGA AG	97
Human <i>CHOP</i> (<i>DDIT3</i>)	GAGATGGCAGCTGAGT CATT	TTTCCAGGAGGTGAAACA TAGG	134
Human <i>Collagen1A2</i> (<i>COL1A2</i>)	AGAGTGGAGCAGTGGT TACTA	GATACAGGTTTCGCCAGT AGAG	100
Human <i>Collagen4A1</i> (<i>COL4A1</i>)	CGGGCCCTAAAGGAGA TAAAG	GAACCTGGAAACCCAGGA AT	115
Human <i>Fibronectin 1</i> (<i>FN1</i>)	CCACAGTGGAGTATGTG GTTAG	CAGTCCTTTAGGGCGATC AAT	104
Human α -SMA (<i>ACTA2</i>)	GATGGTGGGAATGGGA CAAA	GCCATGTTCTATCGGGTAC TTC	94
Human <i>Laminin γ2</i> (<i>LMAC2</i>)	CTCAGGAGGCCACAAG ATTAG	TGAGAGGGCTTGTTTGGA ATAG	101
Mouse <i>Eprs</i>	AAGCGGAAAAGGCTCC TAAG	CCCAGTCTTTTCTTTATAC TCAGCTT	85
Mouse <i>Albumin</i>	GACCAGGAAGTGTGCA AGAA	CAAGTCTCAGCAACAGGG ATAC	115
Mouse <i>Collagen 1A1</i> (<i>Colla1</i>)	AGACCTGTGTGTTCCCT ACT	GAATCCATCGGTCATGCTC TC	113
Mouse <i>Fibronectin 1</i> (<i>Fn1</i>)	TCCTGTCTACCTCACAG ACTAC	GTCTACTCCACCGAACAA CAA	96
Mouse <i>Laminin γ2</i> (<i>Lmac2</i>)	TGGAGTTTGACACGGAT AAGG	GAGTGTGTCTTGGATGGT AACT	104

1.3. RESULTS

Inhibition or suppression of EPRS in LX2 HSCs decreased the production and deposition of ECMs under TGF β 1 signaling

To investigate whether EPRS could regulate the expression of different ECMs including collagen I and fibronectin, a SMARTvector shEPRS doxycycline-inducible knock-down LX2 cell line was established by treatment with lentiviral particles. shCont or shEPRS LX2 cells were treated with EPRS specific inhibitors, DWN compounds. Cells were harvested and immunoblotted for Fibronectin. The expression level of fibronectin was down regulated dose-dependently for DWN 10620, 10624, 10993, 11157, and 11158 compounds.

Next, shCont or shEPRS LX2 cells were tested for following conditions. Cell extracts were immunoblotted for mesenchymal markers of active HSCs and ECMs. Suppression of EPRS did not cause cell death, presumably because the suppression was not complete and residual levels of EPRS were sufficient for other homeostatic functions, such as cell survival and proliferation that would be favored by new proteins synthesized by its proline charging to prolyl-tRNA (data not shown). TGF β 1 treatment resulted in enhanced expression of Snail1, α -smooth muscle actin (α -SMA), fibronectin, and collagen I; this was abolished by suppression of EPRS (Fig. 1. 2A). In contrast, overexpression of the PRS domain of EPRS alone in LX2 cells promoted basal ECM expression, which was further upregulated upon TGF β 1 treatment (Fig. 1. 2B). These data suggest that EPRS can upregulate ECM expression in active LX2 HSCs.

In addition to *EPRS* mRNA levels, mRNA levels for diverse ECM chains, including *COL1A1*, *COL1A2*, *COL4A1*, *FNI*, and *ACTA2* were upregulated by TGF β 1 treatment; this TGF β 1-mediated increase in the ECM chain expression was partially blocked by suppression of EPRS (Fig. 1. 2C). Interestingly, *LAMC2* mRNA levels were enhanced by TGF β 1 but not further blocked by EPRS suppression, suggesting that the laminin γ 2 chain may be regulated

via other signaling pathway(s) and/or in different cell types. Furthermore, different levels of ECM chains were abolished by HF treatment both in EPRS-intact and EPRS-suppressed cells; However, *DDIT3* (also known as *CHOP*) mRNA expression was enhanced by EPRS suppression and further promoted by HF treatment, indicating an involvement of the AAR pathway (Fig. 1. 2C). TGF β 1 had no effect on *DDIT3* mRNA levels. At the protein level, HF treatment abolished TGF β 1-mediated and EPRS-dependent collagen I and fibronectin expression, which was partially rescued by supplementation with additional proline (Fig. 1. 2D, lanes 3, 4, 7, 8, 11, and 12). In addition to the EPRS-dependent ECM proteins, Smad2/3 phosphorylation and pY⁶⁴¹STAT6 levels with or without TGF β 1 treatment were generally abolished by HF treatment but were also partially rescued by additional proline supplementation and HF treatment (Fig. 1. 2D). *COL1A1* and *FNI* mRNA levels also changed similarly under the same experimental conditions (Fig. 1. 2E). However, the TGF β 1-mediated protein and mRNA levels of the ECMs after HF and proline treatment were still lower than those in cells treated with TGF β 1 alone whether EPRS level and/or activity was modulated or not (Fig. 1. 2D; lanes 3, 4, 7, 8, 11, and 12, Fig. 1. 2E; graphic bars 3, 4, 7, and 8). These data suggest that EPRS plays a unique role in ECM production in addition to its tRNA-charging activity, although other molecules may also be involved in STAT-mediated ECM induction. Thus, EPRS might transcriptionally regulate the expression of collagen type I and fibronectin, but may not significantly regulate the expression of laminin γ 2.

We next examined whether suppression of other aminoacyl-tRNA synthetases could be involved in the regulation the ECM expression via analysis of the AAR pathways. Suppression of lysyl-tRNA synthetase (*KRS*), glycyl-tRNA synthetase (*GRS*), or leucyl-tRNA synthetase (*LRS*) led to an increase in *ACTA2* mRNA upon TGF β 1 treatment to a level similar to non-suppressed control LX2 cells. However, *KRS*-suppressed cells had *DDIT3* mRNA levels that

were unchanged despite of TGF β 1 treatment compared with control cells, whereas *GRS* or *LRS* suppression increased *DDIT3* levels (Fig. 1. 3A and 1. 2B). In addition, the mRNA levels of diverse ECM chains were unchanged by suppression of any of the aminoacyl-tRNA synthetases, although TGF β 1 treatment promoted ECM production independent of aminoacyl-tRNA suppression (Fig. 1. 3C). Therefore, EPRS appeared to be involved in ECM production via proline-tRNA charging and non-translational mechanisms, specifically.

Next, I examined whether the EPRS level could affect the extracellular deposition and transcriptional induction of collagen I and fibronectin. Collagen I and fibronectin staining in the extracellular space of LX2 cells was more apparent upon TGF β 1 treatment, whereas suppression of EPRS reduced the intensity of extracellular collagen I and fibronectin staining (Fig. 1. 2F). Furthermore, results from immunoblotting of the conditioned media (CM) of the cells showed that suppression of EPRS reduced collagen I levels and foot-print collagen I (i.e., extracellularly deposited collagen I) (Fig. 1. 2G). These observations demonstrate that EPRS upregulated collagen and fibronectin.

Additionally, the effects of EPRS expression on the regulation of ECM expression were examined using primary human foreskin fibroblasts (HFFs). TGF β 1 treatment upregulated *COL1A1* mRNA levels, and suppression of EPRS reduced *COL1A1* mRNA levels, compared with control HFFs (Fig. 1. 4A). HF treatment decreased TGF β 1-mediated *COL1A1* mRNA levels compared with non-HF-treated conditions (Fig. 1. 4A). Again, *DDIT3* mRNA levels were increased by HF treatment suggesting activation of the AAR pathway (Fig. 1. 4A). Collagen I deposition outside of HFFs was much higher in EPRS-expressing parental cells than in EPRS-suppressed HFFs (Fig. 1. 4B-D). These results suggest that the up-regulatory effect of EPRS on ECM production and deposition can be applied to different types of mesenchymal cells.

EPRS-mediated transcriptional regulation of ECMs involved STAT6 activation

Next, I examined which signaling pathways or molecules could be involved in the EPRS-mediated ECM up-regulation upon TGF β 1 treatment. Because TGF β 1-mediated signaling transduces canonical SMAD-mediated signaling and non-canonical pathways, I explored molecules that are involved in both pathways. Among the molecules I tested, STATs appeared to be involved in the effects of TGF β 1; TGF β 1 treatment promoted the phosphorylation of STAT6 at Tyr641 (i.e., pY⁶⁴¹STAT6), and this was abolished by EPRS suppression. In contrast, phosphorylation of STAT3 at Tyr705 (i.e., pY⁷⁰⁵STAT3) decreased upon EPRS suppression and was slightly reduced by TGF β 1 treatment (Fig. 1. 5A). pY⁷⁰⁵STAT3 was promoted by PRS expression but was inactivated by TGF β 1 stimulation in LX2 cells, whereas pY⁶⁴¹STAT6 was increased by PRS overexpression or TGF β 1 stimulation (Fig. 1. 5B). In addition, I assessed whether STAT6 overexpression could promote the expression of basal or TGF β 1-mediated ECMs in an EPRS-dependent manner. Overexpression of STAT6 in EPRS-suppressed cells could not recover basal and TGF β 1-mediated pY⁶⁴¹STAT6, fibronectin expression, and collagen I expression levels to the levels of cells with intact EPRS expression (Fig. 1. 5C). Meanwhile, suppression of STAT6 decreased basal and TGF β 1-mediated fibronectin and collagen I expression (Fig. 1. 5D). Thus, although sensitive to STAT6 expression, basal and TGF β 1-mediated ECM expression in LX2 cells appeared to depend primarily on EPRS expression. Meanwhile, overexpression of STAT3 did not result in a proportional relationship between pY⁷⁰⁵STAT3 and basal or TGF β 1-mediated collagen I expression (Fig. 1. 5E), suggesting that STAT3 might be irrelevant to EPRS-dependent ECM production in TGF β 1-treated LX2 cells. Additionally, activation of STAT molecules using known cytokines, IL13 and IL6, were tested (Fig. 1. 5F). Although it have been shown that suppression of STAT6 resulted in down-regulation of ECM, phosphorylation of IL13 did not enhance ECM expression.

Thus, the sole activation of STAT3 or STAT6 molecules could not trigger expression of ECM. Accordingly, it could be suggested that activation of both SMAD3 and STAT6 by TGF β 1 may be required for expression of ECM.

Interestingly, the transcriptional activity of the *COL1A1* promoter with STATs-responsive consensus elements in LX2 cells was significantly upregulated by TGF β 1 treatment, but this effect was reduced with EPRS-suppression (Fig. 1. 5G, left). However, TGF β 1 treatment did not induce significant increases in *LAMC2* promoter activity, which was still abolished by EPRS suppression (Fig. 1. 5G, right). Data gathered via qRT-PCR assays revealed that *LAMC2* mRNA levels were increased \sim 2-fold by TGF β 1 but not significantly inhibited by EPRS suppression (Fig. 1. 2C). This discrepancy may be due to either the effects at smaller fold changes (as shown in Y axis values) or different cell types; indeed, I have observed that *LAMC2* expression changed more significantly in hepatocytes than in LX2 or HSCs (unpublished observation). To examine whether STAT6 was important for the EPRS-dependent transcriptional regulation of ECM chains, LX2 cells with or without STAT6 suppression were treated with vehicle or TGF β 1 prior to qRT-PCR analysis. *COL1A1*, *COL1A2*, *COL4A1*, *FNI*, and *ACTA2* mRNA levels were upregulated by TGF β 1 treatment. Suppression of STAT6 alone was not as effective as suppression of EPRS alone, and suppression of both EPRS and STAT6 was only as effective as EPRS suppression alone. Further, when treated with TGF β 1, EPRS-intact control cells decreased ECM mRNA levels upon additional STAT6 suppression whereas EPRS-suppressed cells did not show any changes in ECM mRNA levels. These data thus suggest that EPRS could be upstream of STAT6 in TGF β 1-mediated ECM expression (Fig. 1. 5H). Therefore, *LAMC2* levels were regulated by EPRS expression but were not significantly modulated by TGF β 1 and/or STAT6 (Fig. 1. 5H).

EPRS-mediated signaling occurred downstream of TGFβ1

We investigated how the canonical TGFβ1-mediated SMAD signaling pathway was involved in EPRS-dependent ECM expression. TGFβ1-mediated SMAD2 and SMAD3 phosphorylation was partially inhibited by EPRS suppression (Fig. 1. 6A). Overexpression of the PRS domain, alone, increased basal SMAD3 phosphorylation to a saturated level that was not increased by further TGFβ1 treatment (Fig. 1. 6B). In addition, TGFβ1-mediated pY⁶⁴¹STAT6 was significantly increased by overexpression of SMAD3 but not of SMAD2, and this was abolished by EPRS suppression (Fig. 1. 6C).

Next, I examined whether TGFβ1-mediated signaling molecules could be involved in the phosphorylation of STATs, especially STAT6, presumably through protein-protein complexes, in an EPRS expression-dependent manner. LX2 cells were transfected with strep-tagged EPRS and treated with or without TGFβ1 for different periods of time. Whole-cell extracts were then prepared and precipitation was conducted using streptavidin agarose beads for immunoblotting. Strep-EPRS was precipitated together with TGFβR1, JAKs, and STATs, including STAT6, in a transient manner upon TGFβ1 treatment. Lysyl-tRNA synthetase (KRS), but not ERKs, was co-precipitated constitutively (Fig. 1. 6D). Because EPRS and KRS are members of the multi-aminoacyl-tRNA synthetase complex (MSC) [87], binding of EPRS to KRS was expected. The binding of strep-EPRS to the molecules was dependent on STAT6 expression, with the exception of KRS (Fig. 1. 6E). In addition, endogenous EPRS and TGFβ1-mediated pY⁶⁴¹STAT6 could co-immunoprecipitate each other and TGFβR1 was found also in the immunoprecipitates (Fig. 1. 6F). Furthermore, a point mutation in EPRS Ser999A that does not allow EPRS to dissociate from the MSC [67] maintained the ability of EPRS to form a protein complex with TGFβR1, SMAD3, JAKs, and STAT6 (Fig. 1. 6G). Given the dynamic

dimerization among STATs [88], the TGF β R1-STAT6 complex could potentially include other STATs.

***In vivo* liver tissues from fibrotic mice showed EPRS-dependent STAT6 phosphorylation and ECM production**

To investigate the physiological roles of EPRS in *in vivo* animal models of liver fibrosis, normal wildtype (WT; *Eprs*^{+/+}) and *Eprs*^{-/+} hetero-knockout (KO) mice were treated with CCl₄. Expression of ECMs, including fibronectin, collagen I, and laminins, increased in WT mice with CCl₄ treatment, compared with untreated mice (Fig. 1. 7A). However, CCl₄ treatment of *Eprs*^{-/+} mice showed less-significant increases in fibronectin and collagen I expression without affecting laminin levels; (Fig. 1. 7A). Concomitantly, pY⁶⁴¹STAT6 was increased in WT mice upon CCl₄ treatment, compared with *Eprs*^{-/+} mice (Fig. 1. 7A). Meanwhile, α -SMA levels, pY⁷⁰¹STAT1, and pY⁷⁰⁵STAT3 were not dependent on EPRS expression and pY⁶⁹⁴STAT5 level was not affected by EPRS expression (Fig. 1. 7A). These observations, again, suggest that EPRS-dependent ECM expression may involve STAT6 activation. Furthermore, CCl₄-treated WT mice showed higher amounts of collagen I in liver extracts compared to CCl₄-treated *Eprs*^{-/+} mice (Fig. 1. 7B). CCl₄ treatment of *Eprs*^{+/+} or *Eprs*^{-/+} mice increased Ki67 levels as measured by immunostaining, although the amount of Ki67 in *Eprs*^{-/+} mice livers might be comparable to, or slightly lower than, that of *Eprs*^{+/+} mice livers (Fig. 1. 7C), indicating that heterozygous knockout of *Eprs* did not significantly affect cell proliferation after CCl₄ treatment. Consistently, the mRNA levels of *Colla1*, *Fn1*, *Lamc2*, and *Acta2* were dramatically upregulated by CCl₄ treatment in the livers of WT mice. CCl₄ treatment did not show significant effects in the livers of *Eprs*^{-/+} mice (Fig. 1. 7D).

We then analyzed the liver tissues by immunostaining for different molecules. CCl₄ administration to *Eprs*^{+/+} control mice showed septal fibrosis or cirrhosis with intense collagen I deposition or α -SMA/HSC activation along septa (F3 and F4 of METAVIR score). In WT mice, treatment with CCl₄ increased collagen I deposition, as visualized using Masson's trichrome staining. Activation of α -SMA (presumably in HSCs) staining along scars, pY⁶⁴¹STAT6 stains at nuclear regions, and laminin γ 2 immunostaining were also enhanced (Fig. 1. 7E). Mice without CCl₄ treatment did not show the fibrotic phenotypes (F0 of METAVIR score). However, CCl₄ treatment of *Eprs*^{-/+} hetero-KO mice led to delayed or less-developed fibrotic phenotypes of portal fibrosis with few septa (F2 of METAVIR score) (Fig. 1. 7E), suggesting that CCl₄-mediated fibrotic phenotypes in livers are EPRS dependent. In addition, laminin γ 2 immunostains could be differentiated from collagen I stains suggesting that different cell types might be involved.

Alternatively, I also adapted the liver fibrosis model using a bile duct ligation (BDL) approach. Wildtype *Eprs*^{+/+} and *Eprs*^{-/+} mice were processed to BDL operation. Five weeks later, analysis showed that BDL increased the activity of aspartate transaminase (AST), alanine transaminase (ALT), and alkaline phosphatase (ALP), in animal sera (Fig. 1. 8A). The levels of AST and ALT, which are indicative of fibrotic liver damage, were significantly higher in the *Eprs*^{+/+} BDL mice, compared with *Eprs*^{-/+} mice. However, ALP activity levels did not show significant changes between *Eprs*^{+/+} and *Eprs*^{-/+} mice after BDL. Whereas *Eprs*^{+/+} showed enhanced fibronectin expression and pY⁶⁴¹STAT6 levels after BDL, *Eprs*^{-/+} mice showed much reduced ECM expression and pY⁶⁴¹STAT6 levels (Fig. 1. 8B). In addition, *Acta2*, *Colla1*, and *Fnl* mRNA levels were less increased by BDL in liver tissues of *Eprs*^{-/+} mice, compared with those of *Eprs*^{+/+} mice (Fig. 1. 8C). Further, immunohistochemistry and Masson's trichrome staining for collagen I synthesis showed that BDL of *Eprs*^{+/+} mice led to increases in α -SMA,

pY⁶⁴¹STAT6, and collagen I, as well, whereas BDL of *Eprs*^{-/+} mice showed less of the effect; BDL of *Eprs*^{+/+} mice resulted in severe fibrotic levels (F3 of METAVIR score) but BDL of *Eprs*^{-/+} mice resulted in F2 fibrotic level, although all control mice (without BDL) showed no phenotype (F0 of METAVIR score) (Fig. 1. 8D). This alternative model of liver fibrosis showed that EPRS could play an important role in hepatic fibrogenesis.

Liver organoids in a three-dimensional (3D) Matrigel system revealed EPRS-dependent regulation of ECM induction

Lastly, I prepared liver organoids from ductal stem cells of WT and *Eprs*^{-/+} mice and used 3D Matrigels to examine EPRS-dependent ECM induction. Differentiated liver organoids showed increased *albumin* (*Alb*) mRNA, which is an indicator of hepatocyte differentiation. TGFβ1 treatment reduced *Alb* mRNA levels and increased *Fn1* mRNA levels. In contrast, *Eprs*^{-/+} liver organoids showed lower *Fn1* levels and *Alb* mRNA levels were unchanged (Fig. 1. 9A). Although *Eprs* mRNA expression was not important for the liver organoid growth and TGFβ1-mediated differentiation, *Fn1* mRNA levels were greatly dependent on *Eprs* expression and TGFβ1 treatment (Fig. 1. 9A). *Colla1* mRNA expression did not significantly depend on *Eprs* expression, although *Lamc2* mRNA levels appeared slightly dependent on TGFβ1 treatment and *Eprs* expression (Fig. 1. 9B). Similar to my finding in LX2 cells and mouse models, the TGFβ1-mediated transcriptional induction of fibronectin depended on EPRS expression. However, collagen I expression was dependent on EPRS in LX2 cells and animal models, but not in liver organoids.

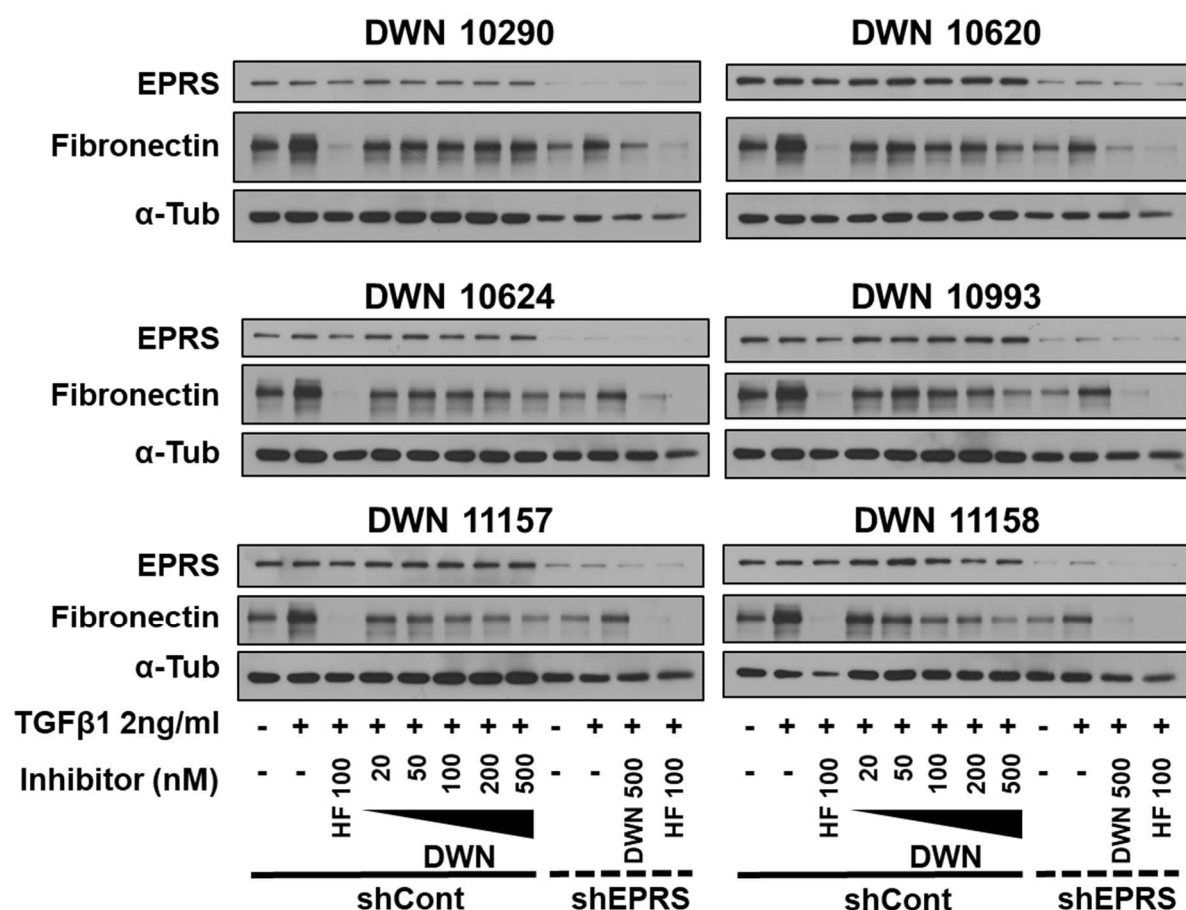
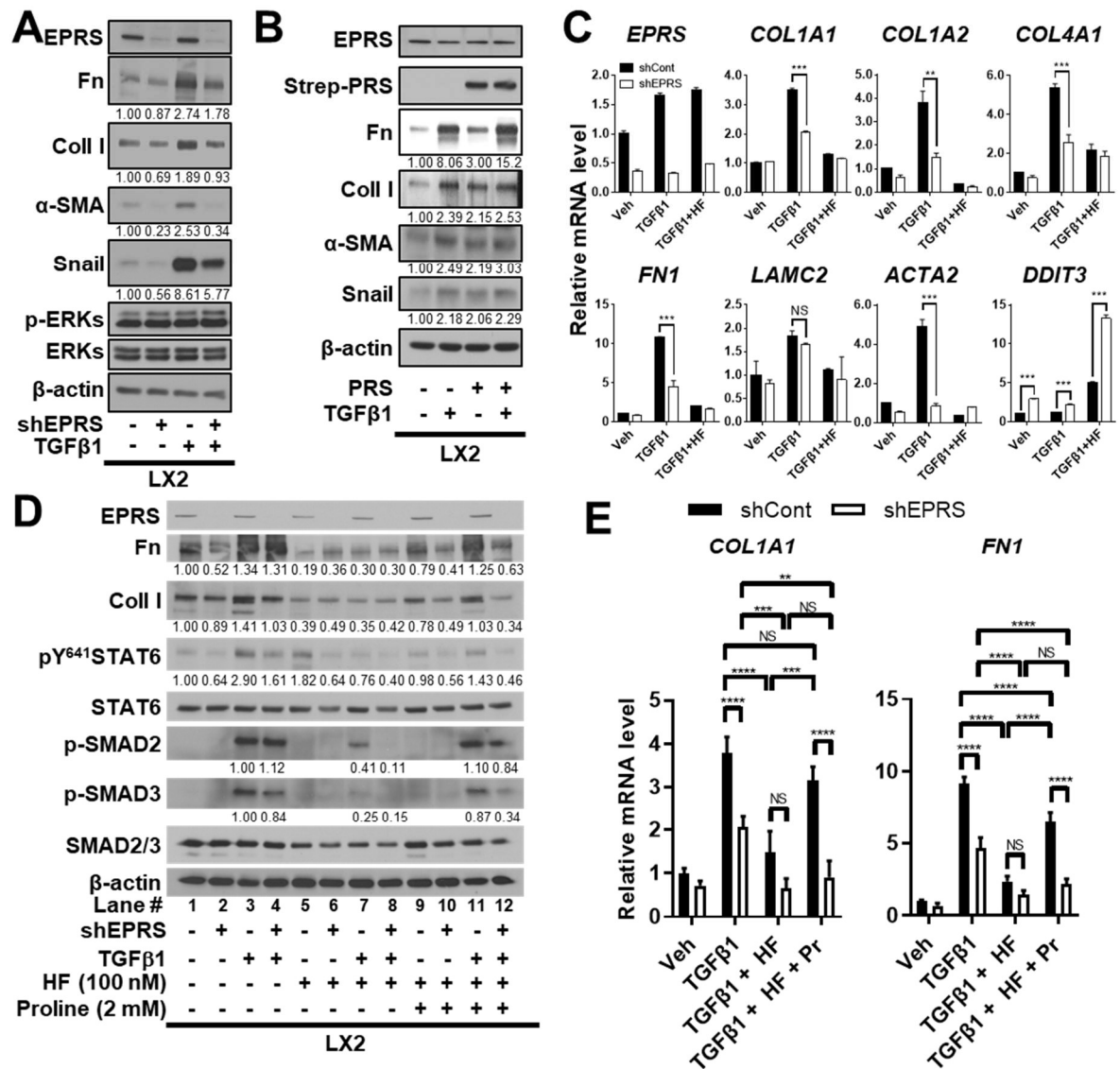


Figure 1. 1. EPRS specific inhibitors can dose dependently down-regulate expression of fibronectin. shCont or shEPRS LX2 cells were treated with EPRS specific inhibitors, DWN compounds. Cells were harvested and immunoblotted for the indicated molecules.



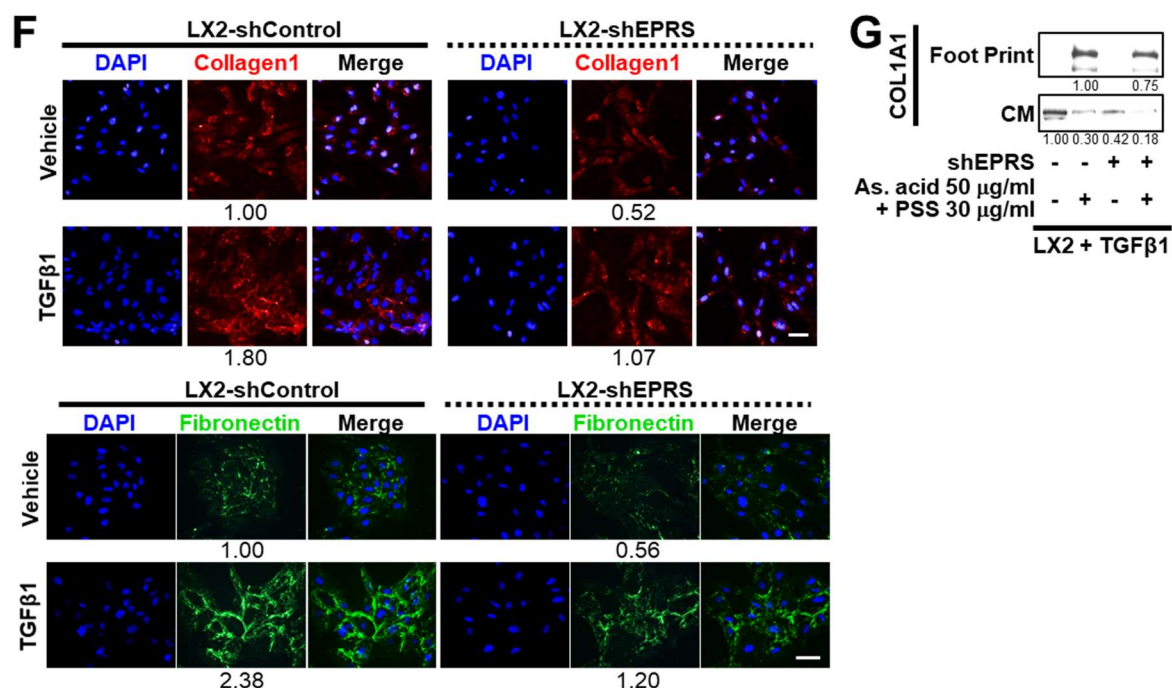


Figure 1. 2. EPRS promotes expression of extracellular matrix (ECM) chains. (A and B) Control LX2 cells, shEPRS doxycycline-inducible knock-down LX2 cell (LX2-shEPRS), or PRS expression vector-transfected LX2 (pEXPR-103-Strep-PRS) cells were harvested prior to immunoblotting for the indicated molecules. (C) Subconfluent control or shEPRS-LX2 cells were treated with TGFβ1 (2 ng/ml) with or without halofuginone (HF; 100 nM) for 24 h, before qRT-PCR analysis. Data are presented as mean ± standard deviation (SD). NS indicates non-significance. *, **, and *** depict statistical significance of $p < 0.05$, 0.01, and 0.001, respectively, according to the Student's t -test. (D and E) Control LX2 or shEPRS-LX2 cells were treated with TGFβ1, HF (100 nM), and/or proline (2 mM) for 24 h, prior to preparation of whole-cell extracts for immunoblotting (D) or qRT-PCR (E) for the indicated molecules. NS indicates non-significance. *, **, ***, and **** depict statistical significance of $p < 0.05$, 0.01, 0.001, and 0.0001 respectively, according to the two-way ANOVA analysis. (F) LX2 (LX2-shControl or LX2-shEPRS) cells on coverglasses were stained for DAPI (for DNA, blue) and collagen I (red, top panel) or fibronectin (green, bottom panel). Relative fluorescence

intensities of ECMs are displayed under the images. White bar indicate 60 μm . (G) LX2-control (-) or LX2-shEPRS (shEPRS, +) cells were treated with ascorbic acid (50 $\mu\text{g/ml}$) and Poly(sodium 4-styrenesulfonate) (PSS; 30 $\mu\text{g/ml}$) for 24 h, along with TGF β 1 (2 ng/ml). Conditioned media (CM) or foot-print extracts (with deposited ECM proteins) were then prepared for immunoblotting against Collagen I α 1 chain (Col1a1). Data shown represent three independent experiments.

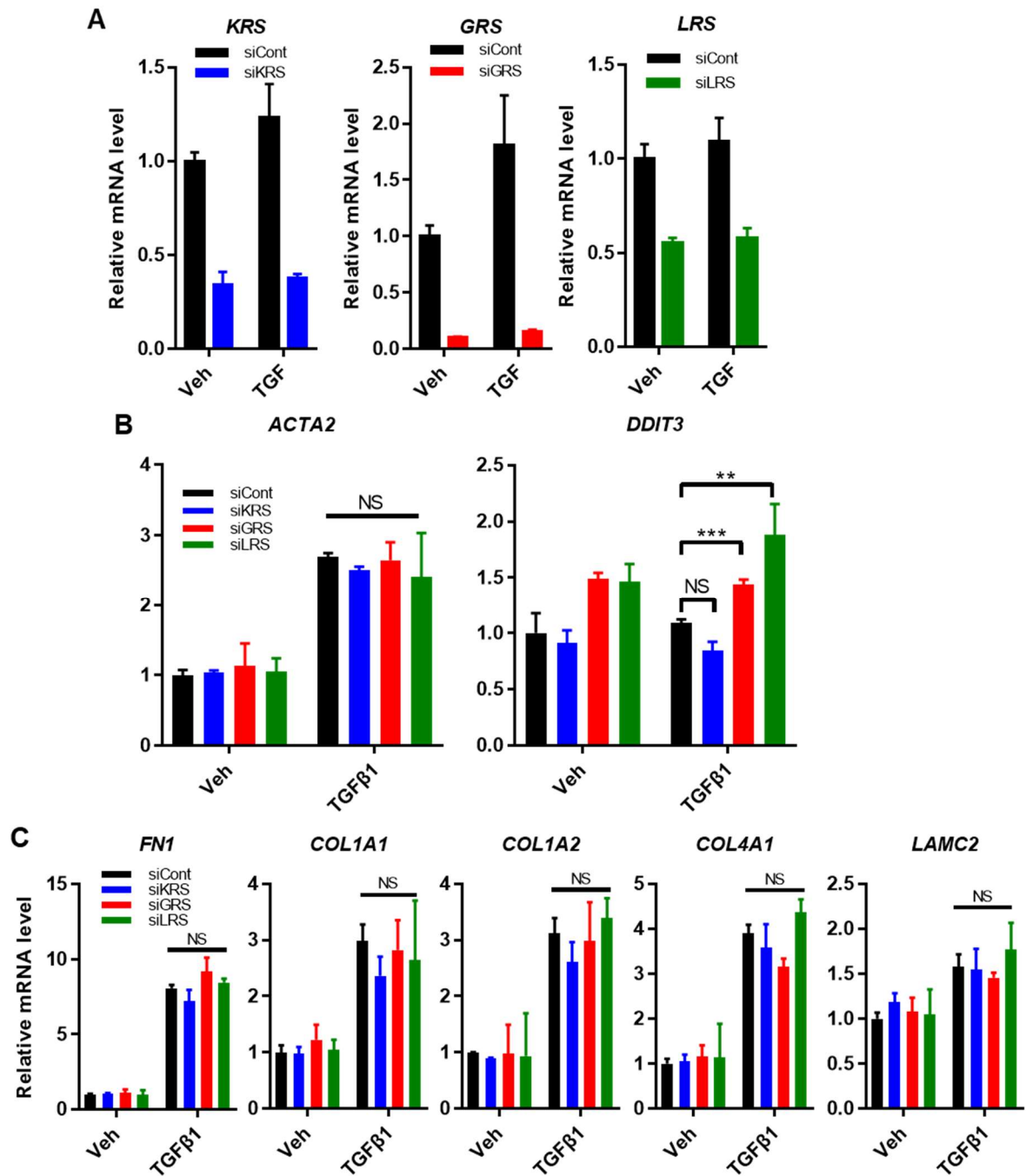


Figure 1. 3. Suppression of different aminoacyl-tRNA synthetases (ARS) showed no significant changes in ECM chain mRNA levels. (A to C) LX2 cells were transfected with siRNAs against a control sequence, KRS, GRS, or LRS sequence and 24 h later the cells were treated with vehicle (Veh) or TGFβ1 for additional 24 h, before qRT-PCR analysis on the

mRNA levels of the indicated genes. NS indicates non-significance. *, **, and *** depict statistical significance of $p < 0.05$, 0.01, and 0.001, respectively, according to the two-way ANOVA analysis. Data shown represent three independent experiments.

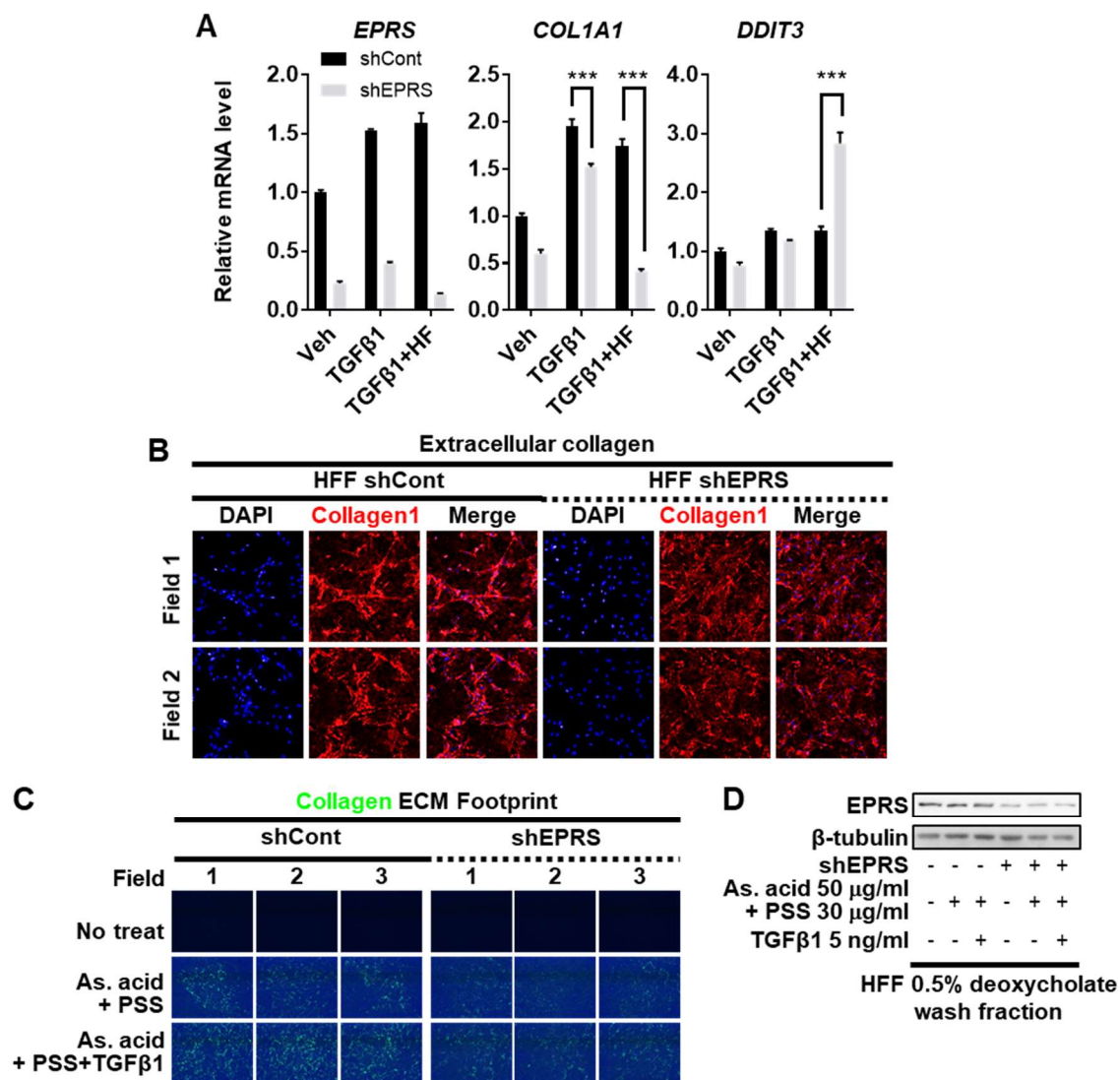


Figure 1. 4. ECM induction and deposition in human foreskin fibroblasts were dependent on EPRS expression. (A) Human foreskin fibroblasts (HFFs) stably infected with shControl (Con) or shEPRS lentivirus were treated with vehicle, TGFβ1, or TGFβ1 plus halofuginone (TGFβ1+HF) for 24 h, before processing to qRT-PCR for the indicated molecules. Data are presented at mean ± SD. *** depicts statistical significance of $p < 0.001$. (B) Control or EPRS-suppressed HFFs cells (shEPRS) on coverglasses were treated with none, with ascorbic acid plus PSS, or with ascorbic acid plus PSS plus TGFβ1 for 24 h, before staining for DNA (DAPI, blue) and immunostaining for collagen I. (C) Cells were manipulated as in (B) and washed

using 0.5% deoxycholate before staining and visualization of collagen foot prints. (D) Successful knock-down of EPRS was confirmed by immunoblot of 0.5% deoxycholate wash fraction in (C). Data shown represent three independent experiments.

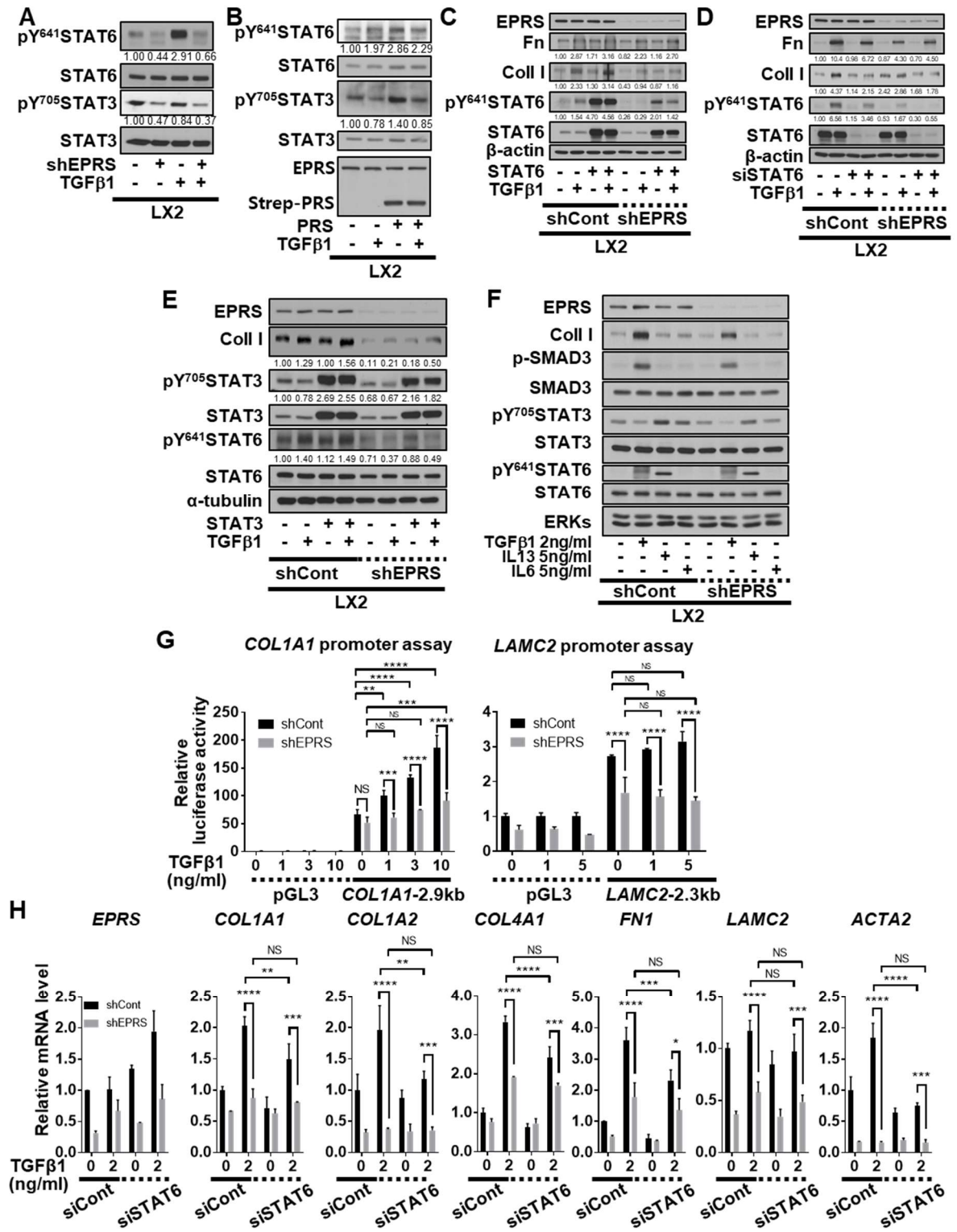


Figure 1. 5. STAT6 phosphorylation upon TGFβ1 treatment to LX2 cells was required for ECM production. (A to F) LX2 cells were stably infected with the control (-) or shEPRS virus (LX2-shEPRS). Control LX2 cells were transiently transfected with different expression vectors, as indicated, in the absence (-) or presence of TGFβ1 (2 ng/ml, +) for 24 h, followed by whole-cell extract preparation and immunoblotting for the indicated molecules. (G) LX2 cells transfected with *COL1A1* or *LAMC2* promoter luciferase constructs with STATs-consensus responsive sequences (*Col1a1*-2.9 kb and *Lamc2*-2.3 kb constructs with upstream promoter regions up to -2.9kb and -2.3 kb, respectively) were treated with TGFβ1 at the indicated concentrations for 24 h, prior to luciferase reporter analysis. (H) Subconfluent control LX2 cells were transiently transfected with siRNA against a control sequence (siCont) or STAT6 (siSTAT6) in the absence (0) or presence of TGFβ1 (2 ng/ml) treatment for 24 h, followed by qRT-PCR analysis. Data are presented as mean ± SD. NS indicates non-significance. *, **, ***, and **** depict statistical significance of $p < 0.05$, 0.01, 0.001, and 0.0001 respectively, according to the two-way ANOVA analysis. Data shown represent three isolated experiments.

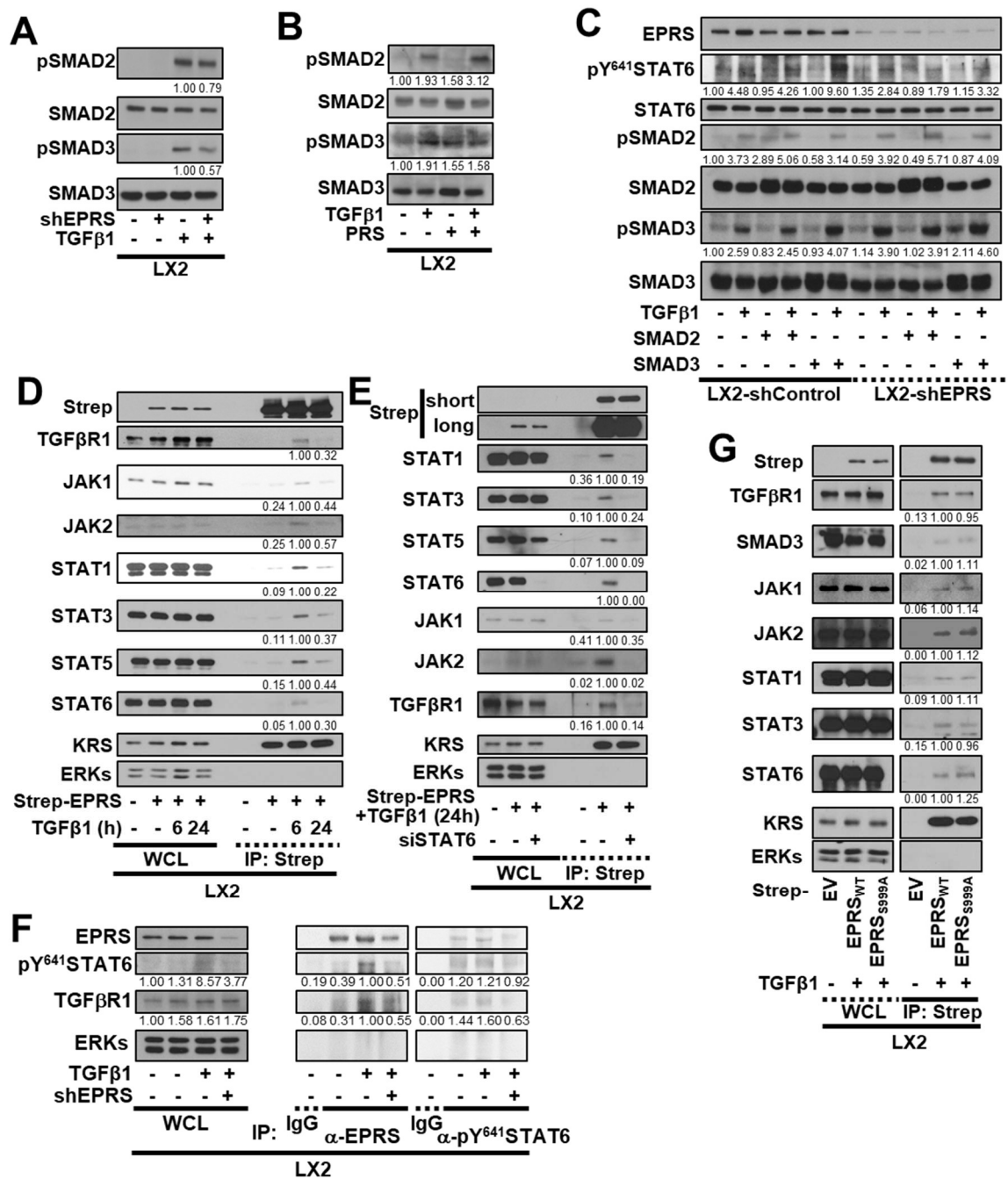


Figure 1. 6. EPRS-dependent regulation of signaling downstream of TGFβ1. (A to C) LX2-shControl (-) or LX2-shEPRS (+) cells (A) or LX2 cells transfected with control construct or pEXPR-103-Strep-PRS (B) were treated with vehicle (-) or TGFβ1 (2 ng/ml, +). (C) Cells were infected adenovirus for SMAD2 or SMAD3 for 24 h, after which they were treated with vehicle (-) or TGFβ1 (2 ng/ml, +). Whole-cell extracts were then prepared before normalization and

immunoblotting for the indicated molecules. (D and E) LX2 cells (-) or stably-expressing Strep-tagged EPRS (Strep-EPRS, +) cells were treated with vehicle (-) or TGF β 1 (2 ng/ml, +) without (D) or with transient transfection of siSTAT6 for 48 h (E). The Strep-EPRS expression levels were exposed for a shorter (short) and a longer (long) time (E). Whole-cell extracts were prepared and processed for precipitation using streptavidin-agarose beads, and the precipitates were immunoblotted. (F) Normal or EPRS-suppressed LX2 cells were treated with vehicle or TGF β 1 for 24 h, before harvests of whole cell lysates (WCL) and then immunoprecipitation with normal immunoglobulin (IgG) or antibody against EPRS or pY⁶⁴¹STST6. The immunoprecipitates were immunoblotted for the indicated molecules. (G) LX2 cells were transiently transfected with Strep-EV (empty vector) or EPRS expression vector for either wildtype (WT) or Ser999A point mutant for 48 h, followed by treatments with vehicle (-) or TGF β 1 (2 ng/ml, +) at 24 h post-transfection. Whole-cell extracts were processed for precipitation using streptavidin-agarose beads, and the precipitates were immunoblotted for the indicated molecules. Data shown represent three independent experiments.

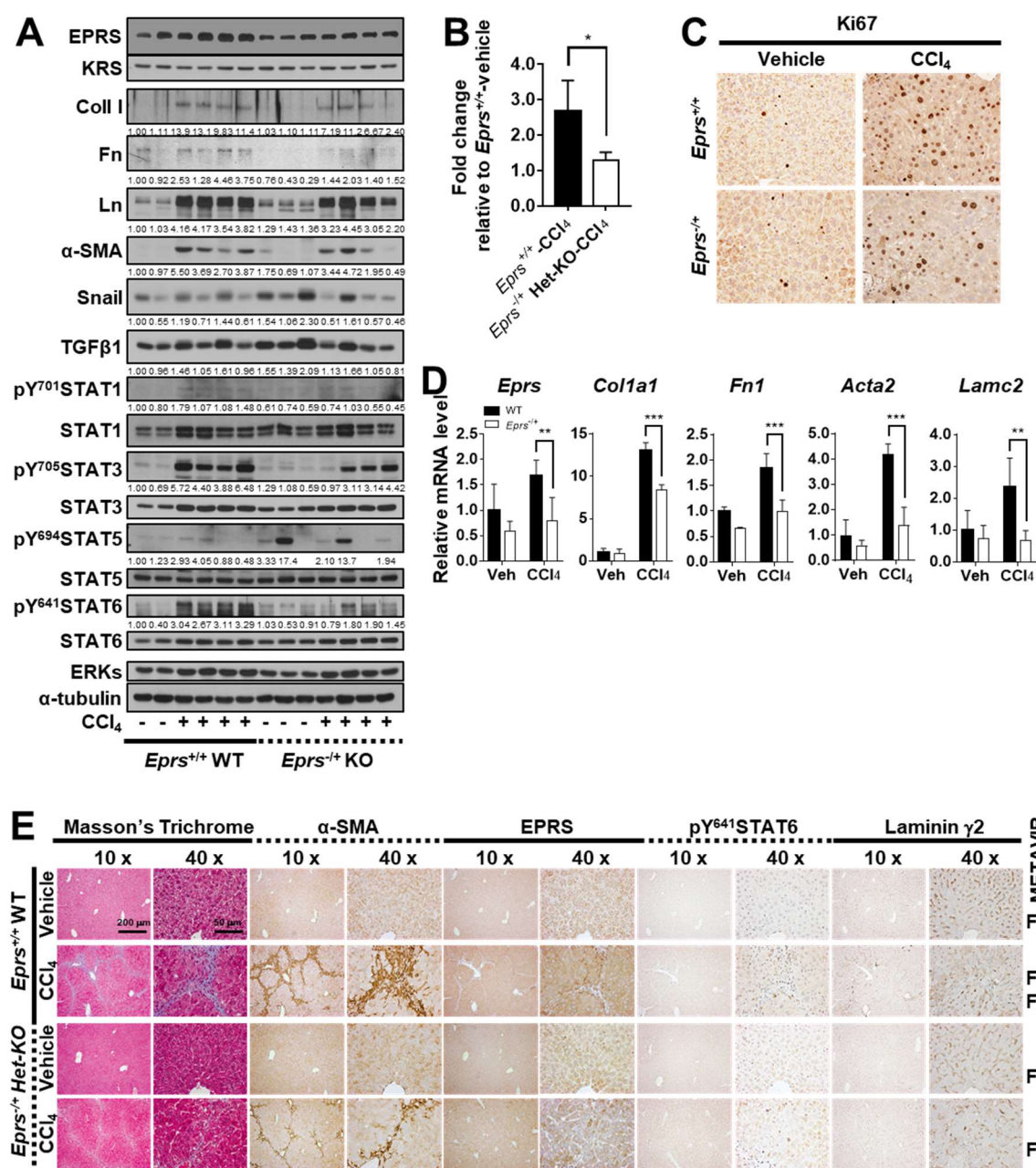


Figure 1. 7. CCl₄-treated mice showed EPRS-dependent ECM production. Wildtype (WT, *Eprs*^{+/+}) and *Eprs*^{-/-} hetero-knockout (KO) C57BL/6 mice were treated with vehicle or CCl₄ (1 mg/kg in 40% olive oil) once a week for 5 weeks. Liver tissue extracts were prepared and processed for immunoblotting (A), the hydroxyproline assay (B), immunohistochemistry using anti-Ki67 antibody (C), and qRT-PCR (D). Data are presented as mean ± SD. *, **, and *** depict statistical significance of $p < 0.05$, 0.01, and 0.001, respectively, according to the

Student's *t*-test. (E) Liver tissues were processed for Masson's Trichrome staining or immunohistochemistry, followed by image capturing at 10× and 40×. Fibrotic grade according to the METAVIR scores are indicated in the right side. Data shown represent three different experiments.

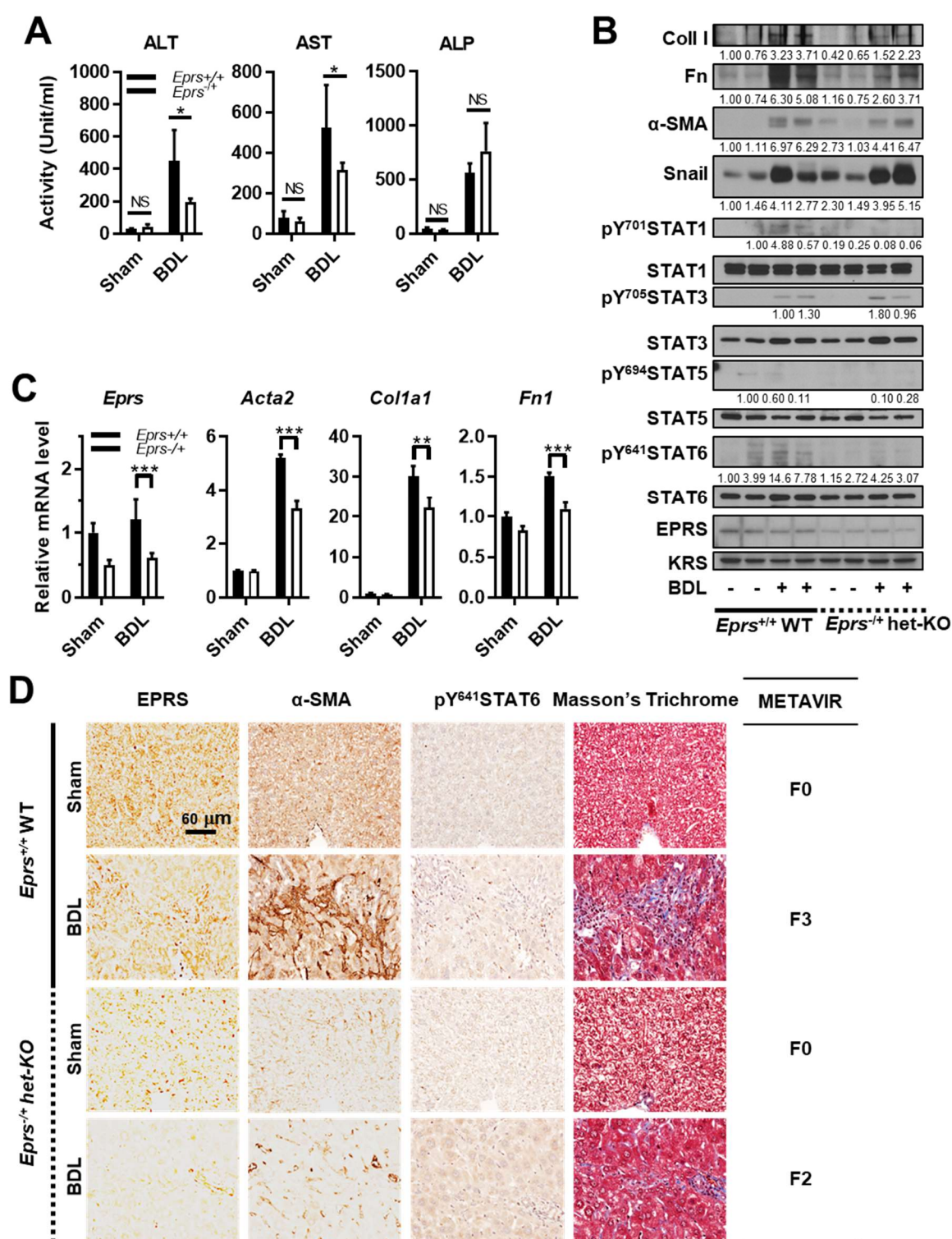


Figure 1. 8. Bile duct ligation in mice showed EPRS-dependent ECM production. (A to D)

Wildtype (WT, *Eprs*^{+/+}) and *Eprs*^{-/-} hetero-knockout (KO) C57BL/6 mice were sham operated or their bile ducts were ligated for 5 weeks. (A) Serum levels of ALT, AST, and ALP were

measured. Liver tissue extracts were prepared and processed for immunoblotting (B) and qRT-PCR (C). Data are presented as mean \pm SD. NS indicates non-significance. *, **, and *** depict statistical significance of $p < 0.05$, 0.01, and 0.001, respectively, according to the Student's *t*-test. (D) Liver tissues were processed for Masson's Trichrome staining or immunohistochemistry, followed by imaging at 40 \times . Fibrotic grade according to the METAVIR scores are indicated in the right side. Data shown represent three different experiments.

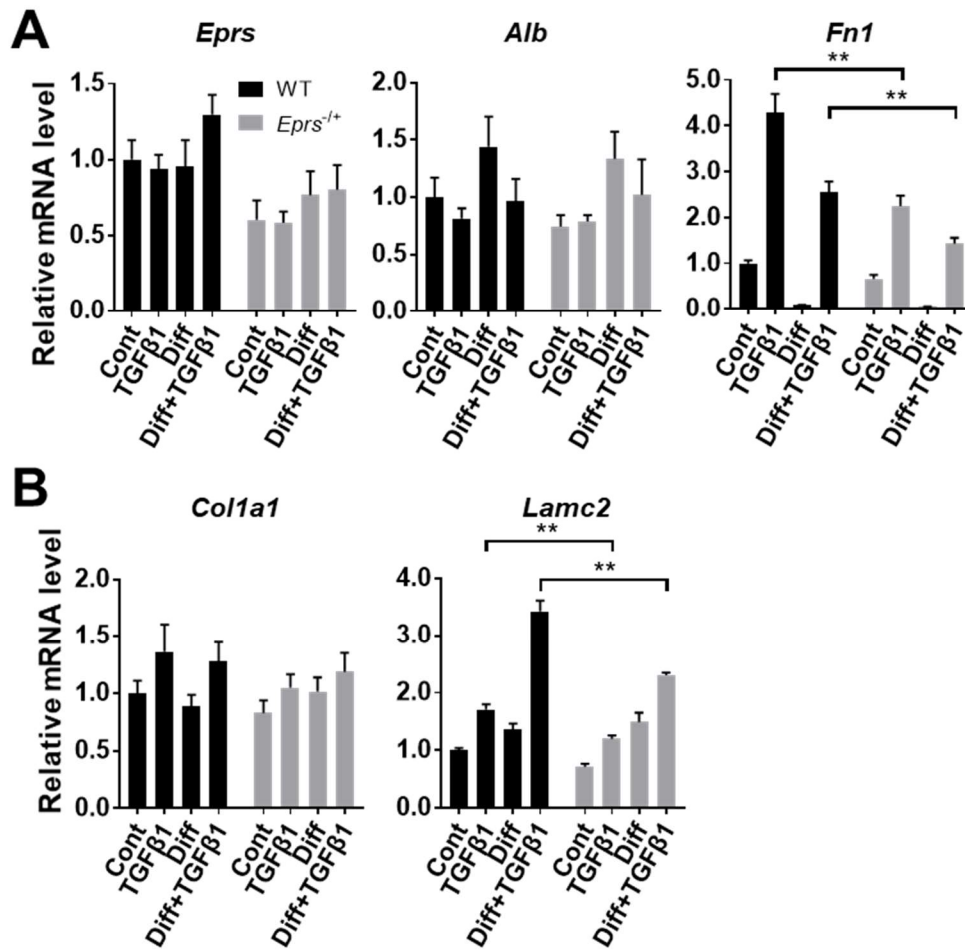


Figure 1. 9. Liver organoid models prepared from WT or *Eprs*^{-/-} hetero-KO mice also showed EPRS-dependent fibronectin expression. (A and B) Organoid cultures following the embedding of ductal cells prepared from WT *Eprs*^{+/+} or *Eprs*^{-/-} hetero-KO mouse livers into 3D Matrigel were treated with TGFβ1 (2 ng/ml) before or after differentiation processes (diff.). After 24 h, the organoids were harvested and processed for qRT-PCR for the indicated molecules. Data are presented as mean ± SD. *, **, and *** depict statistical significance of $p < 0.05$, 0.01, and 0.001, respectively, according to the Student's *t*-test. Data shown represent three independent experiments.

1.4. DISCUSSION

This study demonstrates that EPRS could transcriptionally regulate the expression of ECMs, including collagen I and fibronectin, via TGF β 1-mediated signaling pathways involving a formation of complexes among TGF β R1, SMAD3, JAKs, and STAT6. Furthermore, a TGF β 1-mediated signaling pathway targeted toward STAT6 was observed in a CCl₄-mediated liver fibrosis animal model, eventually leading to ECM induction (Fig. 1. 20). Thus, this study suggests that EPRS can be a promising anti-fibrotic target.

Among *in vitro* LX2 HSCs, CCl₄-treated animal liver tissues, and 3D organoid models, the dependency of ECM chains levels on EPRS expression could be differential, presumably depending on cell type and/or signaling context involved in the experimental models. Fibronectin was clearly shown to be expressed in an EPRS-dependent manner in all three models. Collagen I expression depended on EPRS in LX2 and animal models, but laminin γ 2 only slightly depended on EPRS in the liver organoid model. Compared with collagen I that has been shown to be a main component in fibrotic livers, whereas laminin γ 2 is a biomarker of acute lung injury [89] and an HCC biomarker in the sera of HCC patients [90]. Thus, laminin γ 2 may also be important for the progression of pre-cancerous liver pathology to HCC. However, the regulation of laminin γ 2 expression differed among the three study models. In addition, I observed that α -SMA-positive HSCs were responsible for collagen I expression whereas albumin-positive hepatocytes could be responsible for laminin γ 2 expression in CCl₄-treated fibrotic mouse livers (data not included).

HF is a competitive inhibitor of EPRS activity [22], and reduces TGF β -mediated collagen synthesis in humans [77]. Its anti-fibrotic effects appears to involve influences on TGF β 1/SMAD3 signaling activity and other signaling molecules, depending on cell types [75]. Moreover, prevention of Th17 cell differentiation leads to the inhibition of autoimmune

inflammation [79]. HF is highly efficacious in inhibiting fibrosis [91], but it causes significant side effects characterized by severe GI lesions and hemorrhage [92]. The antagonistic effects of HF on SMAD3 phosphorylation can be at least partially due to the HF-mediated activation of other signaling molecules including AKTs, ERKs, and p38 MAPK phosphorylation [93]. As a multifunctional cytokine, TGF β 1 plays significant roles in several biological activities encompassing various effectors and receptors [94]. Thus, it is likely that HF causes side effects by targeting TGF β signaling that is also important for homeostatic immune and inflammatory functions [34, 75]. Therefore, more studies are needed to develop safer anti-fibrotic reagents that can target specific EPRS- and/or TGF β 1-mediated signaling components of pathways leading to ECM production.

The biological activity of HF also involves the inhibition of proline utilization by EPRS [22]. EPRS is traditionally important for loadings of proline to tRNA^{Pro} during amino acid polymerization following the codon information on mRNA. Although the α 1 chain of collagen I includes a proline composition of 19.0%, this study revealed that EPRS could also regulate the mRNA expression of *COL1A1* and *FNI* (with a lower 7.9% proline content). Furthermore, in EPRS-suppressed cells, proline enrichment could not recover the inhibitory effect of HF on ECM production, thereby indicating another role of EPRS in ECM production beyond proline-charging to tRNA^{Pro}. Additionally, EPRS expression was positively correlated with the extracellular deposition of collagen I, suggesting that EPRS can play positive roles in the synthesis of ECMs.

It was recently reported that TGF β R1 can interact with JAK1, thereby leading to early STAT3 phosphorylation in normal hepatocytes or hepatic cancer cells [95]. In my study, STAT3 expression did not enhance ECM expression in TGF β 1-treated LX2 HSCs. STAT3 was also negatively responded to TGF β 1 stimulation but was positively correlated with EPRS

expression. In contrast, STAT6 phosphorylation was correlated with the upregulatory effects of EPRS and TGF β 1 effects on collagen I and fibronectin expression. Thus, it is likely that different hepatic cell types can adapt different forms of STATs downstream of TGF β 1 stimulation. Results from this study also show that EPRS may be a component of the TGF β R1/SMAD3-mediated protein complex consisting of JAKs and STATs. Importantly, EPRS is also a component for the cytosolic MSC. Once EPRS is phosphorylated at Ser999 by mTORC1-S6K1, EPRS can be dissociated from the MSC and translocate to membrane where it can interact with fatty acid transporter upon insulin stimulation to adipocytes [67]. Thus, EPRS can translocate to the plasma membrane. However, the current study shows that phosphorylation of EPRS at Ser999 in LX2 HSCs was not required for TGF β R1 binding. The discrepancy in the requirement of EPRS phosphorylation at Ser999 to translocate from the cytosolic MSC to membrane might be due to differences in cell types and/or signaling contexts. Alternatively, it cannot be ruled out that EPRS as a component of MSC may still have the capacity to bind to TGF β R1. Overall, results from this study suggest that it may be reasonable to target the EPRS-dependent, TGF β R1-STAT6 signaling axis to inhibit fibrotic ECM production.

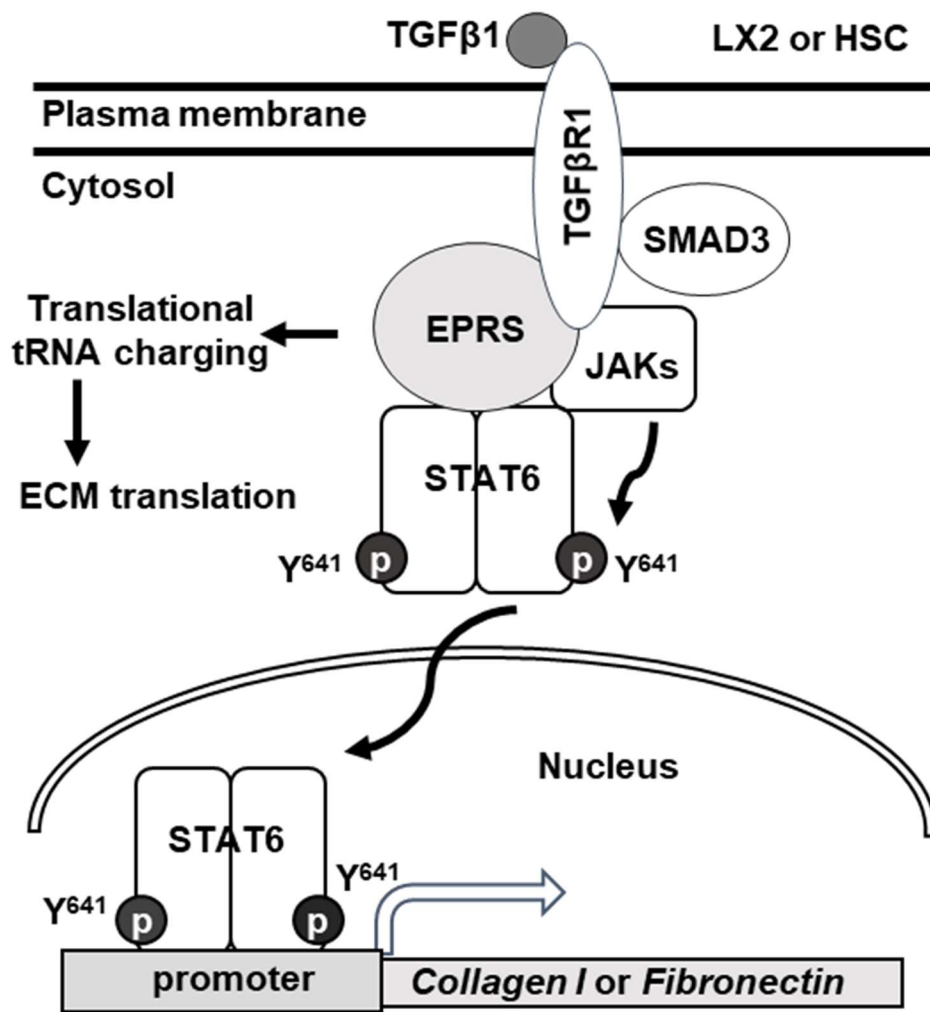


Figure 1. 10. The working model for EPRS-dependent ECM expression on TGFβ1 treatment to LX2 cells. TGFβ1 treatment leads to formation of protein complex among TGFβ1R, SMAD3, EPRS, JAKs, and pY⁶⁴¹STAT6. Active pY⁶⁴¹STAT6 causes transcriptional activations of the promoters of *COL1A1* or *FNI* genes. In addition, EPRS can play role in translational charging of prolyl-tRNAs during ECM expression.

CHAPTER 2.

Glutamyl-Prolyl-tRNA Synthetase Regulates Epithelial Expression of Mesenchymal Markers and Extracellular Matrix Proteins: Implications for Idiopathic Pulmonary Fibrosis

ABSTRACT

Background: Idiopathic pulmonary fibrosis (IPF), a chronic disease of unknown cause, is characterized by abnormal accumulation of extracellular matrix (ECM) in fibrotic foci in the lung. Previous studies have shown that the transforming growth factor β 1 (TGF β 1) and signal transducers and activators of transcription (STAT) pathways play roles in IPF pathogenesis. Glutamyl-prolyl-tRNA-synthetase (EPRS) has been identified as a target for anti-fibrosis therapy, but the link between EPRS and TGF β 1-mediated IPF pathogenesis remains unknown.

Methods: Here, I studied the role of EPRS in the development of fibrotic phenotypes in A549 alveolar epithelial cells and bleomycin-treated animal models. **Results:** I found that EPRS knockdown inhibited the TGF β 1-mediated upregulation of fibronectin and collagen I and the mesenchymal proteins α -smooth muscle actin (α -SMA) and snail 1. TGF β 1-mediated transcription of collagen I- α 1 and laminin γ 2 in A549 cells was also down-regulated by EPRS suppression, indicating that EPRS is required for ECM protein transcriptions. Activation of STAT signaling in TGF β 1-induced ECM expression was dependent on EPRS. TGF β 1 treatment resulted in EPRS-dependent *in vitro* formation of a multi-protein complex consisting of the TGF β 1 receptor, EPRS, Janus tyrosine kinases (JAKs), and STATs. *In vivo* lung tissue from bleomycin-treated mice showed EPRS-dependent STAT6 phosphorylation and ECM production. **Conclusion:** My results suggest that epithelial EPRS regulates the expression of mesenchymal markers and ECM proteins via the TGF β 1/STAT signaling pathway. Therefore, epithelial EPRS can be used as a potential target to develop anti-IPF treatments.

2.1. INTRODUCTION

Idiopathic pulmonary fibrosis (IPF) is a chronic, progressive, fatal, fibrotic interstitial lung disease of unknown cause [27-30]. Typical clinical symptoms include dyspnoea, decreased exercise capacity, and dry cough; most patients survive for 2.5-5 years after diagnosis [31]. IPF is characterized by the excessive accumulation of extracellular matrix (ECM) components, which correlates with the proliferation and activation of fibroblasts, myofibroblasts, and abnormal lung epithelial cells [32]. Although the origins and activation of invasive lung myofibroblasts remain unclear, some potential causes include activation of lung resident fibroblasts, recruitment of circulating fibrocytes and blood mesenchymal precursors; and mesenchymal transformation of alveolar type II epithelial cells, endothelial cells, pericytes, and/or mesothelial cells [33].

Current pharmacologic treatments for IPF include two U.S. Food & Drug Administration-approved drugs (nintedanib and pirfenidone) that improve symptoms but do not cure the disease [27]. Given the limited treatment options, it is urgent to investigate the mechanisms of IPF pathogenesis [30].

Transforming growth factor $\beta 1$ (TGF $\beta 1$) is a multifunctional cytokine that regulates immune responses during homeostasis and inflammation (Luzina et al., 2015). During IPF pathogenesis, TGF $\beta 1$ activates lung fibroblasts and promotes epithelial mesenchymal transformations (EMT) of various cell types, such as alveolar type II cells [30, 76]. Disrupting TGF $\beta 1$ -mediated signaling will be important to develop effective anti-fibrogenesis drugs.

Prolyl-tRNA synthetase (PRS) catalyzes the attachment of proline to transfer RNA (tRNA) during translation. Halofuginone (HF), a plant alkaloid isolated from *Dichroa febrifuga* [22], is an anti-fibrotic agent that blocks PRS catalytic activity. HF inhibits mRNA levels of

collagens, COL1A1 (with 19% proline/total residues) and COL1A2, but this effect is reversed by exogenous proline [22]. HF also blocks non-translational functions of PRS, such as inhibiting synthesis of fibronectin 1 (with 7.9% proline/total residues), an ECM protein that is not proline-rich. HF-mediated inhibition of PRS leads to the accumulation of naked tRNA molecules, which activates the amino-acid response (AAR) pathway to inhibit the synthesis of ECM proteins. Such HF-mediated inhibition of PRS and ECM expression are overcome by exogenous proline treatment, indicating that PRS can be involved in ECM translation via proline charging of prolyl-tRNA [22]. However, it may still be likely that roles of PRS in ECM expression involve non-translational processes, since variable ECMs can be composed with different levels of proline.

Studies have demonstrated a role for the Janus kinase (JAK)-signal transducer and activator of transcription (STAT) pathway in IPF. STAT3 is activated in the lungs of patients with IPF [96-98]. TGF β receptor 1 (TGF β R1) forms a protein complex with JAK1 that activates STAT3 via SMAD3 mediation [95]. STAT3 is essential for activation of the COL1A2 enhancer [99]. A link between STAT3/STAT6 and IPF has also been reported [30, 100]. However, the role of EPRS in TGF β 1/STAT signaling-induced IPF pathogenesis remains.

Here, I studied the functional role of EPRS in TGF β 1-mediated fibrosis. I found that EPRS activated TGF β 1-induced ECM protein expression both *in vitro* and *in vivo*. TGF β 1 treatment resulted in the formation of a multi-protein complex consisting of TGF β R1, EPRS, JAKs, and STATs in alveolar type II epithelial cells. EPRS-dependent STAT6 phosphorylation correlated with ECM production in the lungs of bleomycin-treated mice. My results suggested that epithelial EPRS regulates TGF β /STAT signaling to induce expression of mesenchymal markers and ECM proteins during IPF development.

2.2. MATERIALS AND METHODS

Reagents and plasmids

All cytokines and growth factors including TGF β 1 were purchased from Peprotech (Rocky Hill, NJ, USA). Hydroxyproline assay kits, and CCl₄ were purchased from Sigma-Aldrich (St. Louis, MO, USA). Bleomycin and target specific pooled siRNAs siSTAT3 and siSTAT6 were purchased from Santa Cruz Biotechnology (Santa Cruz, CA, USA). EPRS in pEXPR-103-Strep vector (IBA Lifesciences, Göttingen, Germany) were gifts from Dr. Myung Hee Kim at the Korea Research Institute of Bioscience and Biotechnology (KRIBB, Daejeon, Korea). EPRS (1-1440 amino acids) consists of ERS (1-687 amino acids) and PRS (935-1440 amino acids) linked via non-catalytic WHEP repeat domains (688-934 amino acids) [101]. The PRS domain of EPRS was cloned into pEXPR-103-Strep vector (IBA Lifesciences). pRc/CMV-WT STAT3 was previously described [81] and pCMV-STAT6-IRES-Neo was a gift from Axel Nohturfft (Addgene plasmid # 35482). Adenovirus expressing SMAD2 or SMAD3 were described previously [82].

Cell culture

A549 lung adenocarcinoma cells were purchased from the Korean Cell Line Bank (KCLB, Seoul, Korea) and cultured in RPMI (SH30027.01, Hyclone, South Logan, UT, USA). Media were supplemented with 10% fetal bovine serum (FBS, GenDEPOT, Barker, TX, USA) and 1% penicillin/streptomycin (GenDEPOT) and cells were grown at 37°C in 5% CO₂. The SMARTvector shEPRS doxycycline-inducible knockdown cell line was established by treating lentiviral particles (EPRS mCMV-turboGFP V2IHSMCG_687815, 687823, Dharmacon, Lafayette, CO, USA). Positive clones were enriched by treatment of 2 μ g/ml puromycin (GenDEPOT) and maintained in complete media supplemented with 1 μ g/ml puromycin.

siRNAs or cDNA plasmids were transiently transfected using Lipofectamine RNAiMAX or Lipofectamine 3000, respectively, following the manufacturer's instructions (Thermo Fisher Scientific, Waltham, MA, USA).

Western blot analysis

Subconfluent cells or animal tissues were harvested for whole cell or tissue extracts using RIPA buffer. Proteins in the lysates were separated in Tris-Glycine SDS-polyacrylamide gels at concentrations ranging from 8 to 12%, and transferred to nitrocellulose membranes (Thermo Fisher Scientific). Target-specific antibodies used in this study are summarized in Table 2. 1.

qRT-PCR

Total RNAs from animal tissues or cells were isolated using Qiazol Reagent (Qiagen, Hilden, Germany), and their cDNAs were synthesized using amfiRivert Platinum cDNA synthesis master mix (GenDEPOT) according to the manufacturer's instructions. Quantitative real time PCR (q-PCR) samples were prepared with LaboPass™ EvaGreen Q Master (Cosmo Genetech, Seoul, Korea) prior to analysis in a CFX Connect™ Real-Time PCR machine (Bio-Rad, Hercules, CA, USA). mRNA levels were normalized against GAPDH and CFX Maestro™ software (Sunnyvale, CA, USA) was used to analyze the data. Primers were purchased from Cosmo Genetech (Seoul, Korea). The primer sequences are shown in Table 2. 2.

Co-immunoprecipitation

Whole-cell lysates were prepared using immunoprecipitation lysis buffer (40 mM HEPES pH7.4, 150 mM NaCl, 1 mM EDTA, 0.5% Triton X-100, and protease inhibitors) and precipitated with Pierce High-Capacity Streptavidin Agarose beads (Thermo Fisher Scientific) overnight at 4°C. Precipitates were washed three times with ice-cold lysis buffer, three times

with immunoprecipitation wash buffer (40 mM HEPES pH 7.4, 500 mM NaCl, 1 mM EDTA, 0.5% Triton X-100, and protease inhibitors), and then boiled in 2× SDS-PAGE sample buffer before immunoblotting.

Luciferase assay

To analyze promoter activity, *LAMC2* (laminin $\gamma 2$) promoters (encoding regions of -1871 to +388) and *COL1A1* (collagen I $\alpha 1$) promoters (encoding regions of -2865 to +89) were amplified by PCR and cloned into the pGL3-basic vector. A549 cells were seeded in 48 well plates and the next day the plasmids were transfected using Lipofectamine 3000 transfection reagent (Thermo Fisher Scientific). β -Gal was co-transfected to allow normalization. One day after transfection, TGF β 1 (2 ng/ml) was added to the culture media. After 24 hr, luciferase activity was measured according to the manufacturer's instructions using a luciferase reporter assay kit (Promega, Madison, WI, USA) with a luminometer (DE/Centro LB960, Berthold Technologies, Oak Ridge, TN, USA).

Animal experiments

Wildtype (WT) *EPRS*^{+/+} (n= 4 for vehicle and n=9 for bleomycin) and *EPRS*^{-/+} hetero-knockout (n=5 for vehicle and n=7 for bleomycin) C57BL/6 mice were housed in a specific pathogen-free room with controlled temperature and humidity. Mouse protocol and animal experiments were approved by the Institutional Animal Care and Use Committee (IACUC) of Seoul National University (SNU-161201-1-3). For the lung fibrosis model, bleomycin (Santa Cruz Biotechnology) was dissolved in sterilized saline and intratracheal instillation was performed through surgically exposed trachea as a single dose of 1 mg/kg in 100 μ l solution per animal. Mice were sacrificed 4 weeks post-intratracheal instillation. Lung tissue samples were snap frozen in liquid nitrogen for western blot, qPCR, and hydroxyproline analysis, or

fixed in 4% formaldehyde in PBS for histological analysis.

Immunohistochemistry and staining

Paraffin blocks and sections (6- μ m thickness) of lung tissues were prepared by Abion Inc. (Seoul, Korea) for immunohistochemistry analysis. Primary antibodies and their dilution ratios are listed in Table 1. Vectastain ABC-HRP kit (Vector Laboratories, Burlingame, CA, USA) were used to visualize the stained samples. Mayer's hematoxylin (Sigma-Aldrich) was used for counter-staining the nuclei.

Statistics

Statistical analyses were performed using Prism software version 6.0 (GraphPad, La Jolla, CA). Two-way analysis of variance (ANOVA) in group analysis or Student's *t*-tests were performed to determine statistical significance. A value of $p < 0.05$ was considered significant.

Table 2. 1. Antibodies and their dilution ratio used in Chapter 2.

Name	Company	Catalog	WB dil.	IHC dil.
EPRS	Neomics	NMS-01-0004	1:5000	1:200
Fibronectin	DAKO	A0245	1:5000	1:200
Collagen I	Acris	R1038X	1:1000	1:200
Beta-actin	Abcam	AB133626	1:1000	
pY641-STAT6	Abcam	AB28829	1:1000	1:100
Total-STAT6	Cell Signaling Technology	#9362	1:1000	
pY705-STAT3	Abcam	AB76315	1:1000	
pY705-STAT3	Cell Signaling Technology	#9145		1:200
Total-STAT3	Santa Cruz Biotechnology	SC-482	1:1000	
pS465/467-SMAD2	Cell Signaling Technology	#3108	1:1000	1:100
Total-SMAD2	Cell Signaling Technology	#5339	1:1000	
pS423/425-SMAD3	Cell Signaling Technology	#9520	1:1000	
Total-SMAD3	Cell Signaling Technology	#9523	1:1000	
TGFβ-receptor1	Santa Cruz Biotechnology	SC-399	1:500	
JAK1	Cell Signaling Technology	#3344	1:1000	
JAK2	Millipore	04-001	1:1000	
Total-STAT1	Santa Cruz Biotechnology	SC-346	1:1000	
Total-STAT5	Santa Cruz Biotechnology	SC-835	1:1000	
KRS	Neomics	NMS-01-0005	1:2000	
Erk	Cell Signaling Technology	#9102	1:1000	
Anti-Strep	IBA life Sciences	2-1509-001	1:2500	
Alpha-SMA	Sigma	A2547		1:200
Laminin gamma2	Santa Cruz Biotechnology	SC-28330		1:200
Laminin	Abcam	AB11575	1:1000	

Table 2. 2. qRT-PCR primers used in Chapter 2.

Gene name	Forward	Reverse	Size (bp)
Human EPRS	AGGAAAGACCAACACC TTCTC	CTCCTTGAACAGCCACTC TATT	87
Human Collagen1A1	CAGACTGGCAACCTCA AGAA	CAGTGACGCTGTAGGTGA AG	97
Human DDIT3	GAGATGGCAGCTGAGT CATT	TTTCCAGGAGGTGAAACA TAGG	134
Human Collagen4A1	CGGGCCCTAAAGGAGA TAAAG	GAACCTGGAAACCCAGGA AT	115
Human Fibronectin	CCACAGTGGAGTATGTG GTTAG	CAGTCCTTTAGGGCGATC AAT	104
Human Laminin γ 2	CTCAGGAGGCCACAAG ATTAG	TGAGAGGGCTTGTTTGGA ATAG	101
Mouse Collagen 1A1	AGACCTGTGTGTTCCCT ACT	GAATCCATCGGTCATGCTC TC	113
Mouse Fibronectin	TCCTGTCTACCTCACAG ACTAC	GTCTACTCCACCGAACAA CAA	96
Mouse Laminin γ 2	TGGAGTTTGACACGGAT AAGG	GAGTGTGTCTTGGATGGT AACT	104

2.3. RESULTS

EPRS expression regulated ECM production in A549 alveolar type II cells upon TGFβ1 stimulation

We studied the regulatory effect of EPRS on the expression of different ECM proteins by introducing doxycycline-inducible EPRS knockdown vectors into the A549 alveolar type II cell line. Expression of ECM proteins such as collagen I, fibronectin and laminin γ 2 were tested by immunoblotting EPRS-knockdown and control A549 cells. All the ECM proteins showed increased expression in control cells treated with TGFβ1 and this effect was abolished in EPRS-knockdown cells (Fig. 2. 1A). Expression levels of mesenchymal proteins including α -smooth muscle actin (α -SMA) and snail 1 were also dependent on TGFβ1 treatment and/or EPRS expression (Fig. 2. 1A). Since EPRS protein consists of two glutamyl-tRNA-synthetase (ERS) and prolyl-tRNA-synthetase (PRS), it would be reasonable to see whether PRS alone could achieve these effects. Overexpression of PRS enhanced TGFβ1-induced ECM protein expression (Fig. 2. 1B). However, overexpression of ERS alone did not increase TGFβ1-mediated ECM protein expression (Fig. 2. 1C), indicating that the PRS component of EPRS regulates ECM protein expression. TGFβ1 treatment also increased mRNA levels of *COL1A1*, *COL4A1*, *FNI*, and *LAMC2* in control cells, while EPRS suppression inhibited this effect (Fig. 2. 1D). My results suggest that EPRS positively regulated TGFβ1-induced expression of ECM proteins. A previous report [22] stated that EPRS suppression increases mRNA levels of DNA damage-inducible transcript 3 (*DDIT3*, also known as *CHOP*) to indicate an activation of AAR pathway that supports for tRNA charging processes. However, I found that *DDIT3* mRNA levels were unaffected by TGFβ1 treatment, indicating that TGFβ1-induced regulation of ECM protein expression involves alternative mechanism(s) in addition to the role in tRNA charging (Fig. 2. 1D).

Regulation of TGFβ1-induced ECM protein synthesis by EPRS occurred via STAT activation

To investigate potential signaling molecules or pathways involved in EPRS-mediated regulation of ECM protein synthesis following TGFβ1-treatment, I studied the dependency of STAT3 and STAT6, known mediators of IPF [30, 100], on EPRS expression. I found that TGFβ1 promoted the phosphorylation of STAT3 at Tyr705 (pY⁷⁰⁵STAT3) and STAT6 at Tyr641 (pY⁶⁴¹STAT6), and these effects were abolished by EPRS suppression (Fig. 2. 2A). EPRS overexpression increased pY⁷⁰⁵STAT3 and pY⁶⁴¹STAT6 levels upon TGFβ1 treatment in A549 cells (Fig. 2. 2B). My results suggest that EPRS and TGFβ1 signaling regulate STAT3 and STAT6 phosphorylation. I studied the role of EPRS in STAT-mediated expression of ECM proteins. Overexpression of STAT6 indicate greater increases in basal and TGFβ1-induced levels of α-SMA, snail 1, fibronectin, and collagen I in EPRS-positive A549 cells compared with EPRS-knockdown cells (Fig. 2. 2C). However, basal and TGFβ1-induced expression levels of fibronectin and collagen I were decreased when STAT6 levels were suppressed (Fig. 2. 2D). A similar EPRS-dependent regulation pattern of fibronectin and collagen I was observed when STAT3 was modulated (Figs. 2. 2E and F). I also tested the transcriptional activities of *COL1A1* and *LAMC2* promoters in A549 cells lacking STAT3 or STAT6. *COL1A1* or *LAMC2* promoters containing STAT-responsive consensus sequences showed increased transcriptional activity in A549 cells treated with TGFβ1. However, EPRS suppression reduced these effects (Fig. 2. 2G). Suppression of STAT3 or STAT6 abolished the increased transcriptional activity of *COL1A1* or *LAMC2* in EPRS-positive A549 cells but not EPRS-suppressed cells (Fig. 2. 2G). Together, my results suggested that EPRS regulates ECM protein expression via STAT3 or STAT6 signaling induced by TGFβ1.

TGFβ1-mediated SMAD3 phosphorylation upregulated phosphorylation of STAT6 depending on EPRS expression.

We investigated the role of the TGFβ1-mediated SMAD signaling in EPRS-dependent ECM protein expression and STAT3/6 activity. TGFβ1-mediated SMAD2 and SMAD3 phosphorylation was partially inhibited by EPRS suppression (Fig. 2. 3A). However, EPRS overexpression did not affect the levels of phosphorylated SMAD2 or SMAD3, which might have already been saturated by TGFβ1 treatment (Fig. 2. 3B). TGFβ1-induced levels of pY⁶⁴¹STAT6 were increased by overexpression of SMAD3 but not SMAD2. EPRS suppression abolished that effect (Fig. 2. 3C and D).

EPRS-mediated signaling in TGFβ1-treated cells involved the formation of a multi-protein complex consisting of STAT6 and TGFβ1R

We then tested for potential protein-protein interactions between TGFβ1 signaling and EPRS that regulate STAT6 phosphorylation. A549 cells containing Streptavidin-tagged EPRS (Strep-EPRS) were treated with or without TGFβ1, prior to precipitation of whole-cell extracts using streptavidin agarose beads for immunoblotting assays. Lysyl-tRNA synthetase (KRS), which forms a multi-aminoacyl-tRNA synthetase complex (MSC) with EPRS [87], was used as a positive control. In TGFβ1-treated cells, Strep-EPRS transiently precipitated with TGFβR1, JAKs, and STATs, which included STAT6 (Fig. 2. 4A). I tested the effect of STAT3 or STAT6 suppression on multi-protein interactions. STAT6 expression was required for the EPRS-mediated multi-protein complex formation (Fig. 2. 4B). Specifically, EPRS interaction with TGFβ1R and SMAD2/3 required STAT6 but not STAT3. Interestingly, STAT3 suppression resulted in increased binding of STAT6 to the EPRS/TGFβ1R-containing protein complex (Fig.

2. 4B). Interactions between EPRS and JAKs were independent of STAT3 and STAT6 (Fig. 2. 4B). My results suggest that STAT6 is critical for the formation of the multi-protein complex for TGFβ1-induced signaling of ECM protein expression. STAT3 and STAT6 may be involved in parallel signaling pathways to regulate this process.

Lung tissues from bleomycin-treated mice showed EPRS-dependent STAT6 phosphorylation and ECM protein production *in vivo*

To investigate the physiological roles of EPRS in pulmonary fibrosis *in vivo*, WT (*Eprs*^{+/+}) and *Eprs*^{-/+} hetero-knockout (KO) mice were treated with bleomycin to induce lung fibrosis by intratracheal instillation before analysis, since homozygous *Eprs*^{-/-} is embryonic lethal. Bleomycin-treated WT *Eprs*^{+/+} mice showed the highest increase in expression of ECM proteins, such as fibronectin, collagen I, and laminins, compared with bleomycin-treated *Eprs*^{-/+} hetero-KO mice and untreated WT mice (Fig. 2. 5A). Levels of pY⁷⁰⁵STAT3 and pY⁶⁴¹STAT6 were also elevated in bleomycin-treated *Eprs*^{+/+} mice, compared with *Eprs*^{-/+} hetero-KO mice (Fig. 2. 5A). My results suggest that STAT6 activation is part of EPRS-dependent signaling for ECM protein expression *in vivo*. I observed a slight upregulation in EPRS expression in bleomycin-treated WT *Eprs*^{+/+} mice, compared with other groups, indicating that EPRS might function as a pro-fibrotic molecule.

Hydroxyproline assays to measure collagen I levels in lung extracts showed that bleomycin-treated *Eprs*^{+/+} mice had higher levels compared with bleomycin-treated *Eprs*^{-/+} mice (Fig. 2. 5B). In addition to *IL8*, which is used to characterize idiopathic pulmonary fibrosis (IPF) [102], *Colla1*, *Fnl*, and *Lamc2* mRNA levels were also upregulated by bleomycin treatment in *Eprs*^{+/+} lungs but not *Eprs*^{-/+} hetero-KO lungs (Fig. 2. 5C).

Lung immunohistochemistry revealed more patchy fibrosis and fibroblastic foci in bleomycin-treated *Eprs*^{+/+} mice compared with *Eprs*^{-/+} mice (Fig. 2. 5D). Bleomycin treatment

also led to marked increases in collagen I, fibronectin, and laminin $\gamma 2$ synthesis in *Eprs*^{+/+} mice compared with *Eprs*^{-/+} mice. Levels of phospho-SMAD2, pY⁷⁰⁵STAT3, and pY⁶⁴¹STAT6, which showed intense nuclear staining, were diminished in *Eprs*^{-/+} mice (Fig. 2. 5D). The myofibroblasts marker α -smooth muscle actin (α -SMA) was positive in fibroblastic foci of bleomycin-treated mice lungs. These results suggest that the bleomycin-mediated fibrotic phenotypes in animal lungs are dependent on EPRS expression.

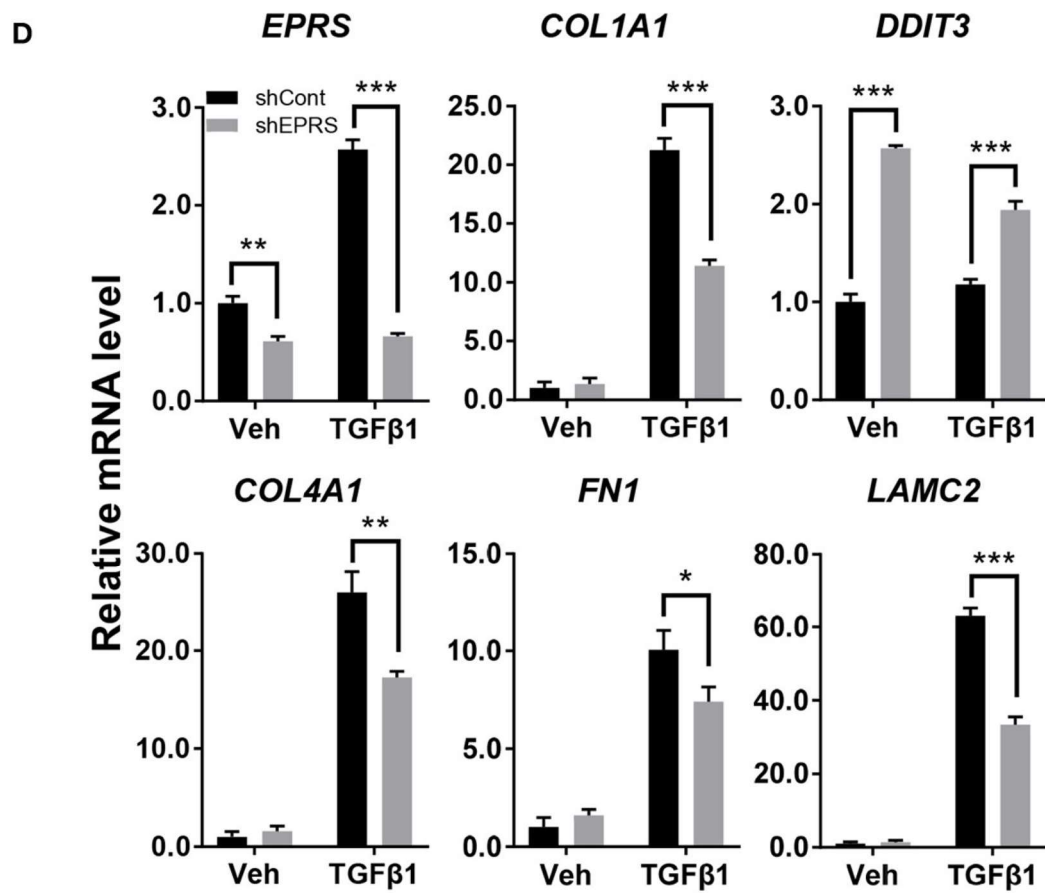
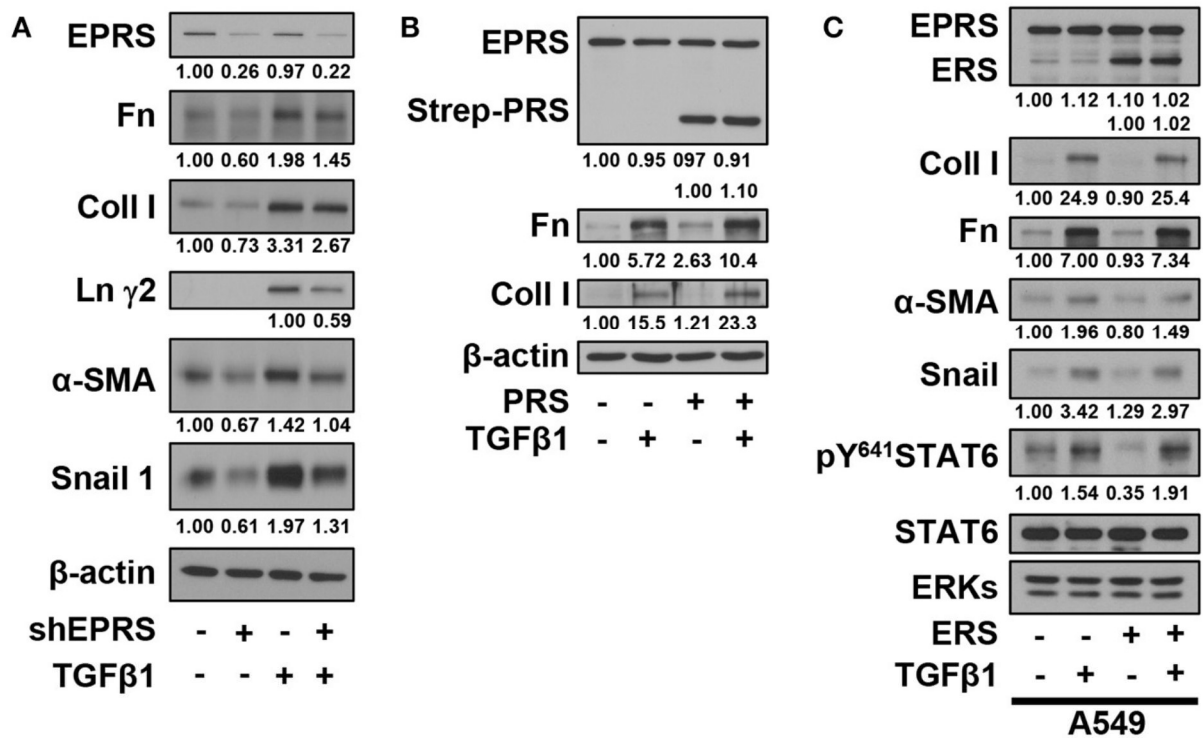


Figure 2. 1. EPRS expression regulates ECM protein production in A549 alveolar type II cells treated with TGFβ1. (A and B) A549-control (-) or shEPRS doxycycline-inducible knockdown (+) A549 cell line or control A549 cells transiently transfected with PRS expression vector (pEXPR-103-Strep-PRS) were treated without or with TGFβ1 (2 ng/ml) for 24 hr, and harvested for immunoblottings for the indicated molecules. (C) A549 cells were transfected without or with ERS expression plasmid for 24 hr and then treated without or with TGFβ1 (2 ng/ml) for 24 hr before lysate preparation and immunoblotting. (D) Subconfluent control (shCont) or shEPRS-A549 cells were treated with TGFβ1 (2 ng/ml) for 24 hr, before qRT-PCR analysis. Data are presented at mean ± standard deviation (SD). *, **, and *** indicate significance at $p < 0.05$, 0.01, and 0.001, respectively (calculated by Student's *t*-tests). Data shown represent three independent experiments. Song *et al.*, *Frontiers in Pharmacology*, 2018. Copyright under Creative Commons Attribution 4.0 License [103].

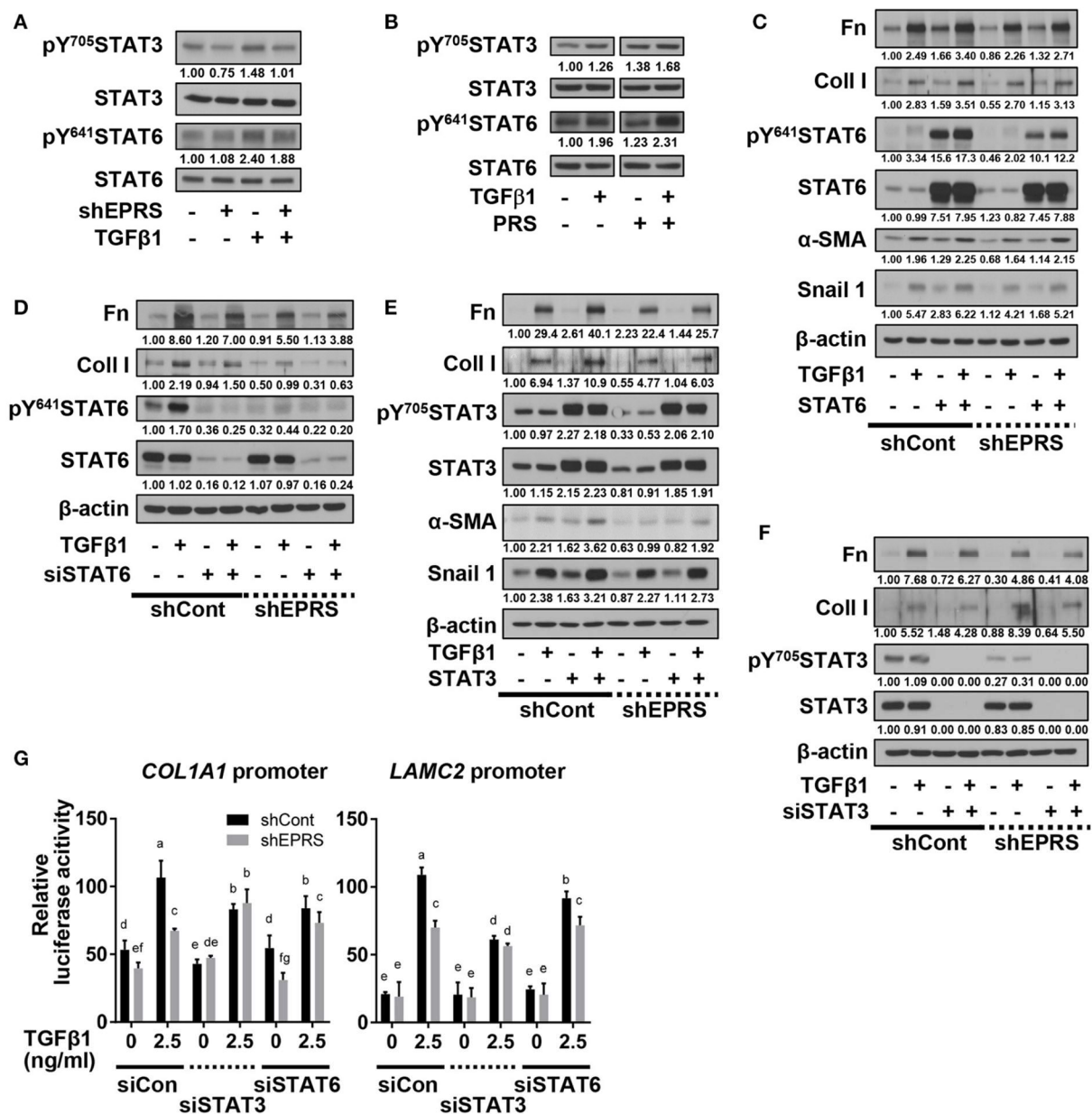


Figure 2. 2. Regulation of TGFβ1-induced ECM protein synthesis by EPRS occurs via STAT activation. (A to G) A549 cells stably infected with control (-) or shEPRS virus (A549-shEPRS) or control A549 cells transiently transfected with different expression vectors or siRNAs as indicated were treated without (-) or with TGFβ1 (2 ng/ml, +) for 24 hr, before whole cell extracts preparation and immunoblotting for the indicated molecules. (G) A549 cells transfected with *COL1A1* or *LAMC2* promoter-luciferase constructs with STATs-consensus responsive sequences (*Colla1*-2.9 and *Lamc2*-2.3 kb constructs with upstream promoter

regions up to -2.9kb and -2.3 kb, respectively) together with either siRNA against control sequence (siCon), STAT3 (siSTAT3), or STAT6 (siSTAT6) were treated with TGF β 1 (0 or 2.5 ng/ml) for 24 hr, prior to luciferase reporter analysis. Data are presented as mean \pm SD. Different letters indicate statistical significance at $p < 0.05$ according to one-way ANOVA. Data shown are from three isolated experiments. Song *et al.*, *Frontiers in Pharmacology*, 2018. Copyright under Creative Commons Attribution 4.0 License [103].

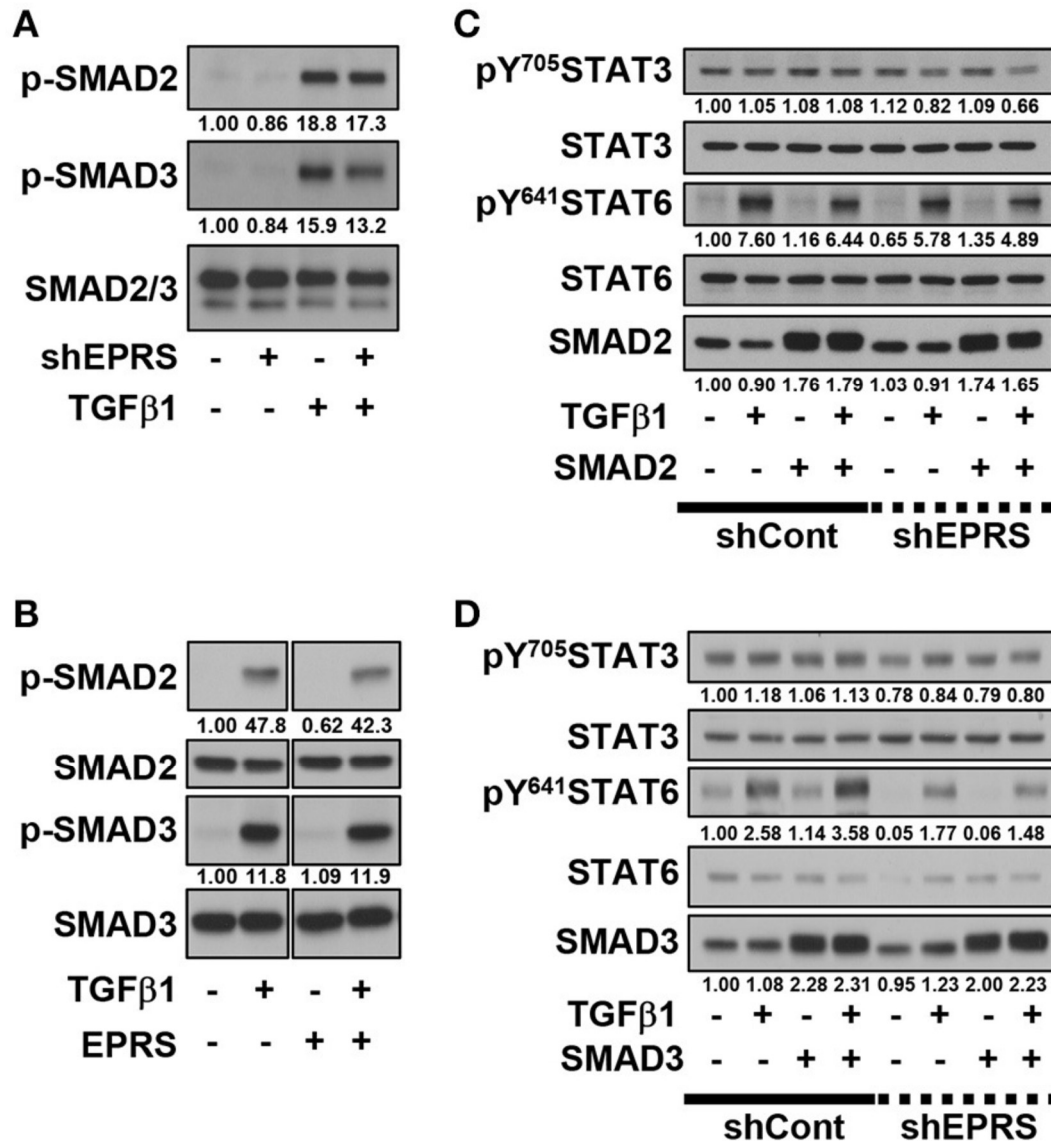


Figure 2. 3. TGFβ1-mediated SMAD3 phosphorylation upregulates phosphorylation of STAT6 depending on EPRS expression. (A to D) A549-shControl (-) or A549-shEPRS (+) cells were treated with vehicle (-) or TGFβ1 (2 ng/ml, +) (A and B) or treated with vehicle (-) or TGFβ1 (2 ng/ml, +) after infection (24 hr) with adenovirus encoding for SMAD2 or SMAD3 (C and D respectively). The whole cell extracts were then prepared before normalization and immunoblotting for the indicated molecules. Data shown represent three independent experiments. Song *et al.*, *Frontiers in Pharmacology*, 2018. Copyright under Creative Commons Attribution 4.0 License [103].

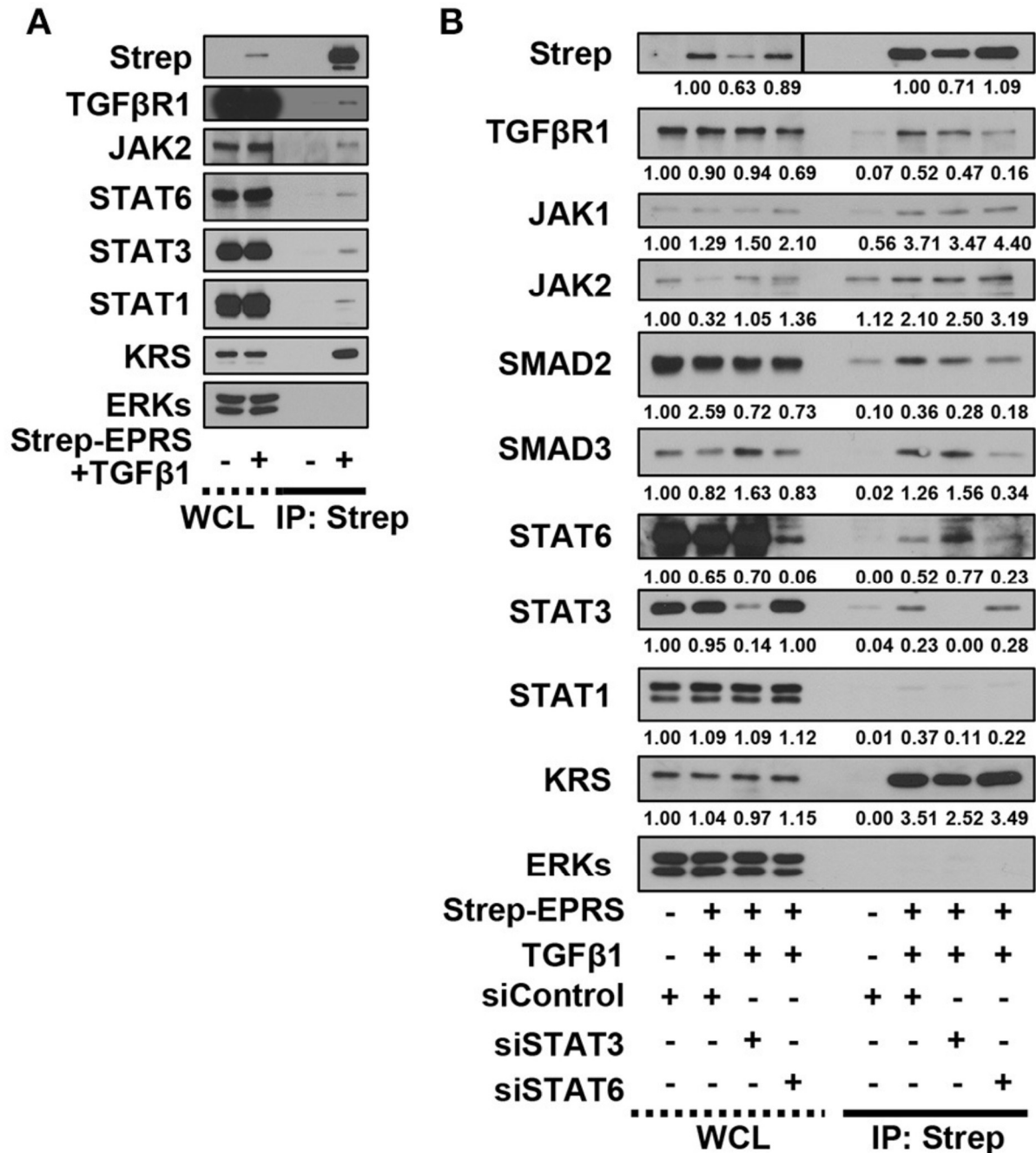


Figure 2. 4. EPRS-mediated signaling in TGFβ1-treated cells involves the formation of a multi-protein complex consisting of STAT6 and TGFβ1R. (A and B) A549 cells (-) or transiently-expressing Strep-tagged EPRS (Strep-EPRS, +) cells without (A) or with transient transfection of siSTAT3 or siSTAT6 for 48 hr (B) were treated with vehicle (-) or TGFβ1 (2 ng/ml, +). Whole cell extracts were then prepared and processed for precipitation using

streptavidin-agarose beads, and the precipitates were immunoblotted for the indicated molecules. ERKs were immunoblotted for the internal loading controls of the lysates. Data represent three independent experiments. Song *et al.*, *Frontiers in Pharmacology*, 2018. Copyright under Creative Commons Attribution 4.0 License [103].

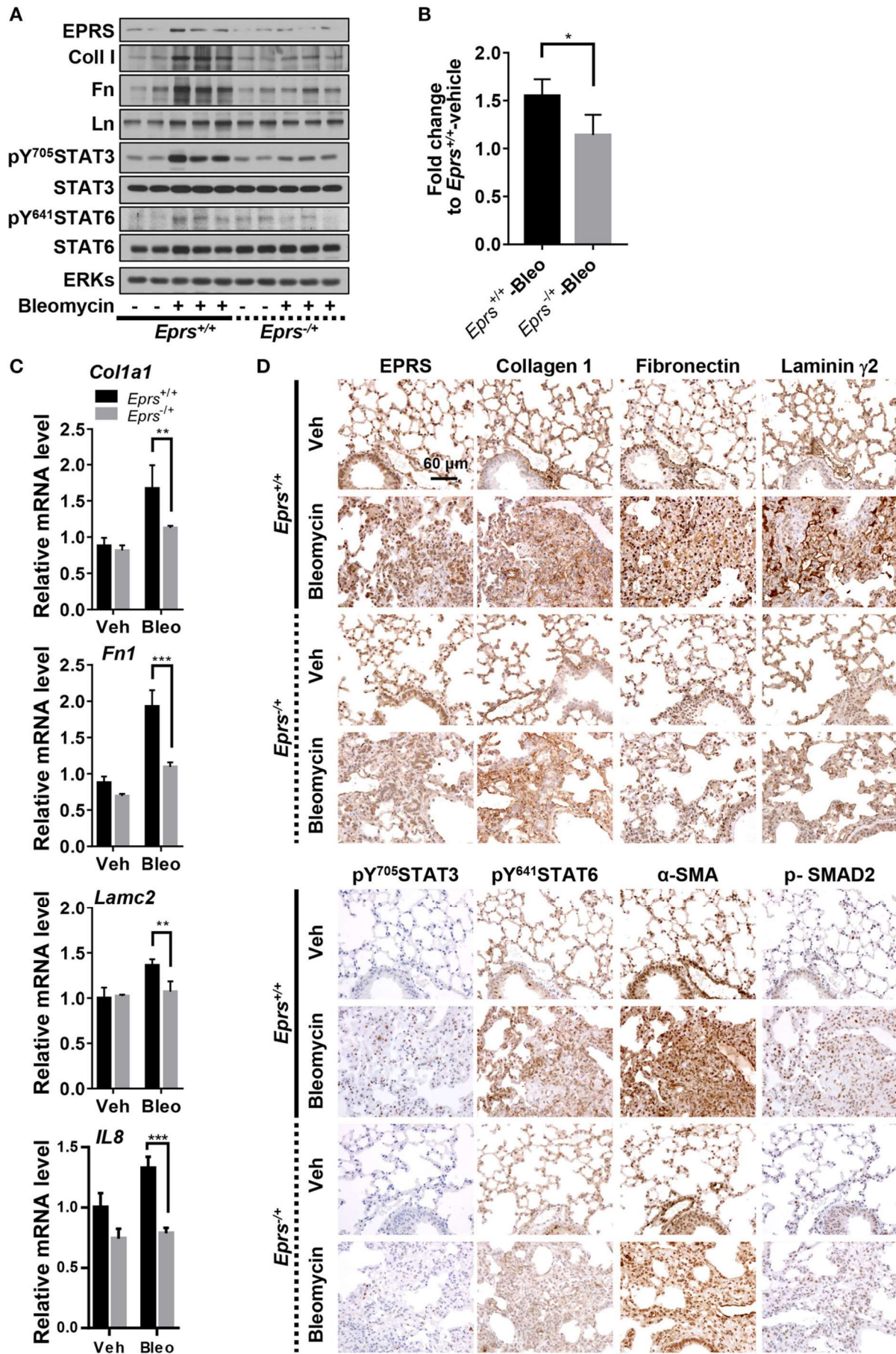


Figure 2. 5. Lung tissues from bleomycin-treated mice showed EPRS-dependent STAT6 phosphorylation and ECM protein production *in vivo*. (A to D) Wildtype (WT, *Eprs*^{+/+}) and *Eprs*^{-/+} hetero-knockout (KO) C57BL/6 mice were intratracheally treated once with vehicle (n=4 for WT and n=5 for *Eprs*^{-/+} hetero-KO) or bleomycin (1 mg/kg in PBS, n=9 for WT and n=7 for *Eprs*^{-/+} hetero-KO). After 28 days, mice were sacrificed, and lung tissues were collected for analyses. Lung tissue extracts were prepared and processed for immunoblots for the indicated molecules (A), hydroxyproline assays (B), and qRT-PCR for the indicated mRNAs (C). Data are presented at mean \pm SD. *, **, and *** indicate significance at $p < 0.05$, 0.01, and 0.001, respectively (calculated by Student's *t*-tests). (D) The lung tissues were processed for immunohistochemistry, before image capturing at 40 x. Data represent three different experiments. Song *et al.*, *Frontiers in Pharmacology*, 2018. Copyright under Creative Commons Attribution 4.0 License [103].

2.4. DISCUSSION

In this study, I showed that EPRS regulates the TGF β 1-mediated expression of ECM proteins such as collagen I and fibronectin. My *in vitro* and *in vivo* analyses demonstrated that the signal for ECM protein synthesis might be transduced via a multi-protein signaling complex composed of TGF β R1, SMAD3, JAKs and STAT6. EPRS may have functions independent of translational tRNA charging that serve as a signaling molecule for TGF β 1-induced ECM protein synthesis and mesenchymal marker expression, presumably leading to fibrotic phenotypes (Fig. 2. 6). Therefore, EPRS is a promising target for anti-IPF therapy.

The binding target of the anti-fibrotic agent, HF, first revealed the link between EPRS and fibrosis [22]. HF competitively inhibits PRS, which activates the AAR pathway because of naked-tRNA accumulation. HF-mediated inhibition of PRS also cause decreased ECM expression, which is overcome by exogenous proline treatment, indicating that PRS can be involved in ECM translation via tRNA charging with proline [22]. However, it cannot be ruled out that PRS play roles in ECM expression at non-translational processes, since variable ECMs can be composed with different levels of proline. Additionally, this previous study had not shown EPRS regulation of TGF β 1-induced ECM protein synthesis. Moreover, although a previous study showed a fibrotic role of EPRS in a lung fibroblast IMR90 cell line, here I found that alveolar type II epithelial cells may lead to the formation of fibrotic foci in IPF under the influence of TGF β 1. TGF β 1 is a master regulator of fibrosis that induces epithelial to mesenchymal transition (EMT) and analyzing its role in EPRS-mediated ECM regulation is critical for developing IPF treatments.

IPF [27] is currently managed with nintedanib and pirfenidone. These drugs slow down the rate of forced vital capacity decline by ~50% over 1-year period [27] but do not completely cure the disease. The anti-fibrotic reagent, HF, causes significant side effects including severe

gastrointestinal lesions and hemorrhage [92]. Novel and safe treatment methods for IPF are therefore needed. Recent studies have begun uncovering the mechanisms of IPF pathogenesis. STAT6-mediated signaling is important for the development of carbon nanotube-induced fibrotic lung disease [100]. The JAK2/STAT3 pathway is activated in IPF, and treatment with JSI-124 (a dual inhibitor of JAK2/STAT3) decreases collagen deposition during lung fibrosis [30]. In the present study, I used *in vitro* and *in vivo* models to reveal a novel relationship between EPRS and STAT6 and their participation in IPF.

In studying TGF β 1-induced activation of the STAT signaling cascade for ECM protein synthesis, I found that EPRS was an upstream regulator of STAT3/6 activation. TGF β 1-induced SMAD3 activation was important for activating STAT6, which was critical for formation of the multi-protein complex of TGF β R1, EPRS, JAKs, and STAT3/6. Both STAT3 and STAT6 appear to act downstream of TGF β 1 stimulation, possibly in parallel signaling pathways. However, STAT3 suppression led to higher levels of STAT6 in the multi-protein complex, indicating that STAT6 was more important than STAT3 for TGF β 1-induced, EPRS-mediated ECM protein synthesis. Previous studies have shown that EPRS forms complexes with other proteins. EPRS translocates to the cell surface to bind to TGF β 1R. Phosphorylation of EPRS at Ser999 causes it to dissociate from the MSC and translocate to the membrane where it interacts with the fatty-acid transporter, FATP1, upon insulin stimulation of adipocytes [67]. TGF β 1 treatment induces TGF β R1-JAK1 and STAT3-SMAD3 to form a protein complex [95]. These studies validate my results regarding the EPRS-containing multi-protein complex. I also found that suppression of STAT6 but not of STAT3 abolished the formation of a complex between EPRS, TGF β R1, and SMAD2/3. My findings suggest that EPRS is a novel component of the TGF β R1-JAK complex and STAT6 is critical for the formation of the EPRS-TGF β R1-JAKs-STATs multi-protein signaling complex that mediates ECM synthesis.

Our *in vivo* animal studies showed that ERPS protein levels were slightly upregulated in bleomycin-treated WT *Eprs*^{+/+} mice compared with *Eprs*^{-/-} KO mice. However, EPRS mRNA levels were upregulated 2.5-fold in TGFβ1-treated A549 cells compared with control cells, although EPRS protein levels were unchanged (Fig. 2. 1C). These differences in EPRS mRNA and protein levels might be the result of variable treatment times between the *in vitro* and *in vivo* experiments (1 vs. 28 days). Because IPF is a chronic disease, EPRS might be upregulated during the development of fibrosis, as seen in my *in vivo* experimental model.

In conclusion, my study showed that EPRS might be a signaling molecule underlying TGFβ1-induced ECM protein synthesis and is a promising potential target for the treatment of IPF.

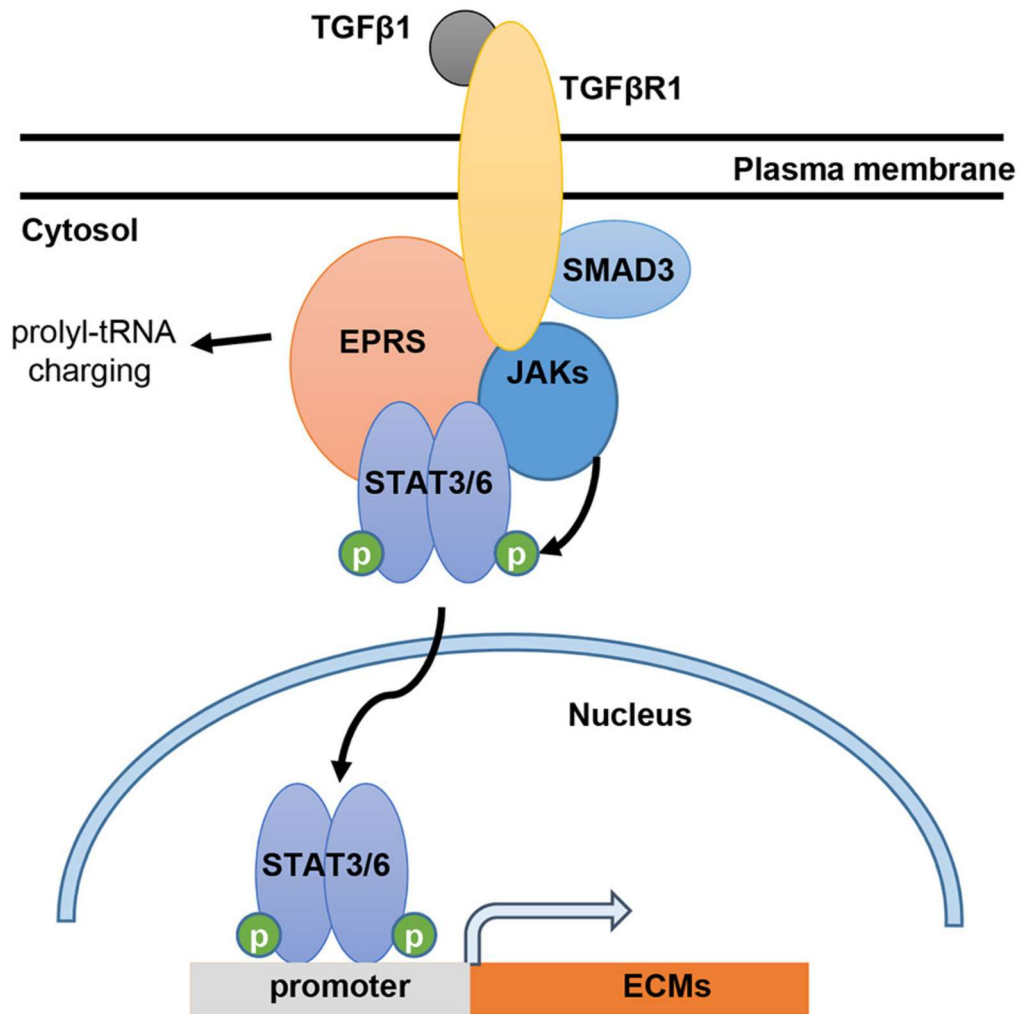


Figure 2. 6. Working model for EPRS-dependent signaling during TGF β 1-mediated ECM expression of ECMs. TGF β 1 binding to TGF β R1 can stimulate formation of a signaling complex consisting of TGF β R1, SMAD3, JAKs, STAT3/6 and EPRS for active JAKs-mediated STAT3/6 phosphorylation. Phosphorylated STAT3/6 can enter the nucleus for transcriptional induction of ECM genes, such as collagen α 1 (*COLA1*), laminin γ 2 (*LAMC2*), and fibronectin 1 (*FNI*). Song *et al.*, *Frontiers in Pharmacology*, 2018. Copyright under Creative Commons Attribution 4.0 License [103].

CONCLUSIONS

&

PERSPECTIVES

In this study, it is shown that EPRS may induce ECMs, especially collagen I and fibronectin, via non-translational activity. When triggered by TGF β 1, EPRS may form binding complex with TGF β -R1. The complex has shown to be able to bind with other binding partners including SMAD2/3, JAK1, JAK2, STAT1, STAT3, STAT5, and STAT6. By the binding of such proteins, TGF β 1 may trigger down-stream phosphorylation of STAT6 and in turn activates the promoter of collagen.

Utilizing the *Eprs* heterozygous knock-out mouse with induced fibrosis model, it has shown that *Eprs* down-regulation may be effective in reducing the fibrotic phenotypes. The fibrotic septa as well as hepatic stellate cell activation have been reduced in *Eprs*^{-/+} mice. At the same time and region, the activation of STAT6 molecules were reduced in hepatic model and activation of both STAT3 and STAT6 molecules were reduced in pulmonary fibrosis. These results were in accordance with respective cell line based studies. The organoid study in the hepatic fibrosis model suggests that organoid based fibrosis model can be applicable in drug development. Additionally, the study has raised some critical points that different cell types may responsible for different types of ECM molecules. Considering the results, it may be important to define the nature of the organoids when developing organoids as a drug screening model for fibrosis.

The study, however, addresses some limiting points. First, the direct activity of EPRS, such as phosphorylation in specific sites, were not fully unveiled. Since the binding of molecules does not necessarily mean it is able to activate binding partners, the result that EPRS forms complex with TGF β R1 and STAT6 does not mean that EPRS can activate down-stream molecules. It was unfortunate that EPRS S999A mutant used in this study showed no difference in binding capacity compared to EPRS WT. Thus rather than EPRS S999A mutant, a phospho-mimetic EPRS S999D mutant can be used in further study to investigate the binding ability of

EPRS. Additionally, deletion mutants could be utilized to reveal the responsible domain which is important in binding the complexes.

Second, the component responsible for phosphorylating STAT6 should also be clarified. Since JAKs are known to phosphorylate STATs, JAK molecules may be the most potent kinases for STAT6 phosphorylation. However, the specific molecule among JAKs (or may be other kinases) should be investigated whether which is the one responsible for EPRS-mediated phosphorylation of STAT6. In order to conduct the experiment, knock-down of JAK molecules could be studied for finding the STAT6 activator. Also, it should be studied whether complex formation is critical in phosphorylating STAT6. Finding of dissociation condition (other than STAT6 knock-down) and following confirmation of down-stream activation could be studied in order to check whether complex formation is critical in signaling or not.

Third limiting point is that the relationship between SMAD and STAT molecules should be studied in detail. Activation of STAT6 either by overexpressing the gene or by treatment with its known cytokine, IL13 or IL4, did not result in significant enhancement of collagen in LX2 cells. However, since collagen was down regulated when STAT6 was knocked-down in LX2 cells, it is certain that STAT6 is somehow related to collagen expression in LX2 cells. Thus I propose that TGF β 1 dependent activation of collagen expression is conducted by co-activating manner with SMAD3 and STAT6. It has been reported that P300 protein is able to bind both SMADs and STAT3 molecules and serves as a co-activator of the glial fibrillary acidic protein promoter during the differentiation process in astrocytes [104]. Thus studying the relevance of P300 protein during TGF β 1-SMAD3-STAT6-mediated collagen production might give us clue on the relationship between SMAD3 and STAT6.

Considering the dual effects of TGF β 1 in human health and disease, it is important to bypass the TGF β 1 signaling pathway and inactivate down-stream ECM production in fibrotic disease. In line with the hypothesis, EPRS might serve as a good target for treatment of fibrosis.

The strategic points may include the followings; 1) developing drug for inhibiting the EPRS binding complex, 2) inhibiting STAT6 activation, and 3) inhibiting non-canonical activity of EPRS.

REFERENCES

1. Gressner, O.A., et al., Monitoring fibrogenic progression in the liver. *Clin Chim Acta*, 2014. **433**:111-22.
2. Nanthakumar, C.B., et al., Dissecting fibrosis: therapeutic insights from the small-molecule toolbox. *Nat Rev Drug Discov*, 2015. **14** (10):693-720.
3. King, T.E., Jr., et al., A phase 3 trial of pirfenidone in patients with idiopathic pulmonary fibrosis. *N Engl J Med*, 2014. **370** (22):2083-92.
4. Shihab, F.S., et al., Pirfenidone treatment decreases transforming growth factor-beta1 and matrix proteins and ameliorates fibrosis in chronic cyclosporine nephrotoxicity. *Am J Transplant*, 2002. **2** (2):111-9.
5. Iyer, S.N., et al., Effects of pirfenidone on transforming growth factor-beta gene expression at the transcriptional level in bleomycin hamster model of lung fibrosis. *J Pharmacol Exp Ther*, 1999. **291** (1):367-73.
6. Nakazato, H., et al., A novel anti-fibrotic agent pirfenidone suppresses tumor necrosis factor-alpha at the translational level. *Eur J Pharmacol*, 2002. **446** (1-3):177-85.
7. Oku, H., et al., Pirfenidone suppresses tumor necrosis factor-alpha, enhances interleukin-10 and protects mice from endotoxic shock. *Eur J Pharmacol*, 2002. **446** (1-3):167-76.
8. Ma, Z., et al., Synthesis and biological evaluation of the pirfenidone derivatives as antifibrotic agents. *Bioorg Med Chem Lett*, 2014. **24** (1):220-3.
9. Hilberg, F., et al., BIBF 1120: triple angiokinase inhibitor with sustained receptor blockade and good antitumor efficacy. *Cancer Res*, 2008. **68** (12):4774-82.
10. Schaefer, C.J., et al., Antifibrotic activities of pirfenidone in animal models. *Eur Respir Rev*, 2011. **20** (120):85-97.

11. Noble, P.W., et al., Pirfenidone in patients with idiopathic pulmonary fibrosis (CAPACITY): two randomised trials. *Lancet*, 2011. **377** (9779):1760-9.
12. Wollin, L., et al., Antifibrotic and anti-inflammatory activity of the tyrosine kinase inhibitor nintedanib in experimental models of lung fibrosis. *J Pharmacol Exp Ther*, 2014. **349** (2):209-20.
13. Richeldi, L., et al., Efficacy and safety of nintedanib in idiopathic pulmonary fibrosis. *N Engl J Med*, 2014. **370** (22):2071-82.
14. Schuppan, D., et al., Liver fibrosis: Direct antifibrotic agents and targeted therapies. *Matrix Biol*, 2018.
15. Huang, Y., et al., Modulation of hepatic stellate cells and reversibility of hepatic fibrosis. *Exp Cell Res*, 2017. **352** (2):420-426.
16. Gressner, A.M., et al., Modern pathogenetic concepts of liver fibrosis suggest stellate cells and TGF-beta as major players and therapeutic targets. *J Cell Mol Med*, 2006. **10** (1):76-99.
17. Maher, J.J., et al., Extracellular matrix gene expression increases preferentially in rat lipocytes and sinusoidal endothelial cells during hepatic fibrosis in vivo. *J Clin Invest*, 1990. **86** (5):1641-8.
18. Karsdal, M.A., et al., Novel insights into the function and dynamics of extracellular matrix in liver fibrosis. *Am J Physiol Gastrointest Liver Physiol*, 2015. **308** (10):G807-30.
19. Hynes, R.O., et al., Overview of the matrisome--an inventory of extracellular matrix constituents and functions. *Cold Spring Harb Perspect Biol*, 2012. **4** (1):a004903.
20. Li, X., et al., Drugs and Targets in Fibrosis. *Front Pharmacol*, 2017. **8**:855.
21. Tu, T., et al., Hepatocytes in liver injury: Victim, bystander, or accomplice in

progressive fibrosis? *J Gastroenterol Hepatol*, 2015. **30** (12):1696-704.

22. Keller, T.L., et al., Halofuginone and other febrifugine derivatives inhibit prolyl-tRNA synthetase. *Nat Chem Biol*, 2012. **8** (3):311-7.
23. Friedman, S.L., Molecular regulation of hepatic fibrosis, an integrated cellular response to tissue injury. *J Biol Chem*, 2000. **275** (4):2247-50.
24. Iredale, J.P., Models of liver fibrosis: exploring the dynamic nature of inflammation and repair in a solid organ. *J Clin Invest*, 2007. **117** (3):539-48.
25. Friedman, S.L., Mechanisms of Hepatic Fibrogenesis. *Gastroenterology*, 2008. **134** (6):1655-1669.
26. Friedman, S.L., Hepatic Stellate Cells: Protean, Multifunctional, and Enigmatic Cells of the Liver. *Physiological Reviews*, 2008. **88** (1):125-172.
27. Lederer, D.J., et al., Idiopathic Pulmonary Fibrosis. *N Engl J Med*, 2018. **378** (19):1811-1823.
28. Zhou, X.M., et al., GHK Peptide Inhibits Bleomycin-Induced Pulmonary Fibrosis in Mice by Suppressing TGFbeta1/Smad-Mediated Epithelial-to-Mesenchymal Transition. *Front Pharmacol*, 2017. **8**:904.
29. Bai, Y., et al., A Chinese Herbal Formula Ameliorates Pulmonary Fibrosis by Inhibiting Oxidative Stress via Upregulating Nrf2. *Front Pharmacol*, 2018. **9**:628.
30. Milara, J., et al., The JAK2 pathway is activated in idiopathic pulmonary fibrosis. *Respir Res*, 2018. **19** (1):24.
31. Raghu, G., et al., An Official ATS/ERS/JRS/ALAT Clinical Practice Guideline: Treatment of Idiopathic Pulmonary Fibrosis. An Update of the 2011 Clinical Practice Guideline. *Am J Respir Crit Care Med*, 2015. **192** (2):e3-19.

32. Wolters, P.J., et al., Pathogenesis of idiopathic pulmonary fibrosis. *Annu Rev Pathol*, 2014. **9**:157-79.
33. Bagnato, G., et al., Cellular interactions in the pathogenesis of interstitial lung diseases. *Eur Respir Rev*, 2015. **24** (135):102-14.
34. Luzina, I.G., et al., The cytokines of pulmonary fibrosis: Much learned, much more to learn. *Cytokine*, 2015. **74** (1):88-100.
35. Varga, J., et al., Transforming growth factor β as a therapeutic target in systemic sclerosis. *Nature Reviews Rheumatology*, 2009. **5**:200.
36. Feng, L., et al., Functional Analysis of the Roles of Posttranslational Modifications at the p53 C Terminus in Regulating p53 Stability and Activity. *Molecular and cellular biology*, 2005. **25** (13):5389-5395.
37. Gordon, K.J., et al., Role of transforming growth factor-beta superfamily signaling pathways in human disease. *Biochim Biophys Acta*, 2008. **1782** (4):197-228.
38. Valle, L., et al., Germline allele-specific expression of TGFBR1 confers an increased risk of colorectal cancer. *Science*, 2008. **321** (5894):1361-5.
39. Zeng, Q., et al., Tgfr1 haploinsufficiency is a potent modifier of colorectal cancer development. *Cancer Res*, 2009. **69** (2):678-86.
40. Saxena, V., et al., Dual roles of immunoregulatory cytokine TGF-beta in the pathogenesis of autoimmunity-mediated organ damage. *J Immunol*, 2008. **180** (3):1903-12.
41. Lo, W.-S., et al., Human tRNA synthetase catalytic nulls with diverse functions. *Science*, 2014. **345** (6194):328-332.
42. Arif, A., et al., Two-site phosphorylation of EPRS coordinates multimodal regulation of noncanonical translational control activity. *Mol Cell*, 2009. **35** (2):164-80.

43. Ibba, M., et al., Aminoacyl-tRNA synthesis. *Annual Review of Biochemistry*, 2000. **69**:617-650.
44. Ribas de Pouplana, L., et al., Aminoacyl-tRNA synthetases: Potential markers of genetic code development. *Trends in Biochemical Sciences*, 2001. **26** (10):591-596.
45. Robinson, J.C., et al., Macromolecular assemblage of aminoacyl-tRNA synthetases: Quantitative analysis of protein-protein interactions and mechanism of complex assembly. *Journal of Molecular Biology*, 2000. **304** (5):983-994.
46. Shiba, K., Intron positions delineate the evolutionary path of a pervasively appended peptide in five human aminoacyl-tRNA synthetases. *Journal of Molecular Evolution*, 2002. **55** (6):727-733.
47. Ko, Y.G., et al., Novel regulatory interactions and activities of mammalian tRNA synthetases. *Proteomics*, 2002. **2** (9):1304-1310.
48. Lee, Y.N., et al., The Function of Lysyl-tRNA Synthetase and Ap4A as Signaling Regulators of MITF Activity in FcεRI-Activated Mast Cells. *Immunity*, 2004. **20** (2):145-151.
49. Park, S.G., et al., Human lysyl-tRNA synthetase is secreted to trigger proinflammatory response. *Proc Natl Acad Sci U S A*, 2005. **102** (18):6356-61.
50. Ko, Y.G., et al., Glutamine-dependent antiapoptotic interaction of human glutaminyl-tRNA synthetase with apoptosis signal-regulating kinase 1. *J Biol Chem*, 2001. **276** (8):6030-6.
51. Tzima, E., et al., Inhibition of tumor angiogenesis by a natural fragment of a tRNA synthetase. *Trends in Biochemical Sciences*, 2006. **31** (1):7-10.
52. Jeong, E.J., et al., Structural analysis of multifunctional peptide motifs in human bifunctional tRNA synthetase: Identification of RNA-binding residues and functional implications for tandem repeats. *Biochemistry*, 2000. **39** (51):15775-15782.

53. Sampath, P., et al., Noncanonical function of glutamyl-prolyl-tRNA synthetase: Gene-specific silencing of translation. *Cell*, 2004. **119** (2):195-208.
54. Jia, J., et al., WHEP Domains Direct Noncanonical Function of Glutamyl-Prolyl tRNA Synthetase in Translational Control of Gene Expression. *Molecular Cell*, 2008. **29** (6):679-690.
55. Park, S.G., et al., Functional expansion of aminoacyl-tRNA synthetases and their interacting factors: new perspectives on housekeepers. *Trends Biochem Sci*, 2005. **30** (10):569-74.
56. Kyriacou, S.V., et al., An Important Role for the Multienzyme Aminoacyl-tRNA Synthetase Complex in Mammalian Translation and Cell Growth. *Molecular Cell*, 2008. **29** (4):419-427.
57. Ray, P.S., et al., Macromolecular complexes as depots for releasable regulatory proteins. *Trends in Biochemical Sciences*, 2007. **32** (4):158-164.
58. Mukhopadhyay, R., et al., DAPK-ZIPK-L13a Axis Constitutes a Negative-Feedback Module Regulating Inflammatory Gene Expression. *Molecular Cell*, 2008. **32** (3):371-382.
59. Ray, P.S., et al., A stress-responsive RNA switch regulates VEGFA expression. *Nature*, 2009. **457** (7231):915-919.
60. Sampath, P., et al., Transcript-selective translational silencing by gamma interferon is directed by a novel structural element in the ceruloplasmin mRNA 3' untranslated region. *Molecular and Cellular Biology*, 2003. **23** (5):1509-1519.
61. Vyas, K., et al., Genome-wide polysome profiling reveals an inflammation-responsive posttranscriptional operon in gamma interferon-activated monocytes. *Molecular and Cellular Biology*, 2009. **29** (2):458-470.
62. Kapasi, P., et al., L13a Blocks 48S Assembly: Role of a General Initiation Factor in mRNA-Specific Translational Control. *Molecular Cell*, 2007. **25** (1):113-126.

63. Dever, T.E., Gene-specific regulation by general translation factors. *Cell*, 2002. **108** (4):545-556.
64. Gebauer, F., et al., Molecular mechanisms of translational control. *Nature Reviews Molecular Cell Biology*, 2004. **5** (10):827-835.
65. Proud, C.G., Signalling to translation: How signal transduction pathways control the protein synthetic machinery. *Biochemical Journal*, 2007. **403** (2):217-234.
66. Mazumder, B., et al., Regulated release of L13a from the 60S ribosomal subunit as a mechanism of transcript-specific translational control. *Cell*, 2003. **115** (2):187-198.
67. Arif, A., et al., EPRS is a critical mTORC1-S6K1 effector that influences adiposity in mice. *Nature*, 2017. **542** (7641):357-361.
68. Aminoacyl-tRNA synthetase. 2012; Available from: https://www.mun.ca/biology/desmid/brian/BIOL2060/BIOL2060-22/22_05.jpg.
69. Lee, E.-Y., et al., Infection-specific phosphorylation of glutamyl-prolyl tRNA synthetase induces antiviral immunity. *Nature Immunology*, 2016. **17**:1252.
70. Thiaville, M.M., et al., Deprivation of protein or amino acid induces C/EBPbeta synthesis and binding to amino acid response elements, but its action is not an absolute requirement for enhanced transcription. *Biochem J*, 2008. **410** (3):473-84.
71. Lu, P.D., et al., Translation reinitiation at alternative open reading frames regulates gene expression in an integrated stress response. *J Cell Biol*, 2004. **167** (1):27-33.
72. Bruhat, A., et al., Amino acid limitation induces expression of CHOP, a CCAAT/enhancer binding protein-related gene, at both transcriptional and post-transcriptional levels. *J Biol Chem*, 1997. **272** (28):17588-93.
73. Harding, H.P., et al., An integrated stress response regulates amino acid metabolism and resistance to oxidative stress. *Mol Cell*, 2003. **11** (3):619-33.

74. Pines, M., et al., Halofuginone - the multifaceted molecule. *Molecules*, 2015. **20** (1):573-94.
75. Luo, Y., et al., The role of halofuginone in fibrosis: more to be explored? *J Leukoc Biol*, 2017. **102** (6):1333-1345.
76. Ghosh, A.K., et al., Molecular basis of organ fibrosis: potential therapeutic approaches. *Exp Biol Med (Maywood)*, 2013. **238** (5):461-81.
77. Halevy, O., et al., Inhibition of collagen type I synthesis by skin fibroblasts of graft versus host disease and scleroderma patients: effect of halofuginone. *Biochem Pharmacol*, 1996. **52** (7):1057-63.
78. Turgeman, T., et al., Prevention of muscle fibrosis and improvement in muscle performance in the mdx mouse by halofuginone. *Neuromuscul Disord*, 2008. **18** (11):857-68.
79. Zhou, H., et al., ATP-directed capture of bioactive herbal-based medicine on human tRNA synthetase. *Nature*, 2013. **494** (7435):121-4.
80. Kaiser, E., et al., The human EPRS locus (formerly the QARS locus): a gene encoding a class I and a class II aminoacyl-tRNA synthetase. *Genomics*, 1994. **19** (2):280-90.
81. Choi, S., et al., Cooperation between integrin $\alpha 5$ and tetraspan TM4SF5 regulates VEGF-mediated angiogenic activity. *Blood*, 2009. **113** (8):1845-1855.
82. Lee, M.-S., et al., The signaling network of transforming growth factor $\beta 1$, protein kinase C δ , and integrin underlies the spreading and invasiveness of gastric carcinoma cells. *Molecular and cellular biology*, 2005. **25** (16):6921-6936.
83. Kim, H.J., et al., Dynamic and coordinated single-molecular interactions at TM4SF5-enriched microdomains guide invasive behaviors in 2- and 3-dimensional environments. *FASEB J*, 2017. **31** (4):1461-1481.

84. Lareu, R.R., et al., Collagen matrix deposition is dramatically enhanced in vitro when crowded with charged macromolecules: the biological relevance of the excluded volume effect. *FEBS Lett*, 2007. **581** (14):2709-14.
85. Tag, C.G., et al., Bile Duct Ligation in Mice: Induction of Inflammatory Liver Injury and Fibrosis by Obstructive Cholestasis. *Journal of Visualized Experiments : JoVE*, 2015 (96):52438.
86. Broutier, L., et al., Culture and establishment of self-renewing human and mouse adult liver and pancreas 3D organoids and their genetic manipulation. *Nat Protoc*, 2016. **11** (9):1724-43.
87. Park, S.G., et al., Aminoacyl tRNA synthetases and their connections to disease. *Proc Natl Acad Sci U S A*, 2008. **105** (32):11043-9.
88. Delgoffe, G.M., et al., STAT heterodimers in immunity: A mixed message or a unique signal? *JAKSTAT*, 2013. **2** (1):e23060.
89. Katayama, M., et al., Laminin gamma2 fragments are increased in the circulation of patients with early phase acute lung injury. *Intensive Care Med*, 2010. **36** (3):479-86.
90. Kiyokawa, H., et al., Serum monomeric laminin-gamma2 as a novel biomarker for hepatocellular carcinoma. *Cancer Sci*, 2017. **108** (7):1432-1439.
91. McLaughlin, N.P., et al., The chemistry and biology of febrifugine and halofuginone. *Bioorg Med Chem*, 2014. **22** (7):1993-2004.
92. Jiang, S., et al., Antimalarial activities and therapeutic properties of febrifugine analogs. *Antimicrob Agents Chemother*, 2005. **49** (3):1169-76.
93. Roffe, S., et al., Halofuginone inhibits Smad3 phosphorylation via the PI3K/Akt and MAPK/ERK pathways in muscle cells: effect on myotube fusion. *Exp Cell Res*, 2010. **316** (6):1061-9.
94. Zhang, Y.E., Mechanistic insight into contextual TGF-beta signaling. *Curr Opin Cell*

Biol, 2018. **51**:1-7.

95. Tang, L.Y., et al., Transforming Growth Factor-beta (TGF-beta) Directly Activates the JAK1-STAT3 Axis to Induce Hepatic Fibrosis in Coordination with the SMAD Pathway. *J Biol Chem*, 2017. **292** (10):4302-4312.
96. Pechkovsky, D.V., et al., STAT3-mediated signaling dysregulates lung fibroblast-myofibroblast activation and differentiation in UIP/IPF. *Am J Pathol*, 2012. **180** (4):1398-412.
97. Pedroza, M., et al., STAT-3 contributes to pulmonary fibrosis through epithelial injury and fibroblast-myofibroblast differentiation. *FASEB J*, 2016. **30** (1):129-40.
98. Prele, C.M., et al., STAT3: a central mediator of pulmonary fibrosis? *Proc Am Thorac Soc*, 2012. **9** (3):177-82.
99. Papaioannou, I., et al., STAT3 controls COL1A2 enhancer activation cooperatively with JunB, regulates type I collagen synthesis posttranscriptionally, and is essential for lung myofibroblast differentiation. *Mol Biol Cell*, 2018. **29** (2):84-95.
100. Nikota, J., et al., Stat-6 signaling pathway and not Interleukin-1 mediates multi-walled carbon nanotube-induced lung fibrosis in mice: insights from an adverse outcome pathway framework. *Part Fibre Toxicol*, 2017. **14** (1):37.
101. Ray, P.S., et al., Origin and evolution of glutamyl-prolyl tRNA synthetase WHEP domains reveal evolutionary relationships within Holozoa. *PLoS One*, 2014. **9** (6):e98493.
102. Carre, P.C., et al., Increased expression of the interleukin-8 gene by alveolar macrophages in idiopathic pulmonary fibrosis. A potential mechanism for the recruitment and activation of neutrophils in lung fibrosis. *J Clin Invest*, 1991. **88** (6):1802-10.
103. Song, D.-G., et al., Glutamyl-Prolyl-tRNA Synthetase Regulates Epithelial Expression of Mesenchymal Markers and Extracellular Matrix Proteins: Implications for Idiopathic Pulmonary Fibrosis. 2018. **9** (1337).

104. Miyazono, K., TGF- β signaling by Smad proteins. *Cytokine & Growth Factor Reviews*, 2000. **11** (1):15-22.

Copyright information.

Parts of this study were accepted for publishing or published in the following journals.

Chapter 1: FASEB journal (accepted on Nov. 20. 2018)

Chapter 2: Frontiers in Pharmacology (published on Nov. 20. 2018) [103]

ABSTRACT IN KOREAN

글루타밀-프롤릴 tRNA 합성효소의 폐 및 간 섬유화에서
STAT Signaling을 통한 Collagen과 Fibronectin의 발현 조절 연구

송 대 근 (Song, Dae-Geun)

약학대학 의약생명과학전공 (Pharmaceutical Bioscience Major)

서울대학교 대학원

섬유화란 염증성 및 대사성 질환에 의해 세포의 과분열과 장기의 기능부전이 일어나 세포외기질 (extracellular matrix, ECM) 이 비정상적으로 과다하게 축적되는 과정을 말한다. 최근 연구에 따르면 상산(常山, *Dichroa febrifuga*) 으로부터 분리된 화합물 febrifugine의 할로젠화 유도체인 halofuginone은 glutamyl-prolyly tRNA synthetase (EPRS)의 활성을 억제함으로써 섬유화를 저해한다고 밝혀졌다. 하지만 기존 연구에서는 halofuginone이 EPRS의 활성을 저해함에 있어서 EPRS의 번역적 활성에만 초점을 맞추었으며 *in vivo* 환경에서는 확인한 바 없으므로 EPRS를 타겟으로한 섬유화 치료제 개발을 위해서는 추가 연구가 필요한 상황이다. 본 연구에서는 폐 및 간의 섬유화 과정에서 ECM을 합성하는 EPRS의 비-번역적 기능을 연구하고 EPRS의 hetero knock-out 마우스를 이용

하여 EPRS의 *in vivo*에서의 역할을 검증하고자 하였다.

우선 섬유화 과정 중 ECM 합성에 있어서 EPRS의 기능을 확인하고자 하였다. EPRS가 knock-down(KD) 되거나 overexpression 된 hepatic stellate cell (LX2 cell) 및 alveolar epithelial cell (A549 cell)에 TGF β 1을 처리하여 섬유화를 유도시킨 후 ECM의 발현을 살펴보았다. 그 결과 EPRS가 KD 된 세포에서는 Collagen I, Fibronectin, Laminin 과 같은 ECM의 발현이 감소했지만 PRS가 과발현된 세포에서는 ECM의 발현이 증가한 것을 관찰할 수 있었다. 이는 western blotting을 통한 단백질 수준뿐만 아니라 qPCR 방식을 이용한 mRNA level 모두 비슷한 양상을 관찰할 수 있었다. 또한, promoter luciferase assay를 통해 EPRS가 KD된 세포에서 collagen I 및 laminin γ 2의 promoter가 down-regulation 되는 것을 확인할 수 있었으므로 EPRS는 ECM 발현의 전사적인 수준에서 수행함을 알 수 있었다.

다음으로 EPRS 가 매개된 ECM 의 합성 조절의 신호전달을 관찰하기 위하여 섬유화와 밀접한 관계가 있다고 알려진 STAT 분자들의 인산화 정도를 분석하였다. 그 결과 STAT6가 EPRS의 발현과 함께 EPRS가 과발현 되었을 때 인산화가 증가되고 EPRS가 KD 될 때 인산화가 저해 되는 것으로 관찰되었다. 또한 SMAD2 단백질이 과발현 될 경우 STAT이 activation되어 SMAD가 STAT의 상위 신호전달에 관여함을 알 수 있었다. Immunoprecipitation 방법을 이용한 실험 결과 TGF β 1 receptor, EPRS, Janus kinase 그리고 STAT6 사이에 단백질-단백질 결합이 이루어 짐으로써 신호전달이 이루어 짐을 확인할 수 있었다.

CCl₄ 처리 혹은 bile duct ligation 방법을 통해 간 섬유화를 유도하거나 bleomycin을 처리하여 폐 섬유화를 유도한 동물 실험 결과 fibrotic septa 주변

에 STAT6의 인산화와 ECM의 발현이 동시에 증가 한 반면, 그 현상이 *Eprs*^{-/+} 마우스에서는 정도가 낮음을 알 수 있었다. 따라서 본 연구 결과 섬유화 과정에서 EPRS는 TGFβ1의존적으로 세포신호전달에 의한 비-번역적 과정을 거쳐 ECM의 발현을 조절하는 것을 확인 할 수 있었다. EPRS 단백질은 향후 간 및 폐 섬유화 억제 치료제의 타겟으로 활용 될 수 있을 것으로 기대된다.

주요어: EPRS, fibrosis, STAT, TGFβ1, SMAD, CCl₄, bile duct ligation, bleomycin

학번: 2015-30498